NOTICE

The quality of this microform is heavily dependent upon the quality of the original thesis submitted for microfilming. Every effort has been made to ensure the highest quality of reproduction possible.

If pages are missing, contact the university which granted the degree.

Some pages may have indistinct print especially if the original pages were typed with a poor typewriter ribbon or if the university sent us an inferior photocopy.

Reproduction in full or in part of this microform is governed by the Canadian Copyright Act, R.S.C. 1970, c. C-30, and subsequent amendments.

AVIS

La qualité de cette microforme dépend grandement de la qualité de la thèse soumise au microfilmage. Nous avons tout fait pour assurer une qualité supérieure de reproduction.

S'il manque des pages, veuillez communiquer avec l'université qui a conféré le grade.

La qualité d'impression de certaines pages peut laisser à désirer, surtout si les pages originales ont été dactylographiées à l'aide d'un ruban usé ou si l'université nous a fait parvenir une photocopie de qualité inférieure.

La reproduction, même partielle, de cette microforme est soumise à la Loi canadienne sur le droit d'auteur, SRC 1970, c. C-30, et ses amendements subséquents.

A STUDY OF CLAY COMPATIBILITY TO HEAVY METAL TRANSPORT IN PERMEABILITY TESTING

by

ALEXANDRE R. CABRAL

A Thesis submitted to the Faculty of Graduate Studies and Research

in partial fulfillment of the requirements for

the degree of Doctor of Philosophy

Department of Civil Engineering and Applied Mechanics

McGill University

Montreal, Quebec, Canada

March 1992

ISBN 0-315-74642-4

ABSTRACT

A clay-contaminant compatibility study was performed using: a) two materials: a kaolinitic clay and a 90% fine sand/10% bentonite mixture (**S/B**); b) concentrated solutions of two heavy metals - *Pb* and *Zn*; and c) a flexible wall (triaxial cell) and a rigid wall (consolidation cell) permeameter. Compatibility was analyzed in terms of changes in the measured coefficient of hydraulic permeability (k) due to percolation of the concentrated heavy metal solutions, and in terms of the capacity of **compacted** clays to retain heavy metals. Testing procedures and sample characteristics were kept as similar as possible for two apparatuses as a means of comparing their performances.

Permeability test results indicated that the k-values for kaolinite ($2 - 5 \times 10^{-7}$ cm/s) were independent of the apparatus employed, among several other parameters. k-values obtained for S/B tested in the rigid wall permeameter remained in the range of $2 - 6 \times 10^{-9}$ cm/s independently of the initial hydraulic gradients applied and of the concentration of the contaminant solution. For S/B tested with the flexible wall, however, the measured k-values varied significantly depending on: a) the initial hydraulic gradient applied; b) the saturation and compaction procedures adopted; c) the concentration of the contaminant solution; and d) type of contaminant used ($k_{Zn} > k_{Pb}$). Differences in performance between the two permeameters were mainly attributed to the more efficient saturation of triaxial samples.

Following permeability tests, the samples were sliced and chemical analyses were performed to evaluate the adsorption characteristics of the compacted materials. In the case of compacted kaolinite, **adsorption characteristic curves (ACC)** were constructed. **ACC** constitute a more realistic approach to the description of the partitioning of contaminants between the solid and liquid phases in a barrier system, as compared to linear adsorption isotherms obtained from batch equilibrium tests (soil solutions). This has major implications in the definition of the retention parameter to be employed in contaminant transport modelling. Retardation factors calculated

based on distribution coefficients (K_d) obtained from **ACC** were found to correlate better to those obtained directly from breakthrough curves than retardation factors calculated based on k_d taken from linear adsorption isotherms.

Chemical analyses of both the compacted samples and the leachate collected indicated that triaxial cell samples adsorbed more contaminant than consolidation cell samples. This was associated with the saturation of the samples. As observed in previous works, *Zn* was found to be more mobile than *Pb* due to its lower selectivity for clay surfaces.

For increased reliability, mass balance calculations were performed. Small discrepancies between amounts introduced and detected were attributed to experimental errors and to limitations in the 'extracting' procedure followed. Larger discrepancies were associated to high affinity adsorption.

RÉSUMÉ

Une étude de compatibilité entre argiles et contaminants a été faite en utilisant : a) deux types de matériaux, soit une argile du type kaolinite et un mélange composé de 90 % de sable fin et 10 % de bentonite (**S/B**); b) des solutions concentrées en *plomb* et en *zinc*; c) un perméamètre à paroi souple (cellule triaxiale) et un à paroi rigide (cellule de consolidation). La compatibilité a été analysée en ce qui a trait : 1) aux changements du coefficient de perméabilité (k) mesuré à la suite de la percolation des solutions, et 2) à la capacité qu'ont les argiles **compactées** de retenir les métaux lourds. Afin de bien comparer la performance des deux perméamètres, la similarité des procédures expérimentales ainsi que celle des caractéristiques des échantillons a été autant que possible maintenue.

Les résultats des essais de perméabilité ont indiqué que, indépendamment du perméamètre utilisé et de la variation de certains paramètres de contrôle, les valeurs de k pour la kaolinite étaient raisonnablement constantes (2 à 5 x 10^{-7} cm/s). En ce qui concerne les tests réalisés avec le mélange sable/bentonite, les valeurs de k obtenues se situaient entre 2 et 6 x 10^{-9} cm/s pour le perméamètre à paroi rigide et ce, indépendamment du gradient hydraulique initial appliqué et de la concentration de la solution de contaminant. Cependant, pour les tests réalisés dans le perméamètre à paroi souple, les valeurs de k mesurées variaient significativement selon : a) le gradient hydraulique initial appliqué; b) la procédure de compactage et de saturation adoptée; c) la concentration du contaminant; et d) du type de contaminant utilisé ($k_{Zn} > k_{Pb}$). La différence de performance entre les deux perméamètres était principalement attribuable à une saturation plus efficace des échantillons analysés dans la cellule triaxiale.

À la suite des tests de perméabilité, les échantillons étaient tranchés puis analysés chimiquement afin d'évaluer les caractéristiques d'adsorption des matériaux compactés. Dans le cas de la kaolinite compactée, les **courbes caractéristiques**

d'adsorption (**CCA**) ont été dressées. Les **CCA** offrent une meilleure description du partage des contaminants entre les phases dissoute et particulaire dans un système où le matériau se trouve compacté que ne le feraient les isothermes linéaires d'adsorption obtenues des «batch equilibrium tests». Ceci a des répercussions importantes sur la définition du (des) paramètres de rétention à employer dans la modélisation du transport des contaminants. Les facteurs de retardement calculés à partir des coefficients de distribution (K_d) obtenus des **CCA** sont en meilleure corrélation avec ceux obtenus directement des courbes de percée («breakthrough curves») que les facteurs calculés en utilisant des K_d tirés des isothermes linéaires d'adsorption.

Des analyses chimiques des échantillons compactés et du lixiviat récupéré ont indiqué qu'il y avait plus d'adsorption dans les échantillons testés dans la cellule triaxiale que ceux testés dans la cellule de consolidation. Ceci a été relié à la saturation des échantillons. Comme il a été observé dans d'autres travaux, le zinc s'est révélé plus mobile que le plomb en raison de sa plus faible sélectivité pour les surfaces argileuses.

Pour une fiabilité accrue, des bilans de masse ont été calculés. Les légères divergences entre les quantités introduites et détectées étaient attribuables à des erreurs expérimentales ainsi qu'à des limites reliées à la procédure d'extraction suivie. Les divergences plus considérables étaient associées à des adsorptions de plus grande affinité («high affinity adsorption»).

To my baby, Laura.

And to Martine.

ACKNOWLEDGMENTS

The author wishes to express his sincere appreciation and gratitude to :

- Dr. **Raymond N. Yong**, William Scott Professor of Civil Engineering and Applied Mechanics, Director of the Geotechnical Research Centre, McGill University, for his invaluable guidance and continued encouragement throughout this study;

- Dr. S. Rao, professor at the Indian Institute of Technology, who provided needed guidance in the early stages of the work;

- Dr. K. Lum, Centre Saint-Laurent, Environment Canada, for the opportunity I was given to be involved with the Saint Lawrence Action Plan.

- Mr. Larry Weber, with whom I had the pleasure to work during most of the time;

- Mr. F. Caporuscio for the technical assistance in the laboratory;

- The staff of both the Geotechnical Research Centre and of the Department of Civil Engineering and Applied Mechanics;

- All the colleagues in room 177, for the good moments together.

Acknowledgement is also extended to the Conselho Nacional de Desenvolvimento Científico e Tecnlógico (**CNPq**) of Brazil, and to the National Sciences and Engineering Research Council of Canada (**NSERC**) for supporting this thesis.

I am specially indebted to my family back in Brazil, and to the Lafortune family, here in Quebec. I deeply appreciate their love and encouragement.

Without the love and support of several friends this work would have been impossible. It is worth repeating here that friendship is the best thing in life. Thanks to all of you; deep from my heart.

Table of Contents

List of Figures

List of Tables

List of Symbols

ρ_b ≡ bulk mass density [M/L^3];

n ≡ porosity;

S ≡ mass of chemical constituent adsorbed to the solid phase of the porous medium per mass of solids [M/M];

C ≡ solute concentration [M/L^3] or concentration of a certain ion in the equilibrium solution;

D_l ≡ coefficient of hydrodynamic dispersion;

v_l ≡ average linear velocity along the flow line;

l ≡ coordinate direction along the flowline;

t ≡ time;

q ≡ equivalent to S

C_0 ≡ concentration of blank *Pb* solution

V ≡ volume of fluid;

M ≡ dry mass of soil;

i ≡ hydraulic gradient applied

K_d ≡ the slope of the adsorption isotherm. Often designated as the partition, or distribution, coefficient.

C_1 ≡ concentration of cations in the inner Helmholtz plane (ions/m^3);

C_2 ≡ concentration of cations in the outer Helmholtz plane (ions/m^3);

k ≡ Boltzmann constant (1.38 x 10^{-16} erg/°K);

T ≡ temperature (°K);

*k*T ≡ 0.4 x 10^{-20} J/ion at 20°C;

E_1 ≡ the potential energy of the ions in the inner Helmholtz plane;

E_2 ≡ the potential energy of the ions in the outer Helmholtz plane;

v_c ≡ the velocity of the $C/C_0 = 0.5$ point on the concentration profile of the retarded constituent;

R ≡ retardation factor; **or**

R ≡ universal gas constant;

T ≡ absolute temperature in °K;

K ≡ equilibrium constant of the reaction describing the exchange phenomena;

$\Delta G°$ ≡ Gibbs free energy;

D ≡ selectivity coefficient;

a_{Pb} ≡ activity of the solute;

CEC ≡ cation exchange capacity;

SSA ≡ specific surface area of the clay mineral;

WDS ≡ total weight of dry soil;

C_c ≡ concentration of the cation in the bulk solution (ions/cm^3);

z ≡ valence of the cation;

e' ≡ electron charge = 4.8×10^{-10} esu;

ψ_{oh} ≡ electric potential in the outer Helmholtz plane (esu);

KT ≡ $0.4 \times 10_{20}$ J/ion at 20°C (0.4×10^{-13} erg/ion);

σ_t ≡ total surface energy density (esu/cm^2) = CEC/SSA;

σ_s ≡ charge density of partially hydrated adsorbed cations (esu/cm^2)

σ_s ≡ $z.e'.\Delta x.C_1$ (where Δx is the thickness of a water layer = 2.8×10^{-8} cm);

σ_d ≡ charge density of hydrated adsorbed cations in the diffuse layer (esu/cm^2).

ε ≡ dielectric constant of the bulk solution = 80 (water);

Y_d ≡ scaled potential = $(z.e'.\psi_{oh})/(2.KT)$;

CHAPTER 1

INTRODUCTION

"Science can amuse and fascinate us all, but it is engineering that changes the world."
Isaac Asimov

1.1 - Statement of the Problem

The contemporary ecological crisis has become one of the most widespread and pressing issues of the late-twentieth century. The contamination of the environment by industrial and consumer waste has reached global proportions and poses unprecedented challenges; to scientists in almost all areas of research, technical experts both inside and outside of industry, policy makers, regulatory agents, and to the public at large.

The safe disposal of hazardous waste is one important component in dealing with the global environmental problem. This is a complex issue requiring the intervention of professionals from many different areas of expertise and backgrounds.

The difficulty of addressing the problem of how to safely and efficiently dispose of hazardous waste is intimately related to the increasing volume of such waste produced by society: 3.3 million tons/yr in Canada (Gore and Storrie, 1982):

The main obstacle to achieving the design and construction of a 'perfect' barrier lies in our limited knowledge of the complex physical, chemical and biological interactions that take place between the myriad of constituents found in any given landfill and the barrier material.

Protection barrier design has received the attention of many researchers in recent years, and is the general topic to which the present research work pertains.

1.2 - Scope and Objectives

The most common types of materials employed in barrier construction are **clays** and **synthetic geomembranes**, often used together to provide double protection. Spray-on asphalt and hydraulic asphalt concrete are also employed in certain cases (Rowe, 1988). In this study, only clays were considered.

In order to function properly as a protection barrier, the clay must have specific physical - or geotechnical - characteristics (e.g.: low hydraulic conductivity, sufficient shear strength and cohesion, etc.), as well as specific chemical characteristics (e.g., high activity, high cation exchange capacity, high buffering capacity, etc.). These characteristics determine whether the barrier material is 'compatible' with the type of waste leachate likely to be generated in a landfill. The structure[1] of the barrier

---

[1] The term "structure" of a soil encompasses the combined effects of fabric (macro or micro), composition, and interparticle forces.

material must not be *altered* significantly when it interacts with the leachate. In other words, their interaction must not cause any major *internal rupture* that would eventually lead to an increased leaching of contaminants from the protected site. In geotechnical terms, such leaching results from an increase in the hydraulic conductivity[2] of the material.

Internal rupture is a term which designates: 1) changes in the interlayer spacing between particles (due, for example, to the collapse of the electric double layer surrounding clay particles, or cracking); 2) changes in the spacial arrangement of groups of particles (due, for example, to the removal of existing bonds); and 3) changes in the equilibrium of forces that define the structure.

Among other tests, the physical characteristics of the clay barrier material are evaluated by obtaining the Atterberg limits and by conducting permeability tests. The chemical characteristics, or retention capability, is accessed by conducting chemical analyses with the samples extruded from the permeameters, and with the leachate collected.

Despite the importance of a proper evaluation of the long term integrity and effectiveness of the engineered clay liner, common regulatory requirements generally establish an upper limiting value for the **coefficient of hydraulic permeability** (***k***) of 10^{-7} cm/s (Zimmie, 1981; Harrop-Williams, 1985; Eklund, 1985; etc.). These pay little or no attention to the many mechanisms of contaminant-clay interactions which

---

[2] The terms: coefficient of hydraulic permeability, coefficient of permeability, hydraulic permeability, and *k*-value will be used indistinctively in this text.

are responsible for the attenuation (or accumulation) of contaminants. How k will respond to these interactions and attenuation mechanisms, and how it can be altered with time are quite often overlooked.

In light of the above, the main questions that led to the development of the present research were:

1) how and to what extent do the contact between contaminants and barrier materials affect the hydraulic conductivity (or hydraulic permeability) of the materials ?
2) how and to what extent is the hydraulic permeability affected by the technique (including the apparatus) used to measure it ?
3) how and to what extent are the contaminants retained by the barrier material ?
4) what type of interactions take place, and what are the key elements interacting ?

Compatibility studies must take into consideration: a) the main contaminants present in landfills that will be either reclaimed or constructed; b) the various materials that can operate as protection barriers; and c) the interactions (rate and dominance) between contaminants and the materials. Depending on certain conditions and types of waste leachate involved, the complexity of the problem may

become overwhelming, and cannot be tackled in one single research program, requiring the combined efforts of many scientists.

With this in mind, this work has attempted to contribute to the solution of the overall problem of safe landfilling of hazardous wastes. **It is proposed here to analyze the compatibility of clay soils with heavy metal leachate**, in terms of:

1) **possible changes in the measured coefficient of hydraulic permeability of a clay due to leaching of concentrated heavy metal solutions; and**
2) **the capacity of the compacted clays to retain the heavy metals: how and how much.**

To address these questions, two clay soils and two heavy metals were selected and the physics and chemistry of soil-contaminant interaction (compatibility) were examined in light of some laboratory experimental results, and of the theories related to the subject.

As can be seen in the scheme presented in Figure 1.1, the experimental work involved mainly: 1) the characterization of the soils in terms of their mineralogical and physico-chemical composition; 2) the performance of laboratory permeability tests using two different apparatuses: a rigid-wall and a flexible-wall cell; and 3) chemical analyses of both the leachate recuperated and of the soil samples. The results of these analyses were interpreted in light of the various models, principles and theories commonly employed in geotechnology and in surface chemistry (e.g.:

Gouy-Chapman's and DLVO diffuse double-layer theories; the Donnan principle applied to cation exchange; the Freundlich model of sorption behaviour, etc.).

1.3 - Statement of Originality

The most important contributions of this research work are presented below.

1.3.1 - Adsorption by Compacted Samples

The partitioning of contaminants between the solid and liquid phases is an important component in the control of contaminant migration through porous media.

In this research, the use of **adsorption characteristics curves of compacted materials** is introduced, and a technique to determine them is proposed. This technique makes use of: 1) the results of chemical analyses of compacted samples after they have been permeated with contaminant solutions; and 2) classical partitioning models. The adsorption characteristic curve of a compacted material, which is a more realistic approach in the evaluation of the partitioning of contaminants between the solid and liquid phases in clay barrier systems, is then compared to the adsorption isotherm of the same material (obtained with soil suspensions).

At certain points, and due to the limited number of results, the subject had to be analyzed more qualitatively than quantitatively. A brief discussion about the limitations of adsorption isotherms is presented in Chapter 2.

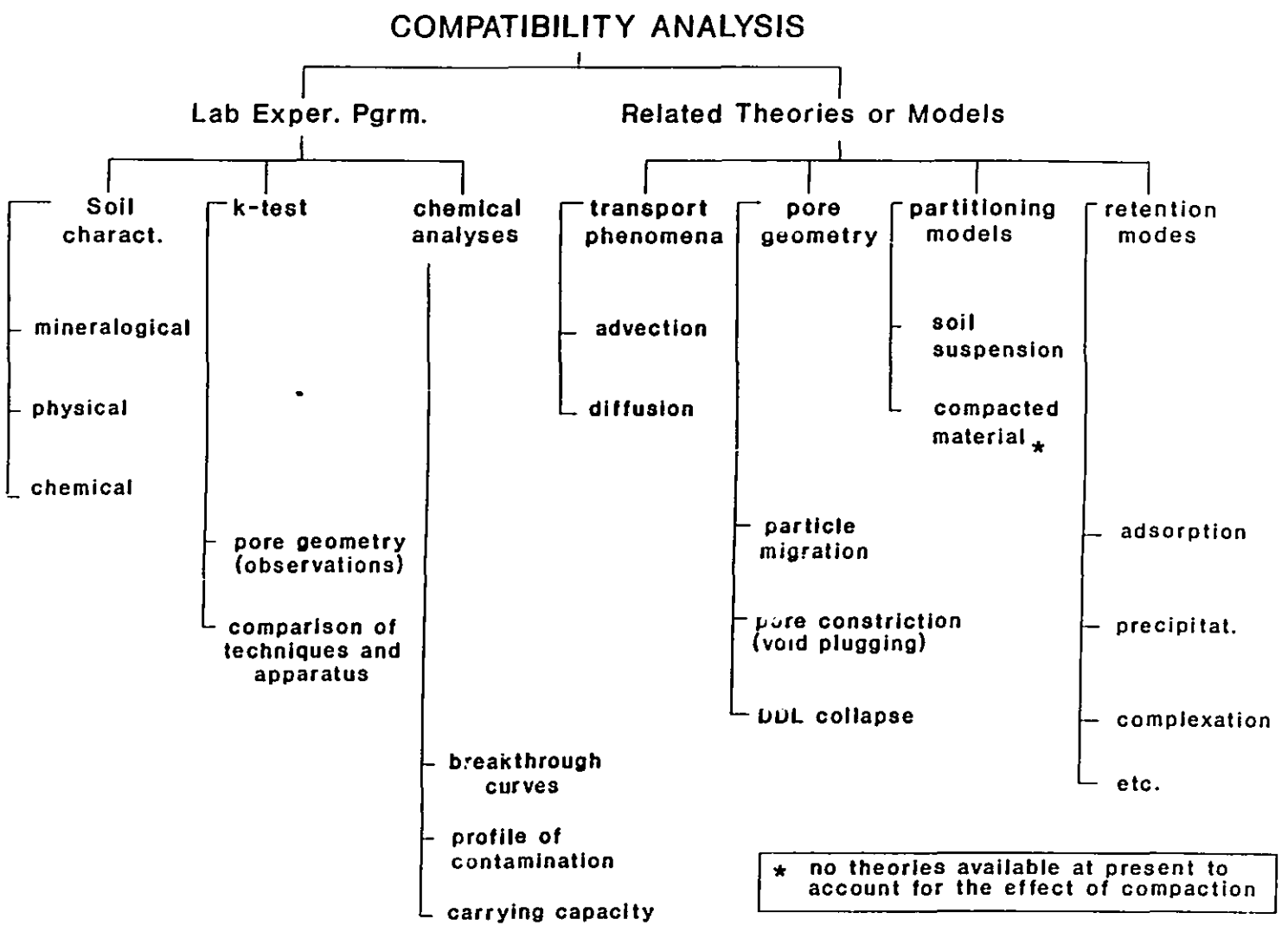

Figure 1.1 - General Scheme of the Present Study

1.3.2 - Permeameter Performance

Although this particular subject is not an original one, it continues to be of great concern in environmental geotechnology (Dunn, 1983; Daniel et al, 1985; Madsen and Mitchell, 1989; etc.).

The performance of the two most common types of permeameters - the triaxial and the consolidation cells - were compared in an original fashion. Previous studies have been concerned mainly with the ability of a certain apparatus to give the 'correct' coefficient of hydraulic permeability of the soils (considering all the parameters that affect it). This study goes a step further and also considers the results of chemical analyses obtained from both the samples extruded and the leachate collected. The initial testing conditions were maintained as similar as possible for a better comparison of performances.

1.3.3 - Permeability and Adsorption

The performance of permeability tests and chemical analyses of both leachate recuperated and soil samples are crucial parts of a complete compatibility analysis. Both were conducted in the present work aiming at a better understanding of the basic phenomena related to contaminant migration and retention. Special importance was given to the identification of adsorption modes (precipitation, low affinity and

high affinity types of adsorption). The results of this two phase study is an important step to answering the four questions mentioned previously.

1.4 - Organization of the Thesis

The thesis consists of 5 chapters and 7 appendices, the contents of which are as follows:

Chapter 1 - Introduction: the statement of the problem, the scope and objectives of the thesis, and the statement of originality are presented;

Chapter 2 - a **review** of the relevant **literature** on compatibility studies: permeability testing, and heavy metal retention;

Chapter 3 - presentation of the equipment, **materials and methods** used.

Chapter 4 - **interpretation of the results** obtained from permeability testing, and subsequent chemical analyses of the samples. In the former, the various parameters influencing permeability measurement are analyzed; in the latter, the results of the analyses with both compacted samples and leachate collected are presented and discussed. In order to help in the interpretation of the chemical analyses and to support the results, ion mass balances were calculated for several tests;

Chapter 5 - a summary of the main **conclusions** of this research work is presented, and a few suggestions for further research are proposed. A personal statement concerning the overall problems of ground water protection closes the present dissertation;

Appendix A - X-ray patterns and details of the procedure used to obtain them;

Appendix B - laboratory sheets with the results of some geotechnical tests performed with the two materials;

Appendix C - description of the procedure used to obtain the CEC of the materials;

Appendix D - details of calculation of *Pb* mass balances;

Appendix E - details of the methodology for sample analysis after leaching with heavy metal solutions;

Appendix F - presentation in tabulated form of: 1) the main physical characteristics of all samples tested in the triaxial cell, before and after permeability testing; 2) all permeability test results; 3) all mass balance calculations.

Appendix G - 1) background on the theory related to adsorption on to charged surfaces, with special emphasis on high affinity types of adsorption; 2) calculation of the theoretical amounts adsorbed in the Stern layer and Gouy diffuse layer (soil suspension), and comparison with experimental data (batch equilibrium tests).

CHAPTER 2

LITERATURE REVIEW

"... all kinds of arguments may be relevant.
A typical procedure is to examine whether our
theories are consistent with our observations."

K. Popper, in "Conjectures and Refutations",
Routledge, London, 1969

Three subjects of interest in environmental geotechnology are addressed in the present chapter:

1) compatibility studies are reviewed focusing on how they are perceived and performed;
2) the development of laboratory permeability tests and the main points of concern related to choice of apparatus and testing procedure are reviewed;
3) the most common heavy metal retention modes are identified and appropriate definitions involving adsorption onto charged surfaces are given. The use (and misuse) of partitioning coefficients (partitioning of contaminants between the solid and liquid phases) are revised and its use in the case of compacted material is criticized.

A brief review about contaminant transport modelling is presented as an introduction to the topics of permeability testing and heavy metal retention. In this fashion, the importance of permeability and retention is evidenced in terms of the need to develop or perfect laboratory (and field) techniques to obtain reliable parameters to apply to the models.

2.1 - Compatibility Studies

With the advent of engineered clay barriers for ground water protection in hazardous waste landfills, there has been an increased interest in clay-leachate compatibility[1] analyses in contaminant migration studies.

By and large, the compatibility of clay barriers with leachate is generally evaluated only in respect to changes in the coefficient of hydraulic permeability (k) of the clay, on the assumption that it reflects changes in the index properties and/or in the internal structure of the soil. If little or no change is observed during permeability testing, and if the k value is below the usual 10^{-7} cm/s established by most regulatory agencies, the clay liner may be eventually considered satisfactory. Here are a few examples:

Alther et al (1985) studied the influence of inorganic permeants on the permeability of bentonite. They concluded that, depending on the nature of the ions

[1] See explanation about the term 'compatibility' in Section 1.2.

in the solution permeated, there was some significant variations in the coefficient of hydraulic permeability of the bentonite.

Lentz et al (1985) investigated the effect of both acidic and caustic permeants on the *k* value of kaolinite and kaolinite-bentonite mixtures. Only at very high pH did the caustic permeant alter the hydraulic conductivity of their test soils. The authors took the care to mention that "future reports of permeability changes should give as much detail as possible about the chemistry and mineralogy of the soil studied." They also suggested "that research is needed into possible reactions which could be induced within the soil pores to create favourable changes in permeability."

Acar et al (1985) used non-polar and polar organic fluids as permeants during permeability tests with kaolinite. They observed significant changes in the *k* value only when some concentrated solutions were percolated. For all dilute organic solutions and some concentrated ones, the coefficient of hydraulic permeability remained unaltered. They explained the variations in flow characteristics "by differences in the surface forces of interaction due to changes in the chemical properties of the pore fluid."

Bowders and Daniel (1987) obtained similar results with dilute organics percolated through kaolinite and an illite-chlorite mixture.

Eklund (1985) compared the effects of water and waste leachate on the performance of soil liners, by the observation of possible changes in the coefficient of hydraulic permeability. They concluded that the barrier materials were "effective

in containing the ... leachate", because the permeability values were lower than 10^{-7} cm/s.

Yong et al (1985) studied the effects of leaching of contaminated solutions on the strength and integrity of a natural clay from Matagami, Quebec, during creep (stress - strain tests). Their results showed that, depending on the type of leachate, there may be fabric/structure reinforcement or degradation, and changes in the relationships between soil particles and the pore fluid.

Bowders et al (1986) suggested the determination of the index properties of the soil prior to permeability testing in compatibility analyses. "If the leachate does not affect the index properties of the soil, it is not likely to affect the permeability."

Peirce et al (1987) analyzed the effect of selected inorganic leachate on the permeability of three natural clays. In order to assess the long term compatibility between clay and leachate, they permeated as many as 50 pore volumes of the chemicals through the samples. Only small changes were observed, even at rather high concentrations of nickel nitrate, which the authors expected to cause significant changes in the measure k value.

Quigley et al (1988) assessed the compatibility between the Sarnia brown and grey clays and domestic waste leachate by means of permeability tests. According to the authors, these clays seemed compatible to the leachate, "at least with respect with hydraulic conductivity".

Storey and Peirce (1989) evaluated the impact of methanol solutions at various concentrations on the hydraulic permeability of an illitic clay. The compatibility

analysis was complemented with: the determination of the Atterberg limits; particle settling tests; and electrophoretic mobility studies. These were used to determine the effects of changing methanol concentrations on clay particle behaviour.

Budhu et al (1991) conducted a series of consolidation tests with three different types of clays, and calculated the coefficient of hydraulic permeability based on the consolidation and compressibility coefficients (c_v and a_v, respectively) obtained. Their samples were prepared by mixing the dry material with organic fluids. They reported a correlation established between dielectric constants and observed changes in permeability.

It is important to note that, in most of the works mentioned above, there is a clear concern about the effects of the testing equipment and technique on the results obtained. This aspect of a compatibility study was also tackled in this research program.

In view of the above, it is clear that the concept of compatibility analysis has not reached consensus yet, i.e., the analysis of the impact of leachate on the geotechnical characteristics of compacted clay soils is not a closed issue.

In fact, scientists have been devoting a great effort to the development of more effective techniques for chemical analyses of test samples and leachate recuperated during permeability tests (or leaching columns). They can serve as powerful tools to help in the assessment of: a) the long term capability of the clay to retain contaminants (Warith, 1987); b) the long term stability of the soil in contact with the

leachate (Yong et al, 1985); and c) the main mechanisms of retention involved (Alammawi, 1988).

Indeed, the quest of the 'ideal' permeameter, and the development of more sophisticated contaminant transport models have received considerable more attention than the study and understanding of retention mechanisms. A qualitative evaluation of the main retention mechanisms, associated with the testing conditions of this research work, is presented during the interpretation of results.

2.2 - Parameters for Modelling

Several authors have discussed over the years the various aspects of contaminant transport and retention through porous media. The many details related to the **advective** transport of pollutants (including the determination of hydraulic permeabilities), as well as their **diffusive** transport (hydrodynamic dispersion and molecular diffusion) have been the subject of numerous recent theses and articles (e.g.: Goodall, 1975; Boynton, 1983; Dunn, 1983; Warith, 1987; Nobre, 1987; Shackelford, 1988, Weber, 1991, etc.; Crooks and Quigley, 1984; Dunn and Mitchell, 1984; Quigley et al a,b, 1987; Yong and Samani, 1988; Yanful et al, 1988; Rowe et al, 1988; Barone et al, 1989; Yanful et al, 1990; Shakelford and Daniel, 1991; Yong et al, 1991; just to mention a few ones).

The **retention** of contaminants has received increased attention from researchers in environmental geotechnology, who have been borrowing from soil sciences not only the theories and concepts developed about the matter (e.g.: double layer theory), but also the techniques to obtain the relevant parameters used to explain retention phenomena during contaminant transport (e.g.: cation exchange capacity, distribution coefficients, buffering capacity, etc.)

In order to predict contaminant migration, a series of advection/dispersion/diffusion models have been proposed and/or adapted, most of them based on the law of conservation of mass and Fick's first law (Freeze and Cherry, 1979).

Ogata (1970) made some modifications to a model early proposed by Ogata and Banks (1961) for granular medium; he included a source-sink term in the advection/dispersion/diffusion equation to account for mass transfer between the solid and liquid phases (**adsorption**). Its one-dimensional formulation is presented in Equation (1.2).

$$D_l \frac{\partial^2 C}{\partial l^2} - \bar{v}_l \frac{\partial C}{\partial l} + \frac{\rho_b}{n} \frac{\partial S}{\partial t} = \frac{\partial C}{\partial t} \qquad (1.2)$$

where :

ρ_b = bulk mass density [M/L^3];

n = porosity;

S ≡ mass of chemical constituent adsorbed to the solid phase of the porous medium per mass of solids [M/M];

C ≡ solute concentration [M/L^3];

D_l ≡ coefficient of hydrodynamic dispersion;

v_l ≡ average linear velocity along the flow line;

l ≡ coordinate direction along the flowline; and

t ≡ time.

This model, or variations of it, have been widely used in environmental geotechnology with different degrees of complexity (Crooks and Quigley, 1984; Desaulniers et al, 1984; Quigley et al, 1987 a,b; Yong and Samani, 1987 and 1988; Rowe, 1988; Rowe et al, 1988; Barone et al, 1989; Yanful et al, 1990; Shakelford and Daniel, 1991), e.g.:

- one- bi- or three-dimensional form;
- assumption of constant or variable diffusion/dispersion coefficients and porosity (Yong and Samani, 1988);
- consideration or not of chemico-osmotic effects (Yong and Samani, 1988);
- inclusion or not of geochemical models to account for precipitation, ion exchange, sorption (adsorption/desorption);
- etc.

Generalized equations have also been proposed (Nobre, 1987; van Genuchten, 1978; Boast, 1973); new terms were added to Equation (1.2) in order to describe: a) radioactive decay; b) biological activity; c) source/sink of fluid into/out of the system; etc.

Mangold and Tsang (1991) made an excellent summary of most hydrological and hydrogeochemical models (codes) for subsurface fluid flow and solute transport. They presented a criterion for selection of the most adequate model, as well as an explanation of their main characteristics.

Independent of the model and its degree of complexity, there remains the problem of finding reliable parameters to feed them. Experimental techniques have to be developed or perfected, either in the field or in the laboratory, in order to obtain such parameters.

In this research work, the interest is placed in the advective and retentive (adsorptive) characteristics of contaminant migration. However, the importance of diffusion and osmotic flow in the study of contaminant migration must not be neglected. In fact, at low advective velocities (associated with a coefficient of hydraulic permeability lower than 10^{-7} cm/s), the principal mechanism of contaminant transport is likely to be diffusion (Cheung et al, 1985). Flow through porous media can also be partly due to differences in solute concentration between 2 points in a clay soil system (Olsen, 1972). The importance of osmotic flow increases with increasing compaction pressures and decreasing water content (Olsen, 1972). The

diffusive and osmotic characteristics of contaminant migration are not analyzed in this thesis.

Velocity is the parameter which describes advective flow, and it can be evaluated by performing permeability tests. The adsorptive capacity is often expressed in terms of distribution coefficients, which are obtained from adsorption isotherms. In the following sections it is presented a brief review of the pertinent literature related to: 1) permeability testing; and 2) the retention characteristics of charged surfaces (adsorption isotherms and distribution coefficients).

2.3 - Permeability Testing

Before the awakening of the environmental problem, the main engineering problems related to permeability testing were: the stability of slopes, seepage, and the settlement of clays (Lambe, 1958; Mitchell et al, 1965).

More recently, however, the attention has been diverted to field and laboratory permeability testing of compacted clays, used in the containment of toxic wastes. Indeed, an impressive number of technical articles have been published about this topic in the past 10 years, e.g.: most papers included in the special publications STP 746 (1981) and 874 (1985) from ASTM (the former includes a state of the art review on hydraulic conductivity measurement by Olson and Daniel, whereas several papers in STP 874 are dedicated to the debate over the best equipment for permeability

measurement); Madsen and Mitchell (1989); etc. Several others were cited in the preceding sections.

It must be remarked the increasing interest in the effect of different leachate in the final results obtained.

According to existing regulations, most of the responsibility for the quality of a liner is attributed to the coefficient of hydraulic permeability of the clay barrier material. According to Zimmie (1981), "[permeability is] probably the most important hydrogeologic parameter in a hazardous waste siting study...", and "estimates of flow quantities and patterns can only be as accurate as the value of hydraulic conductivity used to make them" (Dunn and Mitchell, 1984).

Thus, the development (or perfecting) of reliable methodologies to obtain k, either in the laboratory or in the field, is one of the most serious challenges environmental geotechnologists have been facing.

Hydraulic conductivity is one of the most difficult soil parameters to measure accurately, because of the numerous variables influencing it, including:

- the molding water content, density, method of compaction, and effort of compaction (they all affect the structure of the compacted soil, which also affects k);

- the hydraulic gradient applied;
- the size and distribution of clods;
- the type and concentration of electrolytes in the soil-water;
- the type of permeameter;
- etc. (Lambe, 1958, Mitchell et al, 1965; Dunn, 1983; Dunn and Mitchell, 1984; Daniel et al, 1985; Boynton and Daniel, 1986; Madsen and Mitchell, 1989; Benson and Daniel, 1990; Yong et al, 1991; etc.).

It is not our purpose in this chapter either to review the details concerning permeability testing, or to discuss about the advantages and disadvantages of experimental techniques. The bibliography cited above can be of better service. It needs only to be remarked that the controversy related both the validity of laboratory permeability results (Mitchell and Younger, 1967) and the choice of the most adequate permeameter (e.g.: Daniel et al, 1985; Madsen and Mitchell, 1989) is still very actual, and involves discussions about problems related to: side-wall leakage (e.g.: Edil and Erickson, 1985; Acar et al, 1985), saturation procedures (e.g.: Dunn, 1983; Dunn and Mitchell, 1984; Daniel et al, 1985; Yong et al, 1991), development of desiccation cracks during testing (Bowders et al, 1986); application of high confining pressures (Peirce et al, 1986; Boynton, 1983, in Daniel et al, 1985); application of high hydraulic gradients to accelerate tests (Yong et al, 1991), etc.

2.4 - Heavy Metal Retention

Retention by charged surfaces involves several chemical processes. Of those, ion exchange and precipitation seem to be the most common ones; or rather, the most considered ones in environmental geotechnology. Quite often, the term **sorption** (*ad*sorption and *de*sorption) is used in the technical literature to designate the two phenomena together. Sorption can also include specific and high affinity types of retention (defined later in this chapter). Other retention phenomena, e.g.: diffusion into the lattice, are not discussed in the present text.

The retention of contaminants has received increased attention from environmental geotechnologists, who are aiming at a better understanding of the retention capability of clay soils. As evidenced by the results obtained by Alammawi (1988), the understanding of retention mechanisms can give a better idea of how 'tightly held' the adsorbed species are. In other words, it is possible to evaluate whether or not the adsorbed ion species will remain adsorbed to the particle surface indefinitely - due to Coulomb and short range forces acting in the Stern layer (Kruyt, 1952; Yong and Mohamed, 1991) - or if they will be desorbed, in a situation where a different type of leachate comes in contact with the soil particles.

The rate of retention (adsorption/desorption) term ($\delta S/\delta t$) of Equation (1.2) is often expressed in the form of Equation (1.3):

$$-\frac{\partial S}{\partial t} = \frac{\partial S}{\partial C} \cdot \frac{\partial C}{\partial t} \qquad (1.3)$$

where $\delta S/\delta C$ represents the partitioning of the contaminant between the solid and liquid phases.

The partitioning is often quantified by conducting batch equilibrium tests, followed by the construction of an adsorption isotherm (often the 'Freundlich isotherm') of the material to the specific contaminant species. The slope of the linear portion sometimes observed in the low concentration range (initial portion) of the adsorption isotherm is often used to represent the partitioning, as widely recommended in the geotechnical literature (e.g.: Freeze and Cherry, 1979; Bowders et al, 1986), and by environmental regulatory agencies (EPA, 1987). The slope of the adsorption isotherm is often designated as the partition, or distribution, coefficient K_d (or K_p).

Rowe et al (1988) describe another technique to obtain the distribution coefficient. The results of a modified column test are used to adjust the diffusion coefficient and K_d. Their model also assumed linear sorption, i.e., constant K_d, and reversible sorption.

The hypothesis of a constant K_d (the slope of the 'linear' Freundlich isotherm), and reversible sorption/desorption exchange reactions to describe the partitioning of contaminants between the solid and liquid phases (Freeze and Cherry, 1979; Desaulniers et al, 1981; Bowders et al, 1986; Quigley et al, 1987b; Rowe et al, 1988; Barone

et al, 1988; Barone et al, 1989; etc.) are two of the most serious limitations of common transport models employed in environmental geotechnology.

The consideration of reversible reactions implies the acceptance that only low-affinity physi-sorption, or non-specific adsorption[2], takes place in heavy metal retention phenomena, without paying much attention to high affinity types of physi-sorption, or specific adsorption[3], and to chemi-sorption[4].

The assumption of linearity of the Freundlich isotherm, i.e., a constant K_d, is a very comfortable attitude that does not reflect reality with exactness (Molinari, 1986), particularly when one is dealing with heavily contaminated sites (Rowe et al, 1988; Shackelford and Daniel, 1991). In some cases, the concentration of heavy metals in landfill leachate may be in the hundreds of parts per million (Clark and Piskin, 1977; Moore and Luoma, 1990). At such high concentrations adsorption isotherms are no longer straight lines and the assumption of the contrary can lead to an erroneous evaluation of the retention capability of a material being considered as a protection barrier.

---

[2] Adsorption in the DDL involving only electrostatic forces (Greenland and Hayes, 1978).

[3] Adsorption in the Inner Helmholtz Plane - IHP - and in the Outer Helmholtz Plane, where coulombic, ion-dipole, and dipole-dipole interactions take place (Yong and Mohamed, 1991; Alammawi, 1988). Higher energies of adsorption are involved as the ion becomes partially dehydrated close to the solid surface (Greenland and Hayes, 1978).

[4] Involves valence forces acting in coordinate covalent bonds, and electron transfers (Hayward and Trapnell, 1964).

Although non-linear adsorption isotherms have been considered and used by chemists (surface chemistry) and soil scientists for quite a long time now, most contaminant transport and retention models still make use of **linear** adsorption isotherms to describe the partitioning. Only very recently have geotechnical literature mentioned the necessity of using non-linear adsorption isotherms to describe more realistically the partitioning of contaminants between the waste leachate and the soil particles of a clay liner material (e.g.: Yong et al, 1991; Shackelford and Daniel, 1991).

In fact, even the use of non-linear adsorption isotherms is not sufficient to describe this partitioning. Liners are made of compacted clay material, and compaction causes a reduction of the 'effective' exposed surface area of the material (Yong et al, 1991), which is not the case of a soil in suspension, where all particle surfaces are 'available' for exchange to take place. This may lead to an improper evaluation of the effective capability of the compacted soil to retain heavy metals (Yong et al, 1991).

This subject is discussed in further detail in light of the results obtained (Chapter 4, Section 4.2).

Another point of concern is related to the choice of the appropriate isotherm to describe the partitioning. In the majority of the cases in environmental geotechnology, the Freundlich model is used. However, many other models - e.g.: Langmuir's,

another 'common' model - can eventually better describe the partitioning for specific cases.

The literature related to adsorption models is quite extensive. Although the main characteristics, advantages, disadvantages, and limitations of each are not discussed here, it is worthwhile referring to some of the works we came across:

- Helfferich (1962): basic literature on ion exchange and ion exchangers;
- Kipling (1965): basic literature about different types of adsorption: liquid on liquid, liquid on solid, gas on solid, etc.;
- Griffin and Shimp (1976): shows a straightforward example of the use of the Langmuir model;
- Gregg and Sing (1982): mostly devoted to the B.E.T. general isotherm;
- Kinniburgh (1986): mostly Freundlich and Langmuir with different degrees of sophistication;
- Harter (1986): a very interesting collection of articles, dating from last century to the last decade, dealing with the evolution of concepts of adsorption.

2.5 - General Remarks

From the present review, a few points may be noted. One is related to the increasing importance attributed to chemical testing of both test samples and leachate in compatibility analysis. This is a clear recognition that not only the observation of changes in the physical parameter *coefficient of hydraulic permeability* are of importance in the evaluation of clay-leachate interactions.

A second point to be noted is that the search for the 'ideal' permeameter and permeability testing procedure is not a closed issue yet, although most researchers are not focusing on it now as much as they used to in the early and mid 1980's (Weber, 1991). Lately, the need to well describe the soil's physico-chemical characteristics, as well as the leachate's chemical characteristics, has become more and more important in the evaluation of clay-leachate compatibility and long term stability of clay barriers.

The latter is precisely the next point to be noted: the long term structural stability of clays in the presence of leachate must be viewed also in terms of the retention mechanisms involved. This is certainly one of the most promising topics environmental geotechnologists will have to address in the near future.

Another point to be remarked is related to the need of establishing testing procedures for chemical analyses of samples and leachate collected during permeability testing. As mentioned before, a procedure is suggested in the present research work.

Finally, it must be kept in mind one of the main goals of permeability testing and chemical analyses of samples and leachate: the prediction of seepage quantities and rates of plume advancement. If refined models are to be used for that purpose, the parameters used in them must reflect, as closely as possible, the reality.

CHAPTER 3

MATERIALS AND METHODS

"Experience is the name everyone gives to their mistakes."
Oscar Wilde

The various Sections in this chapter were organized in a sequence that reflects the order of evolution of the experimental work, as summarized in the scheme presented in Figure 3.1. Basically, the experimental work comprises: characterization of the materials, performance of constant head permeability tests, and chemical analyses of the leachate collected and of the samples extruded after the permeability tests.

Laboratory permeability tests were performed throughout the experimental phase of this research work using two types of soils, three types of permeants, and two types of permeameters.

One of the objectives of this research work was to compare the performance of two types of permeameters usually employed in the geotechnical practice, and the results of permeability tests obtained with them. For that purpose flexible wall and rigid wall permeameters were used. The initial testing conditions were as similar as possible for both permeameters; this included: (1) type of soil; (2) type of

contaminant and concentration range in the solution to be flushed; (3) initial water content of soil samples; (4) dry density; (5) the method and energy of compaction; (6) the saturation procedure (in some cases only); (7) hydraulic gradients applied; and (8) the same type of chemical analyses of the samples extruded and leachate collected.

Their performance will also be judged in light of the results of the chemical analyses, i.e., by comparing the retention patterns of samples tested with each of the permeameters for the same set of conditions mentioned above.

Details concerning tests performed with the rigid wall permeameter will be omitted[1], except when they serve the purpose of comparison between the two apparatuses (one of the objectives of this research work).

3.1 - Materials

The two soils chosen, a kaolinitic clay and a mixture of sand and bentonite, have different physico-chemical properties (Tables 3.1 and 3.2), which affects heavy metal migration. Water and two heavy metal solutions were used as permeants. The choice of the two heavy metals (lead and zinc) is related to their different mobility

[1] All the credits for tests executed with the consolidation cell must be given to Lawrence Weber, a graduate student colleague who completed his M. Eng. program in 1991. The reader is referred to Weber (1991) for additional information on the experimental procedures concerning tests with the consolidation cell.

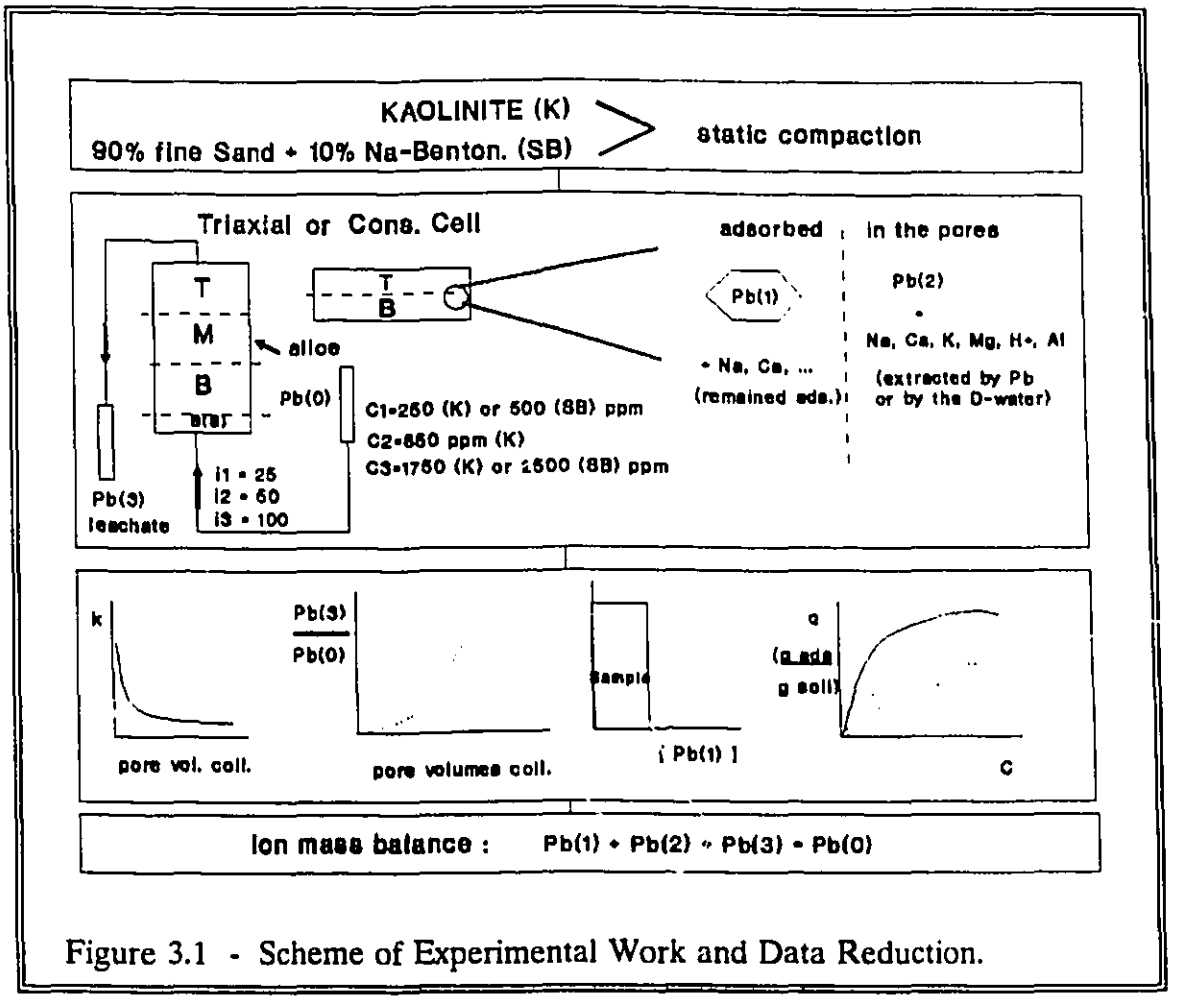

Figure 3.1 - Scheme of Experimental Work and Data Reduction.

in soils (Phadungchewit, 1990), to the different selective affinity of clay minerals for these two metals (Mitchell, 1964 and Soong, 1974; in Forstner and Wittmann, 1981) and to the fact that these two heavy metals are generally present in hazardous waste leachates.

As compared to *Pb*, *Zn* is more mobile and have a lower selectivity for charged surfaces (Farrah and Pickering, 1977; Phadungchewit, 1990). A higher mobility and lower selectivity implies that the contaminant will not be retained as

effectively by the clay particles, thus the interest in studying these two heavy metals. This subject is addressed in more detail in Section 4.2.5.2.

3.1.1 - Soils

A kaolinitic clay, Hydrite PX (Georgia Kaolin Co.) and a mixture of 90% fine to medium sand (Silica 40) and 10% Na-bentonite[2] were tested. Typical sand/bentonite (**S/B**) liners in Quebec have bentonite contents in the 5-15% range (Chapuis, 1990). Although kaolinite is rarely used in environmental geotechnology practice as a barrier material, it has been studied and reported on extensively, thereby permitting one to compare results obtained from this study with other reported results.

X-ray diffraction results indicated very little amorphous materials and no quartz, smectites or organics in the kaolinitic soil. Trace amounts of feldspar and mica were present in the bentonite obtained from Avonlea Minerals Ind. of Saskatchewan. The X-ray patterns for both materials and details of the procedure used are found in Appendix A.

The geotechnical properties of both soils are presented in Table 3.1. The results of some preliminary characterization tests - liquid limits (**LL**), compaction curves, and grain size distribution of the kaolinite and Silica 40 sand - are presented

---

[2] *Na* is the predominant exchangeable cation of the bentonite, as indicated in Table 3.2.

Property	Kaolinite	Sand/Bentonite (90%/10%)
Liquid Limit (LL)	69.0%	355% (bentonite)
LL w/ 200 (or 500) ppm Pb-sol	70.5%	328% (bentonite)
LL w/ 1500 ppm Pb-sol	70.2	-
Plastic Limit (PL)	30.8	55% (bentonite)
Unified soil classif.	CH	CH
Specific gravity	2.6	2.66
Proctor Maximum dry density (kN/m^3)	13.1	17.2
Optimum moisture content	32.0%	16.0%
% clay size material (ASTM)	86.0%	10.0%
Specific surface area (m^2/g)	24.0	855 (Alawawi, 1988) (for bentonite only)
Diam. of sand grains (mm)	-	0.06 - 0.6

Table 3.1 - Geotechnical and Physical Properties of Kaolinite Hydrite PX and a Sand/Bentonite Mixture (90%/10%).

in Appendix B. The influence of one of the contaminant solutions in the LL of the two soils was verified. Changes in the Atterberg limits (e.g.: either lowering or increase of the LL) may be used as a first indicator of the effect of a liquid on a soil (Yong and Selig, 1961; Bowders and Daniel, 1987). A drastic change in the LL indicates that the structure of a compacted clay may be affected when it is in contact with the specific leachate.

As expected, the LL of the kaolinitic clay was not affected even by a highly concentrated lead solution. The slightly lower LL of the bentonite obtained with a

500 ppm *Pb*-solution (328%, as compared to 355% for distilled water) indicated that the structure of the bentonite clay may be affected during percolation of concentrated *Pb*-solutions.

In order to evaluate the dispersibility of the compacted sand/bentonite (**S/B**) material, a pinhole test was performed following the methodology described by Sherard et al (1976). The effluent had a 'milky' colour in the beginning of the test, soon passing to very clear. When the sample was taken out and sliced, it could be noticed that the 1.0 mm hole created by the needle had expanded to several millimetres. The need for a pinhole test appeared during the interpretation of some tests that are discussed in Section 4.1.2.1.

The chemical properties of kaolinite and bentonite are presented in Table 3.2. The cation exchange capacity (**CEC**) was determined using an adaptation of the ammonium acetate method as described in Black (1965; in Chhabra et al, 1975), which also gave origin to the EPA Method 9080 (EPA, 1986). The ammonium acetate method is "a reference to which other procedures are compared (Chhabra et al, 1975)."

The results obtained fall well within the range of reported values (Grim, 1968; Yong et al, 1986). Details of the procedure used to obtain and calculate the CEC are described in the Appendix C.

The CEC of kaolinite - a variable charge type of clay - arises from isomorphous substitution within the crystal lattice, and from hydroxylated edges at

Property	Kaolinite	Bentonite
soil pH (range of 3 tests)	4.3 - 4.7	8.6-8.8
Cation Exchange Capacity (meq/100g) index exchangeable cations :	7.00	109.0
Na^+	0.31	63.7
K^+	0.48	1.9
Ca^{++}	0.16	35.7
Mg^{++}	0.02	7.5
exchangeable H^+	2.86	-
exchangeable Al^{3+}	3.23	-
% by mass of: Al_2O_3	0.48	N.A.
Fe_2O_3 (Galvez, 1989)	0.00	N.A.
SiO_2	0.70	N.A.
carbonate content	N.A.	0.00
total amorphous content	1.18	N.A.
organic content (Galvez, 1989)	0.00	0.00

Table 3.2 - Chemical Properties of Kaolinite Hydrite PX and a Sand/Bentonite Mixture (90%/10%).

broken bonds (Uehara and Gillman, 1981). Due to the latter, it is pH dependent; in the acidic range H^+ and Al^{3+} become very important for the calculation of the total CEC (Grim, 1968). Also, at low pH, the *Al* is dissolved from the crystal structure and has the ability to replace index cations on the exchange sites (Duquette and Hendershot, 1987; Boland et al, 1980). In the present case, the ammonium

acetate solution was acidified to pH = 3.6 by the addition of acetic acid, thus the percentages of H^+ and Al^{3+} in the total CEC of the kaolinite are rather high, as can be seen in Table 3.2. The acidification was performed to increase its extracting capacity (Farrah and Pickering, 1978), and because the permeants were also acidified to this pH (see Section 3.1.3) and these acid conditions should prevail inside kaolinite samples.

For constant charge types of clays - like bentonite - the participation of these two ions in the total CEC is negligible. The exchange capacity arises mainly due to unbalanced charges in the structural unit of the clay that are balanced by adsorbed cations (Grim, 1968; Grim and Guven, 1978).

A Beckman Φ pH/ISE was employed for pH measurements.

The concentration of the various cations was obtained by atomic absorption spectrometry (**AAS**) with a GBC 902 Double Beam Atomic Absorption Spectrophotometer. The exchangeable H^+ was determined using an adaptation of the method described by Jackson (1967). The procedure is described in the Appendix C (Section C.11).

3.1.2 - Adsorption Isotherms

To complete the full characterization of the clays, the adsorption of *Pb* by the two materials was determined by constructing adsorption isotherms, or quan-

tity/intensity (Q/I) plots, as preferred by Barrow (1985), who advocates that the latter designation is a more appropriate nomenclature.

The use and importance of these and other isotherms in the practice of Environmental Geotechnology were discussed in detail in Section 2.4.

Batch equilibrium tests were performed following the procedure described by EPA (1987) (equivalent to the ASTM standards ES-10-85 and D4319, described in a simplified form in Bowders et al, 1986), in order to construct the materials' isotherms. Batch equilibrium tests may also be used to "obtain an estimate of how many pore volumes of flow will be necessary to achieve breakthrough of a constituent into the effluent liquid (Bowders et al., 1986)." Only a very rough estimate can actually be obtained (if any at all !), because the adsorption characteristics of compacted material are not the same as that of soils in a suspension. This is discussed in detail in Chapter 4 (Section 4.2.3).

Initially, different concentrations of lead solutions were prepared dissolving lead nitrate ($Pb(NO_3)_2$) in distilled water. Lead nitrate was chosen because it is very soluble. The pH was then adjusted to 3.6 for the reasons mentioned later in Section 3.1.3. For kaolinite, the concentrations were: 50, 250, 500, 1000, 1500, and 2000 ppm, and for S/B they were: 250, 500, 1000, 1500, 2000, and 3000 ppm.

For each concentration a suspension was prepared by mixing 4 g of soil with 40 ml of the concentrated *Pb* solutions in Nalgene tubes. The 10:1 liquid:solid ratio is recommended by EPA (1987) for batch equilibrium tests. Triplicates were prepared to ensure accuracy.

After mechanical shaking was left for 24 hours, the tubes were centrifuged and the supernatants collected. These supernatants and the blank solutions were then analyzed by atomic absorption for *Pb*.

The amount adsorbed/mass of soil (in grams/grams),*q*, was calculated for each value and plotted against the equilibrium concentrations, *C*, using the formula[3]:

$$q = \frac{(C_0 - C) \times V}{M} \qquad (3.1)$$

where: C_0 = concentration of blank *Pb* solution

V = volume of fluid (40 ml in this case);

M = dry mass of soil (4 g in this case);

V/M = 10 ml/g.

Since C_0 and C are expressed in ppm, a simple conversion was needed to present q in more appropriate units, i.e., grams of *Pb* adsorbed/grams of soil, using the following formula:

$$q = (C_0 - C) \times (10\ ml/g) \times (1 \times 10^{-5}\ g/ml) \qquad (3.2)$$

---

[3] the nomenclature **q** is widely used in the technical (soil science) literature to designate the amount adsorbed/mass of soil.

The adsorption isotherms for kaolinite and S/B are presented in Figures 3.2 and 3.3, respectively.

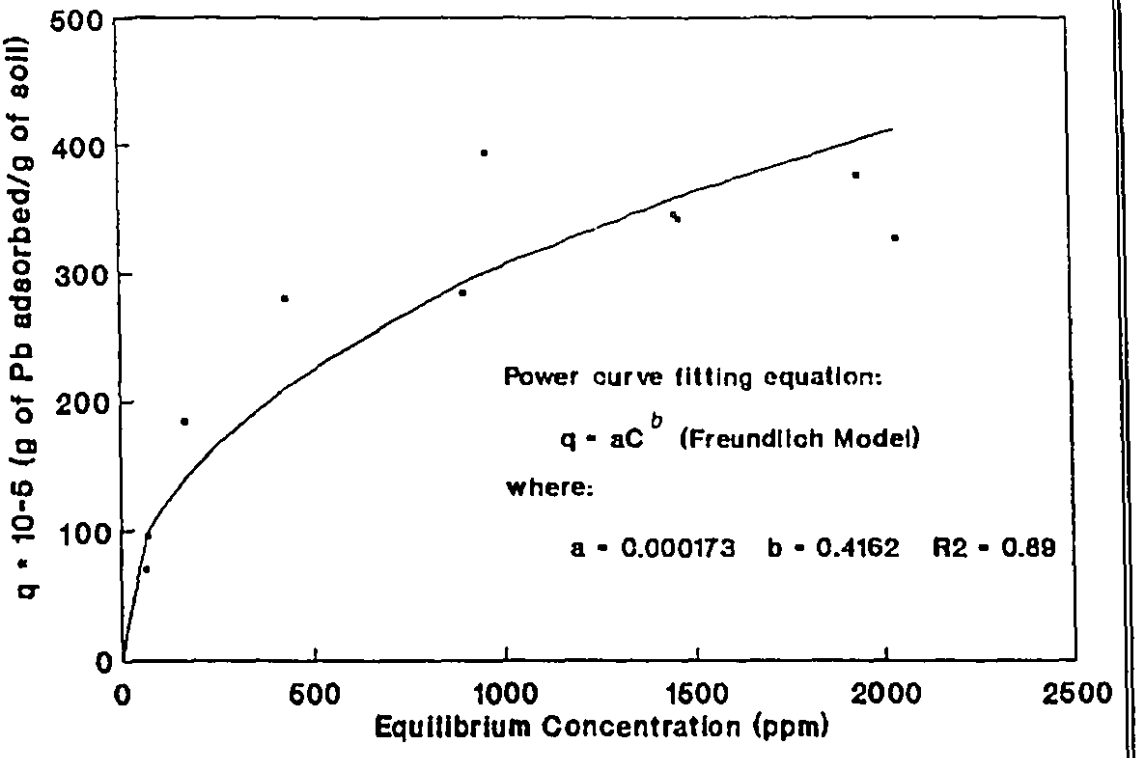

Figure 3.2 - Partitioning of Lead Between the Solid and Liquid Phases in a Kaolinite Suspension (Adsorption Isotherm).

The equations shown in the graphs of Figures 3.2 and 3.3 were obtained by power curve fitting using the Freundlich model: $y = kC^{1/p}$ (Helfferich, 1962). This particular model was selected mainly because it has been widely used in environmental geotechnology (Freeze and Cherry, 1979; Bowders et al, 1986; U.S. National

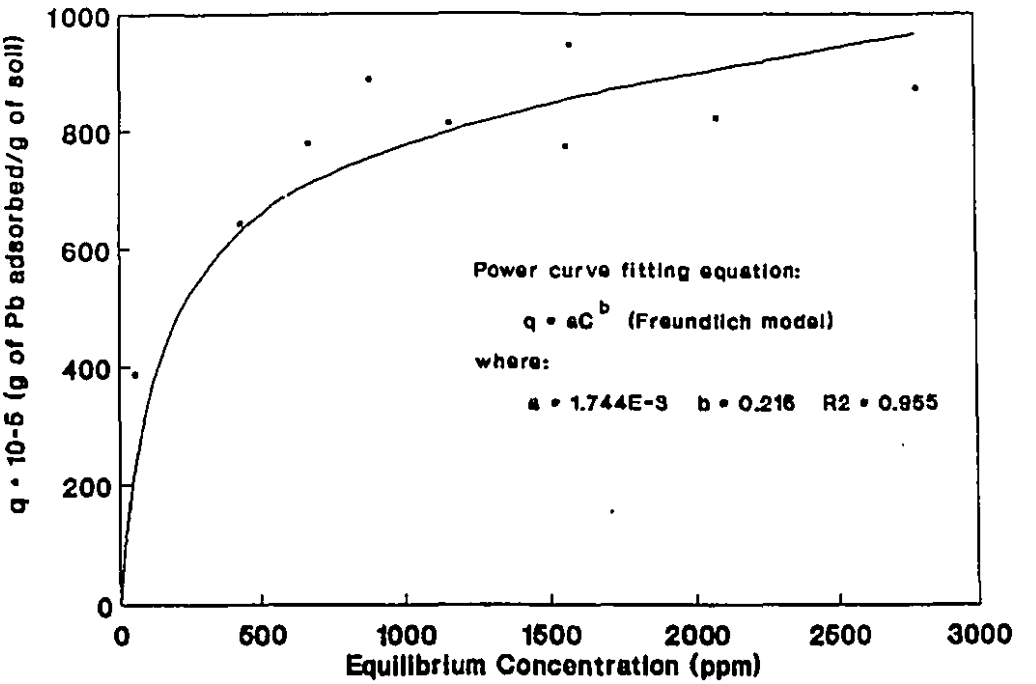

Figure 3.3 - Partitioning of Lead Between the Solid and Liquid Phases in a Sand/Bentonite (90%/10%) Suspension (Adsorption Isotherm).

Research Council, 1990) and "is one of the most extensively used in water and waste water treatment" (Sweeney et al, 1982). According to Hayward and Trapnell (1964), "the Freundlich isotherm is often obeyed over wide ranges of adsorbed amount". Other models, like Langmuir's can also be used with success to fit experimental data (Hayward and Trapnell, 1964).

From the isotherm data, the concentrations of lead solutions to be used in the experimental program were selected.

As a verification of the consistency of the results obtained, the maximum adsorption values of each curve were converted from g_{ads}/g_{soil} into *meq/100g* in order to compare them with the respective CEC's of the materials (obtained with the same acidified ammonium acetate solution). Equation (C.1) (Appendix C) had to be adapted to the volumes used during construction of the isotherms, i.e., 40 ml instead of 100 ml of ammonium acetate. Using the data presented in the Appendix F:

1) for kaolinite: $(C_0\text{-}C)_{max}$ = 393.4 ppm = 0.3934 g/l

$$q_{ads} = \frac{[g/l]\ x\ 40ml\ x\ 100g\ x\ 1000}{1000ml\ x\ 4g\ x\ \ equ.\ weight\ of\ Pb} = 3.8\ meq/100g$$

This value is 46% lower than the total CEC of the kaolinite (7.00 meq/100g). Two arguments can be resorted in order to explain this difference: 1) part of the exchangeable Al^{+++} may have not been displaced by the divalent *Pb*; and 2) the ammonium acetate may not be 100% efficient as extracting solution (Karamanos et al, 1976; Farrah and Pickering, 1977). Supposing 100% efficiency of the ammonium acetate and considering that no aluminum was displaced by lead, the contribution of Al^{+++} to the total CEC - 3.23 meq/100g - can be added up to the value found above - 3.8 meq/100g - and the difference is eliminated.

2) for S/B: $(C_0\text{-}C)_{max}$ = 947.2 ppm = 0.9472 g/l

$$q_{ads} = \frac{0.9472g/l \; x \; 40ml \; x \; 100g \; x \; 1000}{1000ml \; x \; 4g \; x \; equ. \; weight \; of \; Pb} = 9.14 \; meq/100g$$

The CEC of the mixture is approximately 109.0 x 10% = 10.9 meq/100g (the contribution of the fine sand is negligible), which differs from the maximum adsorption calculated above by only 16%. This difference can be attributed to minor experimental errors and, agair., to the fact that ammonium acetate may not be 100% efficient.

In another form of cross check, the present experimental results were compared to the theoretical quantities of *Pb* adsorbed by montmorillonite, as given by a modification of the DDL model discussed by Alammawi (1988) and Yong and Mohamed (1991). The background theory, references and calculations are presented in Appendix G.

3.1.3 - Permeants

Three types of permeants were used during the experimental program: distilled water, lead solutions at several concentrations, and one concentrated zinc solution. In this fashion, not only the influence of the type of permeant (contaminant), but also that of the concentration of the contaminant solution, on the calculated coefficient of hydraulic permeability is evaluated.

The greater affinity of clay minerals for *Pb*, as compared to *Zn* (Mitchell, 1964; Soong, 1974; both in Forstner and Wittmann, 1981; Farrah and Pickering, 1977; Phadungchewit, 1990) suggested the use of these two contaminants.

It is relevant to note that the concentrations of the two heavy metals (*Pb* and *Zn*) in very contaminated sites can be as high as the ones used in this research work (Moore and Luoma, 1990; Clark and Piskin, 1977). From the low 5 ppm of *Pb* existing in municipal landfill leachate (Cartwright, 1984; from various sources) to 695,000 ppm existing in the soil subjacent to a drum site in Miami (Singh et al, 1984) all concentrations can be found depending on the type of waste. Characteristic concentrations of *Zn* in leachate and domestic waste waters may vary from 1 to 1,000 ppm (Cartwright, 1984), and be as high as 11,000 ppm in very contaminated sites (Moore and Luoma, 1990).

Distilled Water

Distilled water was used to saturate the samples prior to leaching with the *Pb* or *Zn* solutions. In some cases (see description on saturation procedure later in this chapter), distilled water was actually flushed through kaolinite samples; this gave a reference permeability of the soil to water. The pH of the distilled water was in the range of 5.2 to 5.7.

Lead Solutions

As in the case of the adsorption isotherms, *Pb* solutions were made by mixing lead nitrate ($Pb(NO_3)_2$) and distilled water.

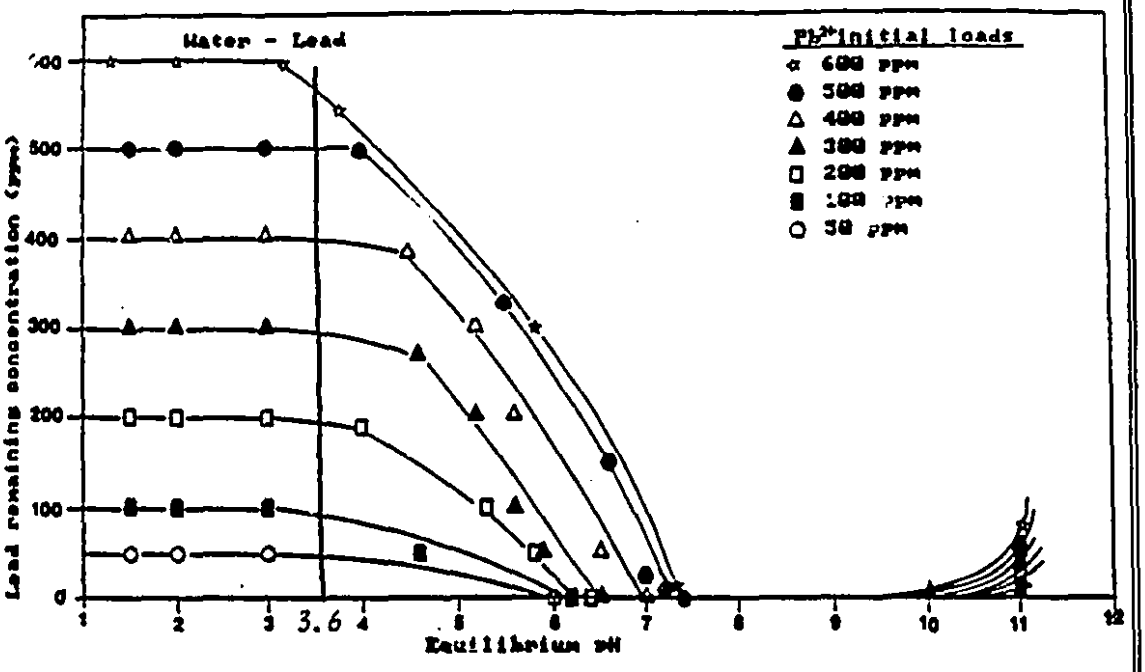

Figure 3.4 - Pb^{++} Solubility Curves for Different Initial Concentrations (from Galvez, 1989).

In order to keep an acidic environment inside the kaolinite samples, it was decided to lower the pH of the lead solution to 3.6 by the addition of nitric acid, for several reasons:

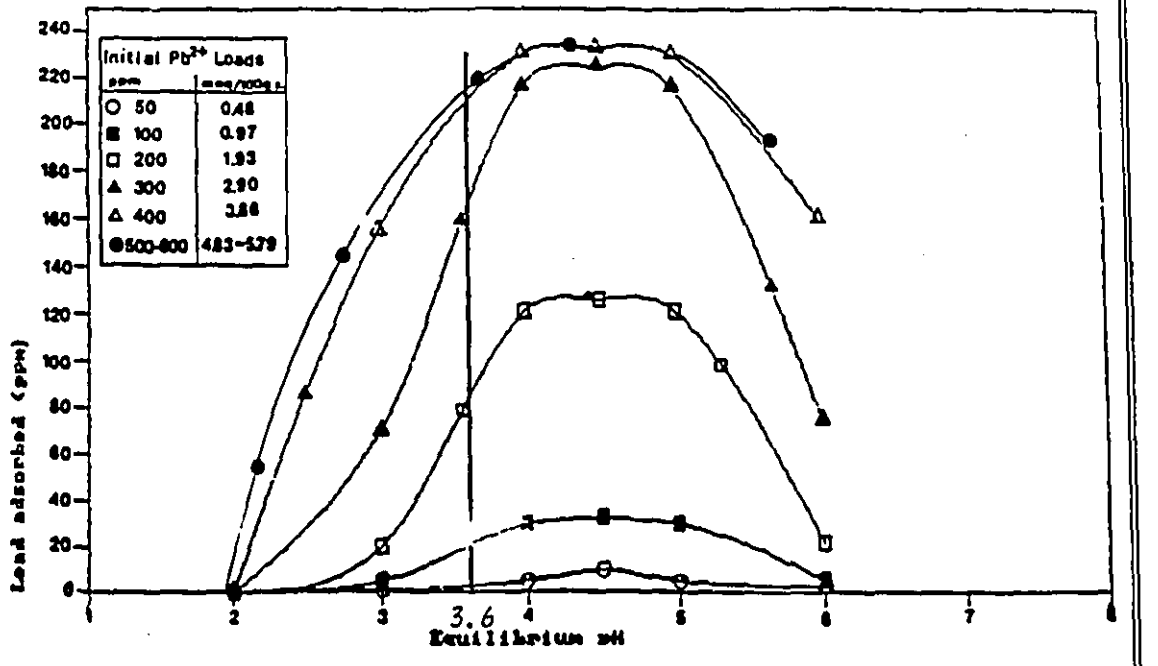

Figure 3.5 - Adsorption of Pb^{++} on Kaolinite as a Function of pH and Initial Load (from Galvez, 1989).

1) Below pH = 3.6, no significant precipitation occurs, i.e., most of *Pb* remains in solution (horizontal lines in Figure 3.4), and the maximum adsorption of *Pb* by kaolinite is achieved (indicated by the peak in Figure 3.5). In this fashion, lead is not adsorbed in the hydroxy form (Farrah and Pickering, 1979), as can be seen in the scheme of Figure 3.6. Precipitation may eventually cause blockage of the pores (Dunn and Mitchell, 1984; Yanful et al, 1988);

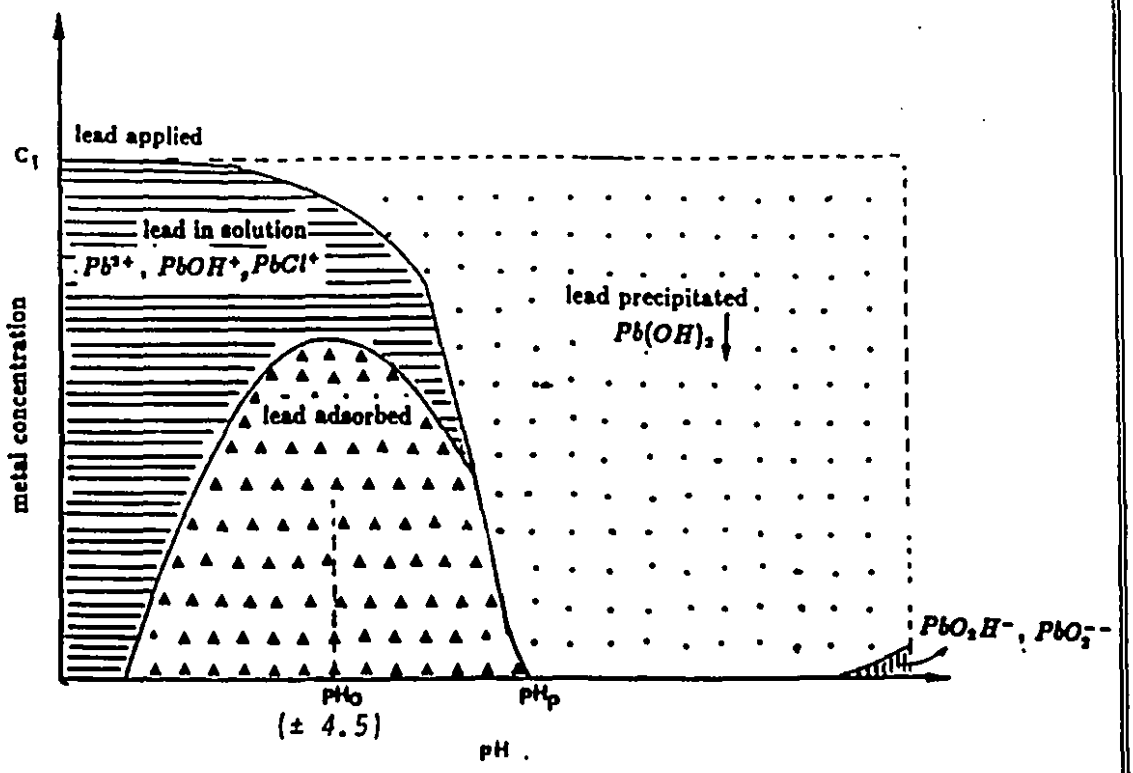

Figure 3.6 - Graphic Representation of Lead Forms (from Galvez, 1989).

2) With increased precipitation at pH > 3.6 the recovery of the adsorbed ions is not facilitated due to stronger bonds, i.e. cation and/or hydrogen bridging, between the precipitate and the clay surfaces (Wang, 1990).

3) The migration of heavy metals is facilitated in acidic conditions (Yanful et al, 1988a). It was also the purpose here to create the worst scenario of contamination.

Because the natural pH of the kaolinite used is low (see Table 3.2), this simplification worked very well; the pH of the effluent dropped during leaching of the very first pore volumes from 4.7 (values as high as 5.3 were also measured) to 3.5.

The practice of acidifying the contaminant solution was maintained for tests with the S/B mixture. In this case, however, the natural pH of the mixture was high (see Table 3.2) - and so was the pH of the collected leachate - indicating that precipitation may have occurred during leaching (see discussion in Section 4.1.2).

For kaolinite, three concentrations of *Pb* solutions were selected based on the material's adsorption isotherm, which was presented in Section 3.1.2 (Figure 3.2). They were chosen to cover a wide range of concentrations: the lowest - **C1** = $\pm$ 250 ppm of *Pb* - was taken from the initial increasing portion of the graph; the intermediate - **C2** = $\pm$ 850 ppm - was taken from where the curve begins to level off; and the highest - **C3** = $\pm$ 1750 ppm - from the near horizontal section, at which point the material is not able to adsorb any more contaminant.

Due to time constraints only two concentrations of *Pb* solutions were selected for the tests with the S/B mixture: **C1** = $\pm$ 600 ppm and **C3** = $\pm$ 2500 ppm. They represent the first part and the horizontal (levelled off) section of the material's adsorption isotherm (Figure 3.3 in Section 3.1.2).

Zinc Solution

A *Zn* solution was made by mixing $ZnSO_4 7H_2O$ and distilled water to obtain a *Zn* concentration of $\pm$ 2000 ppm. The solution was also acidified to pH = 3.6 by addition of concentrated sulphuric acid.

Due to time constraints, only one sand/bentonite sample was percolated with *Zn* solution.

The *Zn* solution was prepared to percolate a S/B sample in a test designed to: 1) compare the mobility and retention pattern of the two heavy metals (*Pb* and *Zn*) under similar test conditions, i.e, the same type of permeameter, gradient, saturation procedure, confining stress, etc., and 2) evaluate the effect of a concentrated solution of this heavy metal in the measured coefficient of hydraulic permeability of the sand/bentonite mixture.

3.2 - Permeameters

Three standard triaxial cells were modified to flexible wall permeameters for this experimental program. A schematic diagram of the cell is presented in Figure 3.7. "Double drainage lines to both the top and bottom of the specimen facilitate the flushing of air bubbles from hydraulic lines..." (Daniel et al, 1985). The base, top cap, and hydraulic lines, were made of Teflon; the fittings were made of stainless steel to

prevent rusting and reaction with the contaminant solution. Side-wall leakage is minimized by the application of a confining pressure which also simulates overburden pressure on the sample (Yanful et al, 1990)." The two latex membranes surrounding the samples were tested in a highly concentrated lead solution (5000 ppm), and found non-reactive. Figure 3.8 shows the total setup. Regulators were self adjusted for changes in atmospheric pressures.

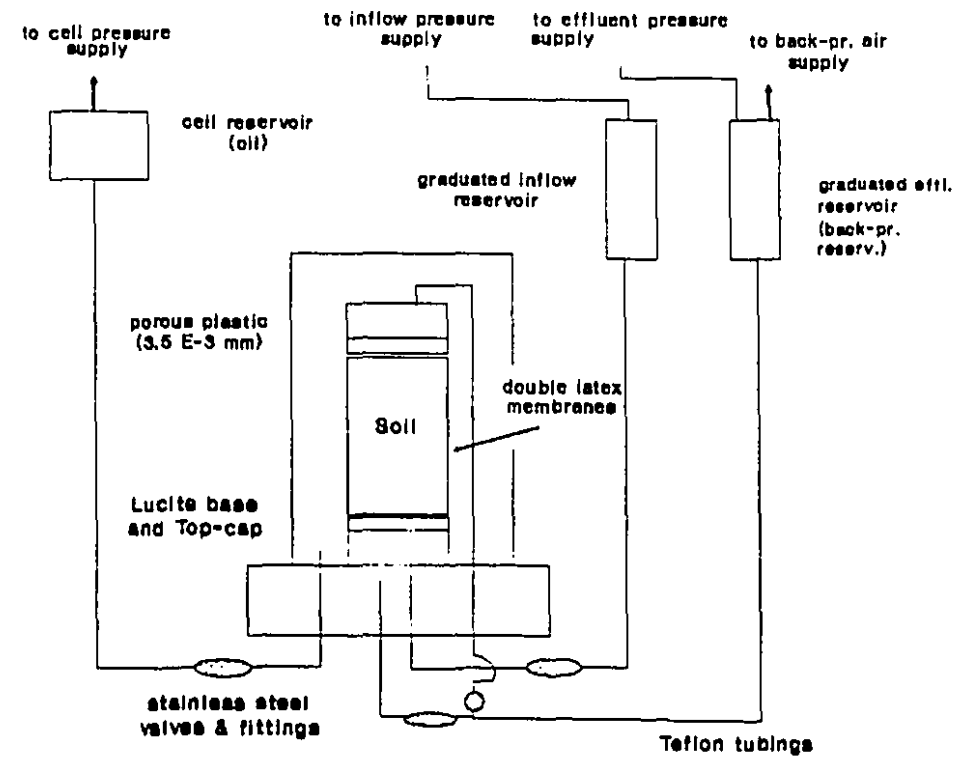

Figure 3.7 - Schematic Presentation of the Flexible Wall Permeameter (Triaxial Cell).

The rigid wall permeameter was a modified consolidation cell, as shown in Figure 3.9. The outer ring was made of stainless steel, with a Delrin inner ring and Teflon top cap. All fittings were stainless steel. Several improvements were made to two cells which were especially manufactured for this experimental program (Weber, 1991).

The advantages and disadvantages relative to these two permeameters, as well as their main characteristics were discussed by Daniel et al (1985), Madsen and

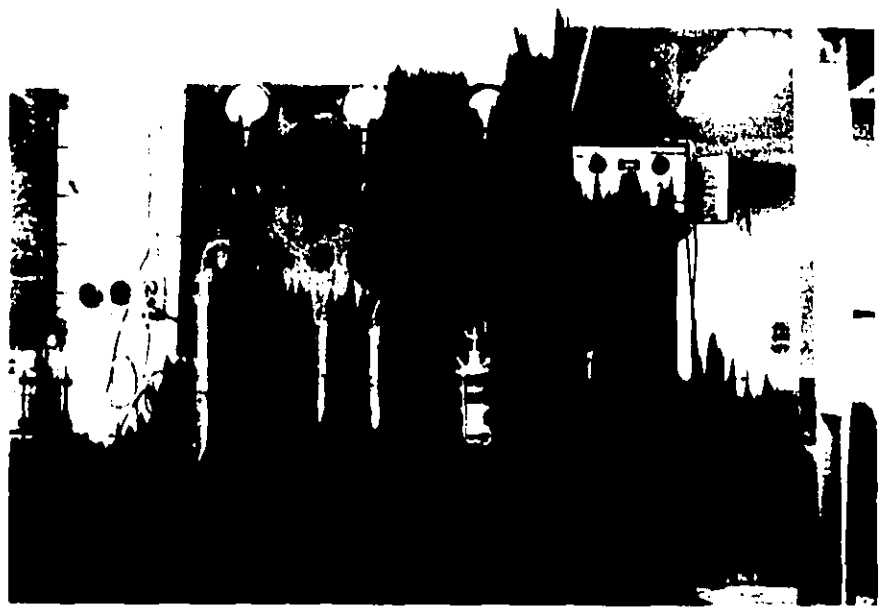

Figure 3.8 - Photograph of the Complete Setup Used for Permeability Testing with Triaxial Cells.

Mitchell (1989), Weber (1991), Yong et al (1991), among others.

3.3 - Sample Preparation

In this section details of the methodology used to mix and compact samples is given in the order of their execution. Care was taken to ensure consistency and repeatability.

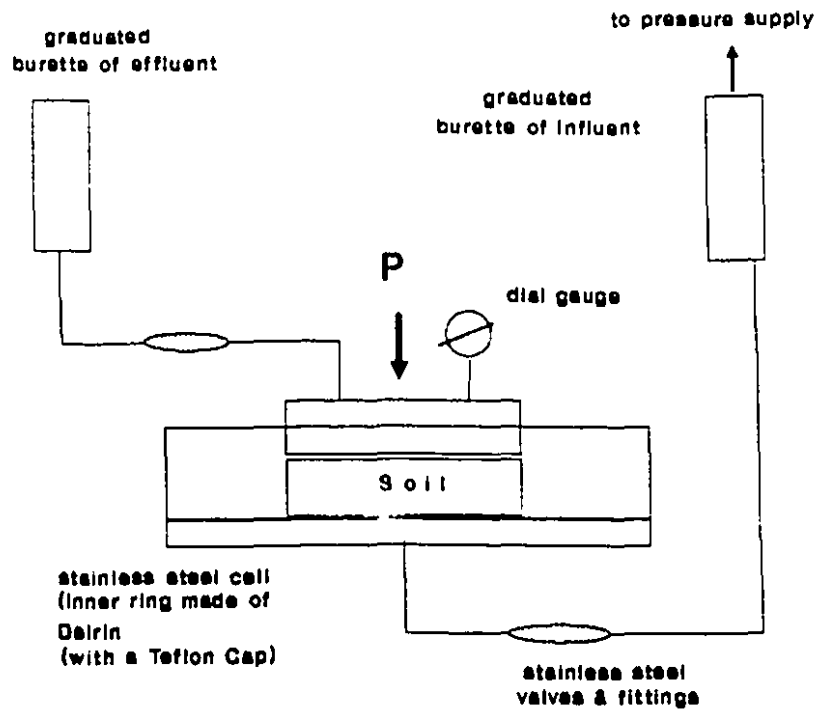

Figure 3.9 - Schematic Presentation of the Rigid Wall Permeameter (Consolidation Cell).

3.3.1 - Soil Mixing

All soil samples were initially mixed with distilled water and left in a humid room for equilibration. In the case of kaolinite samples, a minimum of 24 hours was allowed. S/B samples were left 72 hours to equilibrate. The longer time for the latter samples is due to the bentonite's affinity for water (Grim and Güven, 1978). To obtain the best uniformity possible with S/B samples, the Silica 40 sand was first

mixed with the Na-bentonite (dry mix), and only then water was slowly added without allowing the formation of pools. This conforms with most recommended procedure for S/B preparation in actual field work (Lundgren, 1981). It is nonetheless illusory to assume total uniformity of the samples.

3.3.2 - Compaction

Samples were statically compacted on the wet side of the Proctor curve, i.e., optimum moisture content (**OMC**) + 2 to 3% for kaolinite, and OMC + 2% for S/B. It was decided to compact wet of the Proctor optimum to minimize the influence of clod size and interclod void size on the hydraulic conductivity of the materials (Benson and Daniel, 1990; Daniel and Benson, 1990). The maximum dry densities and OMC of the materials are shown in Table 3.1. According to Dunn and Mitchell (1984) "static compaction induces the lowest level of shear strain, and thus should produce a less dispersed fabric, with higher hydraulic conductivity", and laboratory permeability values of statically compacted samples tend to relate better with field values. Dunn and Mitchell (1984) also indicated that the static compaction method "produce[s] replicate samples of the best quality". This is of utmost importance if the effect of structure on the coefficient of hydraulic permeability is to be minimized (Mitchell et al, 1965).

Samples tested in the in the rigid wall permeameter were compacted directly in the cell in two equal lifts, each requiring a pressure of approximately 1400 kPa -

for kaolinite, and 10,000 kPa - for S/B, to attain the desired height of approximately 1.9 cm (diameter = 6.3 cm). Compacting directly in the cell minimizes the risk of side-wall leakage (Weber, 1991).

An 80 cm^3 compaction mold was used to prepare samples for the triaxial cell.

All kaolinite samples were compacted in 5 lifts requiring a pressure of approximately 1,475 kPa (per lift) to attain the desired height of 8 cm (diameter = 3.56 cm). Some S/B samples were compacted in 5 lifts, whereas, for comparison, others were compacted in 3 lifts.

The soil was scarified between lifts for enhanced uniformity. It was particularly difficult to maintain a constant pressure for all lifts during compaction of S/B samples, the variation being more significant for samples compacted in 5 lifts than those compacted in 3 lifts. In the former case the pressure varied from approximately 4,500 kPa in the first lift to 10,500 kPa in the final lifts. In the latter case the pressure varied from 8,300 to 12,400 kPa. It is also very possible that these values vary from test to test, although not significantly.

In order to assess the uniformity of S/B samples prepared by static compaction, a sample was sliced into 5 sections just after being compacted in 5 lifts. Contrary to the lack of uniformity found by Mitchell et al. (1965), who statically compacted silty clay samples in a mold with the same dimensions as the one used in this experimental work, the results presented in Table 3.3 show very clearly that S/B samples were, for all practical purposes, quite uniform.

slice ⇒ parameter ⇓	top	top-mid	middle	mid-bot	bottom
w% [1]	18.8	19.0	18.9	18.9	18.9
vol (cm^3)	17.91	15.68	15.13	15.42	16.82
W (g)	35.18	30.81	29.72	30.30	33.05
G_s	2.66 [2]				
WDS [3]	29.61	25.89	25.00	25.48	27.80
e_0	0.61	0.61	0.61	0.61	0.61
S%	82.1	82.7	82.4	82.4	82.4

1 w% of the material before compaction = 18.3%
2 tested apart
3 weight of dry soil

Table 3.3 - Results of a Test to Access the Uniformity of S/B Samples.

A slurry consolidation test was performed with kaolinite in a separate apparatus, and from the consolidated material obtained one sample was trimmed. A permeability tests was performed with it in the triaxial cell. This test was designed to evaluate the influence of the compaction procedure on the coefficient of hydraulic permeability of kaolinite.

3.3.3 - Installation

There are, as yet, no definite specifications for sample dimensions, as far as permeability testing is concerned. Based on the literature reviewed, it seems that the rationale normally used is to adjust sample dimensions either to the type of equipment available, or to the type of test.

In the present case, triaxial kaolinite samples were trimmed to a final height of 7 cm. The amount of material used was sufficient to perform all the necessary chemical analyses with the samples after permeability testing with spare material available for water content measurements. Following the suggestion of Edil and Erickson (1985), who also worked with a sand/bentonite mixture, it was decided to trim S/B samples to a final height of approximately 4 cm. In this way, there was sufficient material for subsequent chemical analyses (see Appendix D), and high gradients could be applied with lower driving pressures, thus reducing the risk of bentonite migration. From the trimmed material, some was kept for initial water content measurements.

After trimming, the sample was weighed, its dimensions were measured with a caliper, and quickly wrapped up in plastic film (cellophane) to maintain the moisture content.

Installation proceeded under water (in a container big enough to fit the cell base) to minimize the possibility of entrapped air between the first latex membrane and the sample. Two Whatman filter papers, Grade 1, were placed on each of the two 3.5 μ porous polyethylene (a non-reactive substitute for the usual porous stone) and mois ned before installing them at each end of the sample. After the second

membrane was in place, 6 rubber O-rings, 3 at each end (top cap and base), were installed to prevent leaks. The lines were filled with water by means of a plastic bottle with a nozzle to minimize - again - the effect of entrapped air.

The cell was then mounted on its base.

In the case of the consolidation cell, trimming was not necessary, because the sample already had its final height after compaction. As a consequence, no excess material was available for initial water content measurement. After weighing the cell with the compacted soil, and placing a porous stone on each end of the sample, with Whatman filter papers (Grade 1) making the contact between the porous stones and the sample, the cell was mounted on its base, and the top cap was fitted. Further procedural details are given by Weber (1991).

3.4 - Consolidation

The next step involved the consolidation of the sample to the maximum overall (confining) stress to which the sample would be submitted. The completion of primary consolidation occurred very quickly for both materials, because compaction pressures were quite high compared to the consolidation pressures applied.

A new consolidation step was performed whenever there was an increase in gradient during testing.

3.5 - Permeability Testing

Constant head permeability tests were performed with inflow and outflow volume rates monitored. Large discrepancies between the two are associated with leaks - causing interruption of the test; small discrepancies may be associated with continuing saturation of the samples.

The contaminant was introduced from the bottom and collected at the top.

Permeability testing using hydraulic gradients much higher than actual field conditions can cast doubt on the validity of laboratory results (Mitchell and Younger, 1967), because of particle migration, among other reasons (see discussion in Section 4.1.2.1).

To evaluate the influence of the hydraulic gradient on the coefficient of hydraulic permeability of the soils when heavy metal solutions are permeated, three different gradients were applied: the lower was **I1** = 25, which is not much higher than gradients existing across clay barriers in certain waste ponds, where values as high as 20 are the case (Dunn and Mitchell, 1984); the intermediate gradient was **I2** = 50, and the higher **I3** = 100. Higher gradients (up to 400) were applied in the end of certain tests to investigate the response of the samples to very high gradients.

3.5.1 - Description of Test Samples

A nomenclature was created to help identifying each sample. With a few exceptions, the designations are composed of:

1) the identification of the permeameter: **C** for consolidation cell, and **T** for the triaxial cell;
2) the identification of the soil: **K** for kaolinite, and **SB** for the sand/bentonite mixture;
3) the identification of the contaminant: **Pb** for lead, and **Zn** for zinc;
4) the identification of the initial gradient: **I1**, **I2**, and **I3** (see description above). If the gradient is changed during the test, it is indicated in the graphs with the results;
5) the identification of the concentration of the permeant solution: **C1**, **C2**, and **C3** (described previously in Section 3.1.3);
6) an eventual extension may be given. For example, **BP** means back pressure applied, and **NB** means no BP applied. The meaning of the extension is always explained in the text.

Thus, sample **TSBPbI3C3NB** was tested in the **T**riaxial cell using the **S**and/**B**entonite mixture, under a gradient **I3** = 100, the concentration of the permeant solution was **C3** = 2500 ppm, and **N**o **B**ack pressure was applied, i.e., the sample was saturated by flushing with approximately 2 pv of distilled water. Sample **TSBPbI3C3BP**, had the same characteristics, but was saturated by **B**ack **P**ressure.

3.5.2 - Saturation

Kaolinite samples tested in both cells were saturated by flushing with ± 2 pore volumes (**pv**) of distilled water, except for two tests performed with the triaxial cell, for which the back pressuring was employed. For S/B tested in the consolidation cell, the saturation phase was considered complete after ± 2.5 pv had been leached.

Several authors, referred to by Peirce and Witter (1986), consider that the saturation phase is reasonably complete after two pore volumes of permeant have been flushed. In fact, the flushing method is not ideal for fine clays, because partially saturated conditions may exist, therefore rendering the measurement of the coefficient of hydraulic permeability more complex: osmotic head and adsorptive head may have to be considered (Hamilton et al, 1981).

The back pressure technique was not used with the consolidation cell because of the increased risk of side-wall leakage (Edil and Erickson, 1985). Samples had to be assumed 'saturated' after flushing with the 2 or 2.5 pv. During saturation, a significant amount of air was eliminated from the samples. Measurements taken during this procedure provided a reference permeability value of the soil to water, i.e., a basis for comparison to the values measured with the contaminants.

The first S/B sample tested in the triaxial cell was also saturated by flushing with 2 pv, and Skempton's parameter B (Skempton, 1954) was measured after the first and second pv had leached. In both occasions, quite low values were measured, indicating that saturation was far from being complete. It was decided, however, to

proceed with the leaching of *Pb*-solution to maintain similarities with tests performed in the consolidation cell.

Due to the above, all other samples tested in the triaxial cell were saturated by application of back pressure (**BP**) to distilled water simultaneously at the bottom and at the top. Although this constitutes a significant difference from tests performed with the consolidation cell, it was considered that the comparison between the two permeameters had to take into considerations the advantages each had. For a detailed discussion about the different methods of BP application the reader is referred to Dunn (1983).

In this experimental program, BP was always applied in steps of 34 kPa ($\approx$ 5 psi). According to Dunn (1983), "if back pressure is applied too rapidly, or using increments which are too large, with applied effective stress held constant, some of the sample may be overconsolidated as compared to other portions of the sample."

The chamber pressure was always 3.4 kPa ($\approx$ 0.5 psi) higher than the back pressure to maintain the seal between the sample and the membrane.

Following recommendation of Edil and Erickson (1985), it was first decided to allow 30 minutes for equilibration between the first steps. This interval turned out to be too short: in the first tests, BP as high as 340.0 kPa ($\approx$ 50 psi) had to be applied to obtain a B-value of 0.95. It was then decided to increase the intervals for equilibration, resulting in lower final BP's (136.0 to 170.0 kPa). However, saturation procedures were rather lengthy, taking almost 5 consecutive days. Figure 3.10 shows the evolution of the measured B-value for a representative test; the time intervals

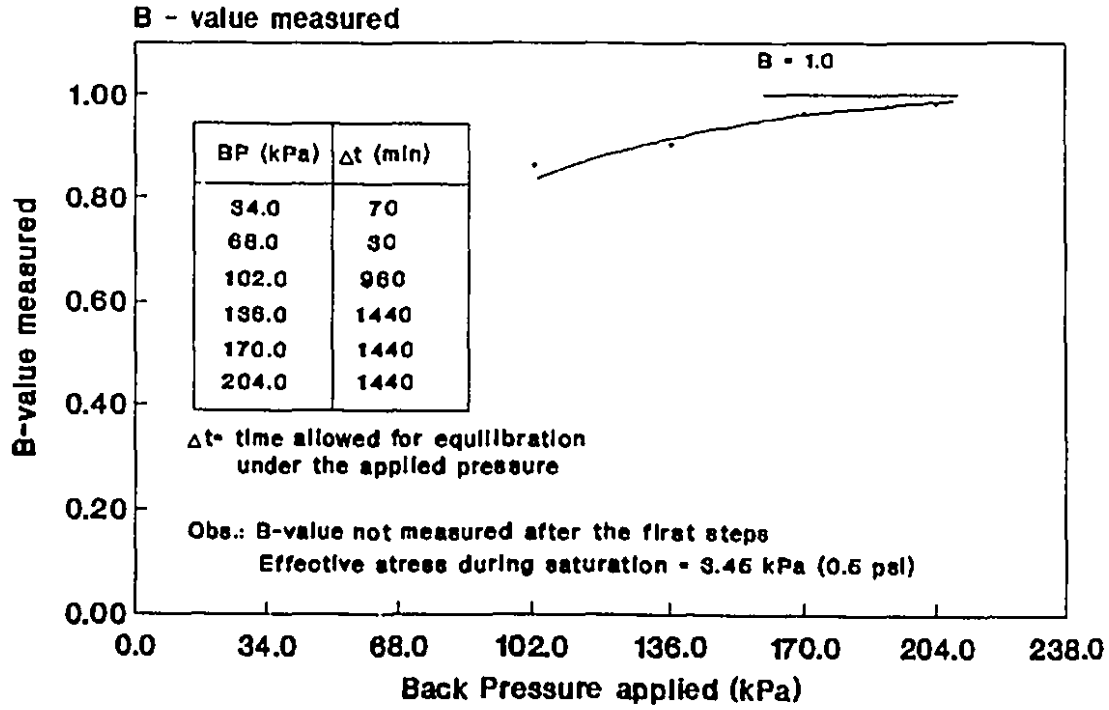

Figure 3.10 - Variation of the Measured B-value with Increasing Back Pressure Application.

between steps are indicated.

BP was maintained throughout the tests, otherwise dissolved air would "immediately begin to come out of solution, and the measured hydraulic conductivity would decrease (Dunn, 1983)."

3.5.3 - Details of Tests

As mentioned before, the rates of flow in the burettes 'in' and 'out' were measured throughout the tests in order to verify the steady state condition. The interval between readings was quite short in the beginning of each test so that any possible leaks, or other kind of problems could be promptly identified. As the coefficient of hydraulic permeability levelled off, readings were spaced. When testing low permeability materials, it is preferable to wait for a clear rise (or fall) in the burette level, otherwise it can lead to a wrong calculation of the value of the coefficient of hydraulic permeability.

The pressure levels were controlled throughout the duration of the tests. The chamber pressure was always 13.6 kPa ($\approx$ 2 psi) higher than the pressure applied at the burette 'IN' in order to maintain the seal between the sample and the membrane, thus avoiding leaks along the membrane. This level of confining pressure does not seem to influence the measured value of the coefficient of hydraulic permeability (Boynton, 1983; in Daniel et al, 1985). It was also sufficient to prevent swelling of the samples; measurements taken after extrusion of the samples did not indicate any change in sample dimensions. A vertical piston placed on top of the triaxial samples also helped to prevent vertical swelling.

It is important to note that the confining pressures applied were well within the range of actual overburden pressures existing in hazardous waste landfills - 60 to 370 kPa (Peirce et al, 1986; from various sources).

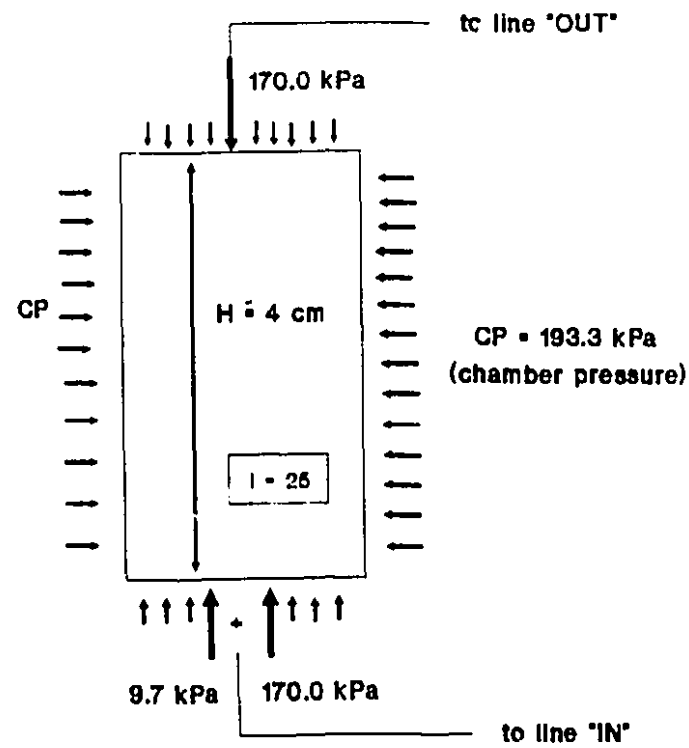

Figure 3.11 - Scheme of Applied Pressures for a Typical Test Conducted in the Flexible Wall Permeameter (Back Pressure = 170 kPa).

The pressure configuration for a typical test is shown in the scheme of Figure 3.11.

Leachate was collected approximately after each pore volume had been percolated. It was poured into glass tubes, labelled and stored for future analyses. To execute this step, the valves had to be closed for a few minutes.

As mentioned in Section 3.4, every time the gradient had to be increased, the sample was consolidated to the new level of effective stress to be applied.

3.5.4 - Termination of Tests

Although the termination criteria suggested by Peirce and Witter (1986) was normally followed (the slope of the curve k versus pore volumes collected must not differ significantly from zero), the moment to stop a test varied according to its purpose. Thus, some tests were terminated after only 4 or 5 pv's had been collected, whereas others would be terminated after as much as 16.5 pore volumes had been collected. The latter were designed to evaluate the long term stability of the samples percolated with concentrated heavy metal solutions. Whenever cell leaks occurred, tests were terminated immediately.

3.5.5 - Sample Extrusion

In the context of the present work, extrusion is the removal of the sample from the permeameter. Once the cell has been completely disassembled, lines disconnected, o-rings, top cap and filter papers removed, the membranes surrounding the samples are carefully cut. The sample was then weighed, its dimensions were measured with a calliper, and then cut into 4 (kaolinite) or 3 (S/B) slices, each being weighed. The height of each slice was also measured. Some material was taken from each for final water content measurement and calculation of the final saturation (S)

along the sample. They were then wrapped in plastic film and stored in labelled plastic bags for future analyses.

For the purpose of this experimental work, the slices were designated **T**, **M**, **B**, and **B(s)** - the latter for kaolinite only. **B(s)** was a very thin slice taken from the very bottom, where the contaminant solution was introduced. With **B(s)** it was possible to obtain the concentration of the contaminant very close to the point where the contaminant was introduced. According to Griffin et al (1976), Warith (1987), among others, heavy metals are retained in the very first centimetres of clay barriers. It was later decided to abandon **B(s)** for tests with S/B because of difficulties associated with trimming a thin slice from this particular material.

3.6 - Chemical Analyses

In this section, the methodology for chemical analysis of soil samples extruded after permeability testing, and of the leachate collected is presented and discussed. The chemical characterization of the soils and solutions were introduced previously in this chapter.

Chemical analyses of soil samples are fundamental for a proper evaluation of the compatibility between soils and contaminants. The methodology presented here is adequate for soil samples which were percolated by inorganic contaminants. For

organic contaminants the approach is quite different, and vary according to the type and concentration of the elements in question, among other factors.

In order to standardize the samples to be analyzed by AAS and for enhanced efficiency, **the pH of every supernatant and leachate was adjusted to 3.6 by adding acetic acid (or sulphuric acid, in the case of *Zn*). In this fashion, precipitation of *Pb* or *Zn* as oxides was minimized** (Figure 3.4). Since the soils contain no organic matter, chelation, or sequestering of the metals was not of concern.

3.6.1 - Leachate

The effluent collected during permeability testing was analyzed chemically for the contaminants of interest (*Pb* and *Zn*).

When needed, dilutions were made by using distilled water with a pH of 3.6, adjusted with concentrated nitric acid (*Pb*) or sulphuric acid (*Zn*). When the concentration in the leachate was within the limits of detection of the AAS apparatus, the leachate itself was acidified.

The results of these analyses were used to help in the calculation of *Pb* mass balances, and to construct breakthrough curves, which give an indication of the potential for breakthrough by a particular contaminant through a soil; they serve as well as tools for calculation of retardation factors, which are then used in contaminant transport models (Freeze and Cherry, 1979; Bowders et al, 1986). The use of retardation factors obtained from adsorption isotherms is criticized and compared to

retardation factors obtained from adsorption characteristic curves of compacted material[4] (Chapter 4).

3.6.2 - Soil Samples

There are, as yet, no definite standardized procedures to analyze soil samples after leaching with contaminants. A methodology is proposed in this research work. Its outlines are described below and the details are specified in the Appendix D. The results of these analyses serve as tools in the assessment of the long term performance of a protection barrier material.

The material obtained from each slice was first washed with distilled water to remove the contaminated pore fluid. Washing was performed in two steps, each involving mechanical shaking and centrifugation. The supernatants obtained were stored in labelled glass bottles for future analysis by AAS (Pb^{++}). The soil was then removed from the Nalgene centrifuge tubes and dried before preparing triplicates for each slice. Some material was spared for the determination of the exchangeable H^{+}.

This procedure had to be slightly adapted for S/B samples: due to their different densities, bentonite and sand do not settle together during centrifugation, making it very difficult to recuperate the soil from the Nalgene tubes without changing the ratio 90% sand/10% bentonite. For this reason, it was decided to avoid

---

[4] Term defined later in this chapter.

two steps: removal of the soil from the centrifuge tubes and drying. To make up for the amount of dry material desired (4.0 g), the amount of wet material to be placed in each tube was calculated by adding a surplus equivalent to the final water content of the slice - previously calculated. For example, if the final water content was 24%, and 4 g of dry material was specified, then 4.96 g of wet material had to be used. Kaolinite samples can be analyzed using the same procedure as S/B samples; thus, only the procedure used to analyze S/B samples was detailed in the Appendix D.

Washing was followed by the 'extraction' procedure. In the present case, extraction involved the exchange of the adsorbed contaminant by ammonium ions (NH_4^+) by effect of concentration. A concentrated solution of ammonium acetate was used and its pH was adjusted to 3.6 by adding acetic acid. In this fashion metals are found as ionic species in solution (Figures 3.1.3). Other efficient extractants, e.g.: silver-thiourea (Chhabra et al, 1975; Phadungchewit, 1990) were not tested for comparison due to time constraints. Fortunately, the results of lead mass balances (presented later, in Section 4.2.5) showed that, in most of the cases, the technique adopted was quite successful.

Triplicates for each slice were made by mixing the material with a specified quantity of ammonium acetate solution in Nalgene tubes. The mixture was left to shake, centrifuging followed, and the supernatants were collected in plastic bottles. This was repeated three times in order to optimize the extraction.

For tests with kaolinite, the contents of 10 bottles had to be analyzed by AAS for Pb^{++}, Na^{+}, K^{+}, Ca^{++}, Mg^{++}, and Al^{3+}: 3 for the Top, 3 for the Middle section, 3 for the Bottom, and 1 for **B(s)**. In the case of S/B, the contents of 9 bottles (3 for each slice - **T**, **M**, and **B**) were analyzed for the same elements, except Al^{3+}. The exchangeable H^{+} was not measured either - the reasons for which are explained in Section 3.1.1.

As mentioned before, the bottles containing the supernatants of the washing procedure were analyzed only for Pb^{++}.

The average quantities adsorbed by each slice were plotted against the concentration in the equilibrium solution, in the same graph used to plot the material's adsorption isotherm. Regression analyses (power curve fitting) were performed and 4 curves were obtained, one for each kaolinite slice. The Freundlich model was again used. The curves obtained were called 'adsorption characteristic of compacted materials'.

3.6.3 - Mass Balance Calculations

The procedure for lead mass balance calculations is presented in the Appendix E. Basically, the amount of *Pb* (or *Zn*) introduced in the system is

compared to the sum of amounts found in the system as: adsorbed species; as ionic species in the acidified leachate, or in the pore fluid.

"The estimation of these retained ions by mass balance is of great importance in designing the required depth and/or the volume of clay soil which would be required to perform effectively as a barrier system in the landfill site" (Yong et al, 1986).

This form of 'book keeping' gives more reliability to the results of chemical analyses. However, there are several difficulties - or limitations - associated with lead or zinc mass balance calculations, the most important being:

1) Possibility of contamination of the glassware during the numerous dilutions when highly concentrated solutions are being tested;
2) The fact that almost no 'extractant' is 100% efficient (Karamanos et al, 1976; Farrah and Pickering, 1977);
3) The occurrence of high affinity adsorption (adsorption in the Stern layer), rendering the metal thus adsorbed less available for exchange (Alammawi, 1988); and
4) The possible presence of colloids in the supernatant due to imperfect separation of phases (Gschwend and Wu, 1985; Servos and Muir, 1989). In this case, some of the adsorbed species would not be identified by AAS.

These limitations are commented in detail during the presentation of results.

CHAPTER 4

RESULTS AND DISCUSSIONS

"Nature seems to abhor hundred percent"
Karl Terzaghi, in "About Life and Living"
Geotechnique, 1961

Some of the results presented and discussed here were also discussed by Yong et al (1991).

Following the order that the experiments were performed, the results of permeability tests are presented and discussed first, followed by those of chemical analyses of both leachate and test samples, according to the scheme shown in Figure 4.1.

Test results will often be presented in groups in order to simplify the discussion. In this fashion, the effect of several parameters on the coefficient of hydraulic permeability of the materials, and on their adsorption capability may be addressed in a more straightforward manner, avoiding reference to many scattered figures.

4.1 - Permeability Tests

In this section, the terms triaxial cell and consolidation cell will quite frequently be employed to designate, respectively, the flexible wall and rigid wall

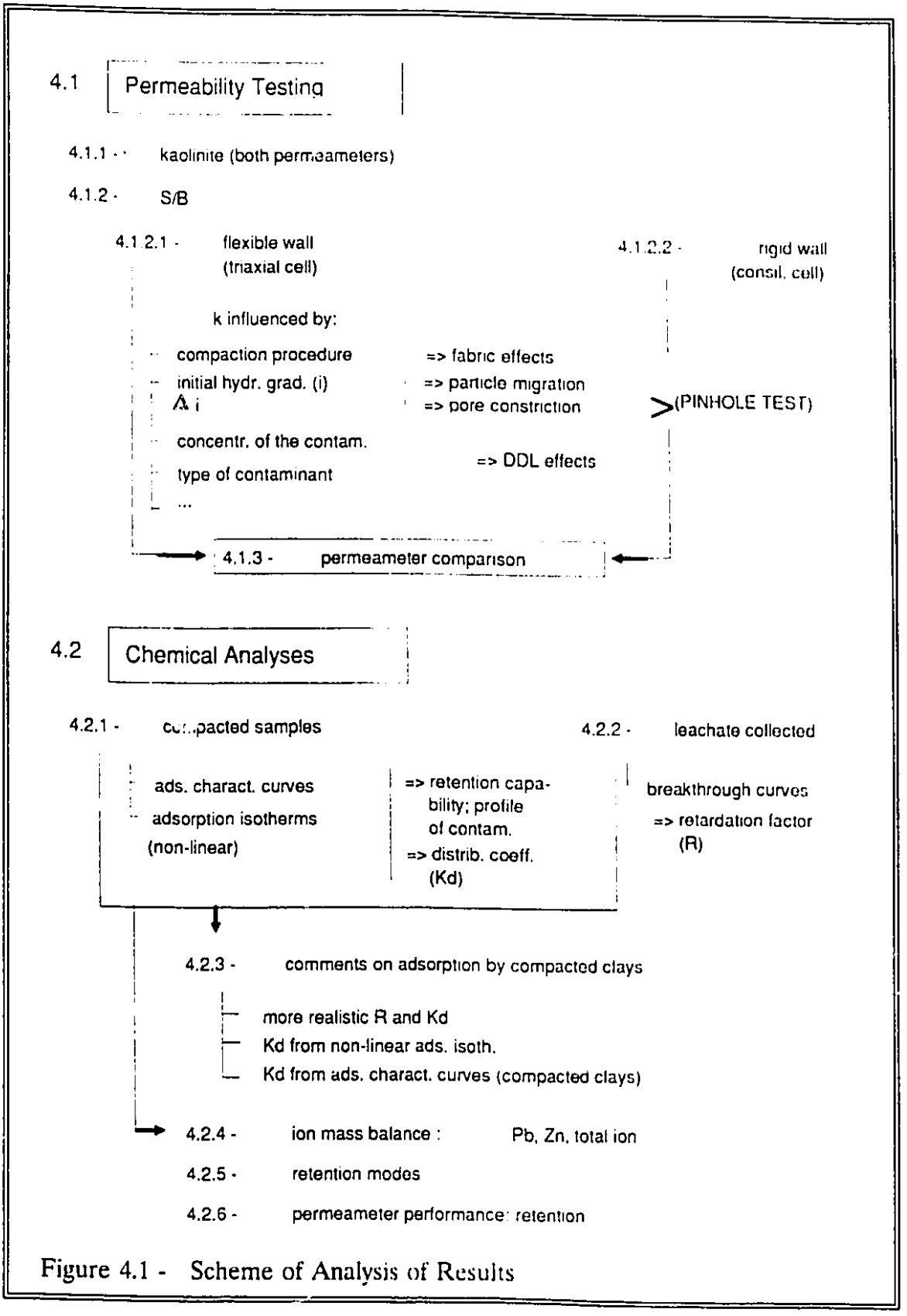

Figure 4.1 - Scheme of Analysis of Results

permeameters used in this research work; the designation sand/bentonite mixture will be abbreviated to S/B; and **the terms 'high' or 'low' coefficient of hydraulic permeability (or *k*-value, or coefficient of permeability, or simply permeability) will be employed in comparison to the 1.0×10^{-7} cm/s usually required as a minimum value by environmental agencies for clay barrier materials** (Zimmie, 1981; Eklund, 1985; Harrop-Williams, 1985).

The results of tests performed with each one of the two materials will be presented separately; for kaolinite, results obtained with both permeameters are presented together, whereas for the S/B mixture they are discussed separately, i.e., one section for each permeameter. A comparison of the performance of the two apparatuses to measure the coefficient of hydraulic permeability of S/B samples is presented.

Some tests were continued to almost total breakthrough[1] in order to access the long term contaminant/clay compatibility. Continuous monitoring of the soil permeability (k) was one of the means used to detect eventual failure mechanisms due to physico-chemical interactions in the clay-leachate system (Eklund, 1985).

Chemical breakdowns, reflected in internal structural changes of the compacted soils, were partly evaluated by the measurement of the samples characteristics and dimensions before and after testing for permeability, and by visual

---

[1] The condition $C/C_0 = 1$, i.e., the concentration of contaminant in the effluent equals that of the input solution.

inspection of the samples after testing. These characteristics are summarized in the Appendix F.

In general, the dimensions of the kaolinite and S/B samples did not change significantly due to percolation of contaminant solutions, independently of the concentration and/or type of contaminant. This indicates that any changes are limited to internal rearrangements of micro and ultra-microscopic structures (domains and clusters) without affecting the macro structure. In fact, void ratios did not change significantly due to percolation; they were always calculated before and after testing. Also, the excess chamber pressure of 13.6 kPa was sufficient to prevent swelling from occurring, as discussed in Section 3.5.3.

Following sectioning of the samples, measurements taken for each slice generally showed little or no difference between water contents. This indicates a certain uniformity within test samples. The final degree of saturation for each sample was also calculated; the values obtained were always very close to S = 100%, as opposed to the 84 to 88% (kaolinite) and 74 to 79% (S/B) in the beginning of tests.

4.1.1 - *k*-tests with Kaolinite

From the results of permeability tests with kaolinite, shown in Table 4.1, it is seen that the range of k values for all tests lies between 1.3×10^{-7} cm/s and 6.5×10^{-7} cm/s, i.e., the k value of the material was not substantially affected by the introduction of the lead permeant. These results agree with previous experience with kaolinite

Sample	γ_t (kN/m³)	e_o/e_f (measured)	ω (%) OMC = 32	I	C (ppm)	k to H_2O (10^{-7} cm/s)	k to Pb (10^{-7} cm/s)
TKPbI2C1	16.8	1.03/1.04	31.3	50	250	3.8	3.2
TKPbI3C1	17.5	0.95/0.96	32.0	100	250	2.5	2.7
TKPbI3C2	17.2	1.05/1.03	35.6	100	800	3.2	3.2
TKPbI1C3	17.3	1.02/1.06	34.3	25	1700	4.2	2.0
TKPbI2C3	17.5	N.A.	31.0	50	1700	3.0	3.4
TKPbI3C3b	17.2	1.04/1.05	35.2	100	1700	2.2	2.9
TKPbI3C3γ_a	17.8	0.94/0.96	33.2	100	1700	6.5	5.0
TKPbI3C3γ_b	16.2	1.14/1.10	33.0	100	1700	2.2	2.3
TKPbI3C3*	17.3	1.04/N.A.	35.5	100	1700	-	4.0
TKI3SLURR	16.8	N.A.	33.7	50	-	4.3/3.7	-
TKI2BP1	17.0	N.A.	31.0	0	-	0.1	-
TKPbI3C3BP2	17.3	0.99/1....	3.0	100	1700	2.4	2.4
CKPbI2C1	17.3	0.98/1.06	**	50	250	3.3	3.7
CKPbI3C1	17.2	0.99/1.01	**	100	250	1.3	1.7
CKPbI2C2	17.5	0.96/0.96	**	50	800	2.7	2.9
CKPbI3C2	17.3	0.99/1.00	**	100	800	1.8	2.7
CKPbI1C3	17.4	0.99/1.00	33.3	25	1700	2.1	3.2
CKPbI2C3	17.3	0.99/N.A.	**	50	1700	3.5	3.2
CKPbI3C3	17.4	0.98/0.98	**	100	1700	1.9	2.4
CKPbI3C3*	17.4	0.98/1.01	**	100	1700	-	3.6

** No measurement was taken; assumed 32%.

Table 4.1 - Hydraulic Conductivity Results for Kaolinite.

(e.g.: Peirce and Witter, 1986) and testify to the relative insensitivity the clay to pore-water chemistry changes, i.e. substantial increases in the rate of flow (possibly associated with 'cracking') are not as severe a problem as in the case of clays with more

pronounced surface active forces. This is not totally unexpected, and can be explained in terms of the buffering capacity of the material (Yong et al, 1990).

The same range of results was found for virtually all the variations used - e.g.: a) samples tested under various levels of hydraulic gradient (**I1** = 25; **I2** = 50; and **I3** = 100); b) samples compacted to different densities - **TKPbI3C3**γ_a and **TKPbI3C3**γ_b; c) samples prepared with a 1700 ppm lead solution instead of distilled water - **TKPbI3C3*** and **CKPbI3C3***; d) application of back pressure (**TKPbI2BP1**; **TKPbI3C3BP2**); and e) a sample prepared by slurry consolidation - **TKI3SLURR**, for which only distilled water was leached (results also shown in Table 4.1). In addition, there appears to be no appreciable difference between the k values measured in the triaxial and consolidation cells, an observation made by other authors (e.g.: Daniel et al, 1985; Bowders and Daniel, 1986; Peirce and Witter, 1986).

Any variations between the actual values obtained in this research program and those reported by other researchers may be attributed to several factors, including: the type of kaolinite; the pH and type of the permeant (0.01N $CaSo_4$, tap water, or concentrated organic permeants); the type of compaction; sample water content and density; etc.

4.1.2 - k-tests with Sand/Bentonite

Contrary to kaolinite, tests with the S/B mixture indicated that the coefficient of hydraulic permeability can be influenced by: 1) the testing system; 2) the hydraulic

gradient applied; 3) the compaction procedure; 4) the concentration of the contaminant; 5) the saturation procedure; and 6) the type of contaminant leached through.

4.1.2.1 - S/B Tested in the Triaxial Cell

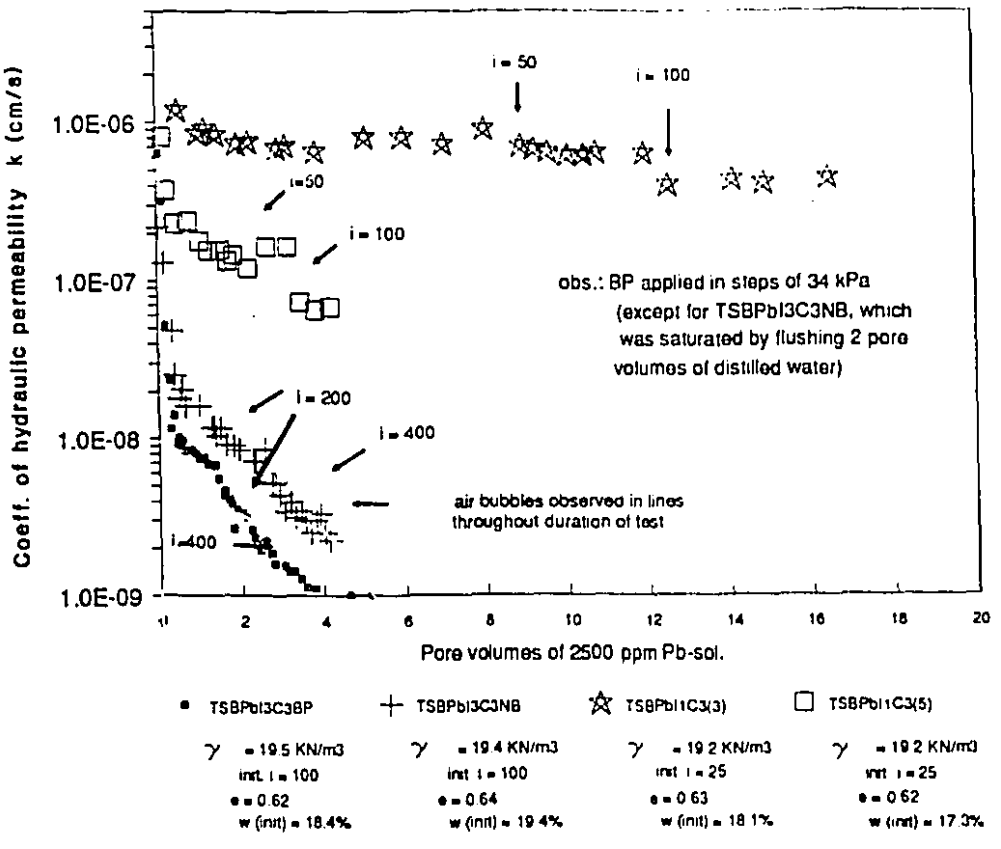

Figure 4.2 - Variation of the Coefficient of Hydraulic Conductivity of Sand/Bentonite Samples Tested in the Triaxial Cell.

In the permeability test results shown in Figure 4.2, similar test conditions were used for all four tests, i.e.:

1) the samples were saturated by back pressure in steps of 34 kPa (except sample **TSBPbI3C3NB**, which was saturated by flushing 2 pore volumes of distilled water) and the permeant solution would not be introduced before B-values close to unity were measured;
2) the concentration of lead permeant was approximately 2500 ppm (**C3**);
3) the total densities of the samples were very similar, varying between 19.2 and 19.5 kN/m^3; and
4) the confining effective stress used for all tests was 13.6 kPa.

Note that the arrows indicate the stage at which hydraulic gradients were changed. The initial gradient for the top two curves was **I1** = 25, whereas for the bottom two curves it was **I3** = 100.

Based on the results presented in Figure 4.2 a thorough evaluation of the effect of many parameters on the coefficient of hydraulic permeability of S/B can be made:

Effect of Compaction Procedure

The equilibrium permeability of sample **TSBPbI1C3(3)**, which was compacted in 3 lifts (upper curve in Figure 4.2), was one order of magnitude greater than that of sample **TSBPbI1C3(5)**,compacted in 5 lifts ($k \approx 5.0 \times 10^{-7}$ cm/s for the former, and $k \approx 7.0 \times 10^{-8}$ cm/s for the latter). Similar results were obtained by Mitchell et

al (1965) who observed a two orders of magnitude difference in the permeability of silty clay samples, due to compaction in different numbers of layers to the same final density and molding water content, and tested in the triaxial cell.

Since the initial water content of samples **TSBPbI1C3(3)** and **TSBPbI1C3(5)** are very similar and on the wet side of the Proctor optimum, a seductive argument to explain the difference would be that a more oriented fabric was obtained with 5 compaction lifts due to a better distribution of the bentonite in the voids of the sand fabric. Whereas this reasoning might be sustained in a system composed uniquely of clay, the mixture of sand and clay presents complications in clay distribution that would need further fabric study before final definitive arguments can really be offered (a few more comments are presented later in this Section).

Effect of Precipitation

Due to the high pH of the S/B mixture (8.6 to 8.8), precipitation of lead as oxides or carbonates may have occurred. This can eventually cause pore blockage (pore constriction), leading to a decrease in the coefficient of hydraulic permeability of the S/B samples. This range of pH is higher than the pH range that hydroxides of *Pb* precipitate (3.5 to 6.0) as obtained by Galvez (1989) for various concentrations of *Pb* solutions (Figure 3.4). The precipitated amorphous material can form various types of bonds (H-bond, cation bridging, electrostatic attraction, etc.) with the clay surfaces (Wang, 1990), eventually giving origin to a more 'tight' structure.

According to Farrah and Pickering (1977, 1979) the adsorption of *Pb* (and of *Zn*) ions increases with increasing pH. Beyond a threshold pH (pH > 6 for *Pb*) "virtually all the metal ion is removed from the aqueous phase, presumably as hydroxy species adsorbed on the surface of the ... solid particles." As mentioned previously, this is one of the reasons the ammonium acetate ('extracting') solution - and the leachate collected - had to be acidified to pH = 3.6: at this pH, lead is found as ionic species (Figure 3.4).

It seems that, in this particular case, precipitation did not play a major role in altering the calculated coefficient of hydraulic permeability of S/B, otherwise it would have been apparent in the results of the permeability tests with samples **TSBPbI1C3(3)** and **TSBPbI1C3(5)** (Figure 4.2), for which the calculated *k* value was not altered significantly, despite the high concentration of *Pb* in the solution (C3 ≈ 2500 ppm). This agrees with results obtained by Finno and Schubert (1986) who observed precipitation of dissolved metals near the top a liner without any apparent effect on the fluid conductivity of the barrier material.

Precipitation can eventually be of importance if considered as a compounding phenomenon to pore restriction due to high gradients applied. Unfortunately, this could not be verified in this research work.

Effect of Hydraulic Gradient

Figure 4.2 shows that the equilibrium permeabilities of samples **TSBPbI3C3NB** and **TSBPbI3C3BP** were two orders of magnitude lower than the permeabilities of the two other samples described above. The initial gradient applied to them (i = 100) was 4 times higher than the gradient applied to samples **TSBPbI1C3(3)** and **TSBPbI1C3(5)**.

Two possible reasons exist for this significant reduction in the coefficient of hydraulic permeability of samples **TSBPbI3C3BP** and **TSBPbI3C3NB**:

1) **densification** of the outflow end of the samples associated with the application of high hydraulic gradients (Daniel et al, 1985);
2) displacement of particles and/or groups of particles (**particle migration**) due to seepage forces, thus causing **partial pore blockage** (Yantul et al, 1988).

1) **Densification:** the application of a hydraulic gradient result in different effective stresses along the samples (Daniel et al, 1985). Thus, nonuniform void ratios may develop inside the sample (Mitchell and Younger, 1967) causing an eventual expansion of the inflow end (higher pore pressure), and the **densification** of the outflow end (higher effective stress). "The importance of this effect may vary with the magnitude of the hydraulic gradient" (*ibid*). However, Edil and Erickson

(1985) made the following remark about sand/bentonite mixtures: "Since the sand grains were compacted into a very dense configuration, it is doubtful that the specimens would experience significant differential consolidation from stress differences between the top and the bottom." In this work, the problem was partially avoided by shortening the S/B samples (Section 3.3.3), and by trimming the material from both ends and keeping the central part of the compacted sample for permeability testing.

2) **Particle Migration:** the results obtained with samples **TSBPbI3C3NB** and **TSBPbI3C3BP** indicate that the drop in k values occurred very rapidly over the permeation of the first pore volume (**pv**) of *Pb*-solution, with a less rapid but still fast drop over the subsequent 3 pore volumes. This contrasts quite dramatically with the results demonstrated by the other two tests shown in Figure 4.2 (samples **TSBPbI1C3(3)** and **TSBPbI1C3(5)**), tested under an initial gradient $i = 25$. Since the porosity (n) of all four samples are practically the same, and the calculated k in the very beginning of the tests were almost the same ($k \approx 10^{-6}$ cm/s), it is expected that the advective velocities ($v_n = v_{darcy}/n$; where $v_{darcy} = k.i$) of the samples tested under an initial gradient of 100 be 4 times greater than those found for samples tested under $i = 25$.

These initial observations indicate that detachment of particles (**particle migration**) may have occurred under the initially 'high' gradient of 100 (Mitchell et al, 1965), thereby leading to **pore constriction** (partial blockage). Observations of the

collected leachate did show that the effluent from samples **TSBPbI3C3BP** (lowest curve in Figure 4.2) became cloudy as the permeability dropped from 4.0×10^{-7} cm/s, in the beginning of the test, to the equilibrium value of about 1.0×10^{-9} cm/s.

To verify the dispersibility of the mixture, a pinhole test was performed as a complementary investigation (Section 3.1.1). The results indicated that this material is easily erodible, considering the situation existing during the pinhole test. Figure 4.3 shows a photograph of the sectioned sample. It can be observed that the 1 mm hole had increased to nearly 5 mm due to erosion.

It must be noted that an increase in the hydraulic gradient, once the coefficient of hydraulic permeability had stabilized, did not lead to a significant change in the *k* values of the four test samples shown in Figure 4.2. A similar pattern of results was obtained by Mitchell and Younger (1967), who did not observe significant changes in *k* following an increase by four times of the hydraulic gradient. They attributed it to the "formation of a stable structure" during the initial phase of their test.

In the case of samples **TSBPbI1C3(3)** and **TSBPbI1C3(5)** (two upper curves of Figure 4.2), the structure/fabric was developed without apparent particle migration (from observation of the effluent collection), pore constriction or significant changes in the calculated *k*.

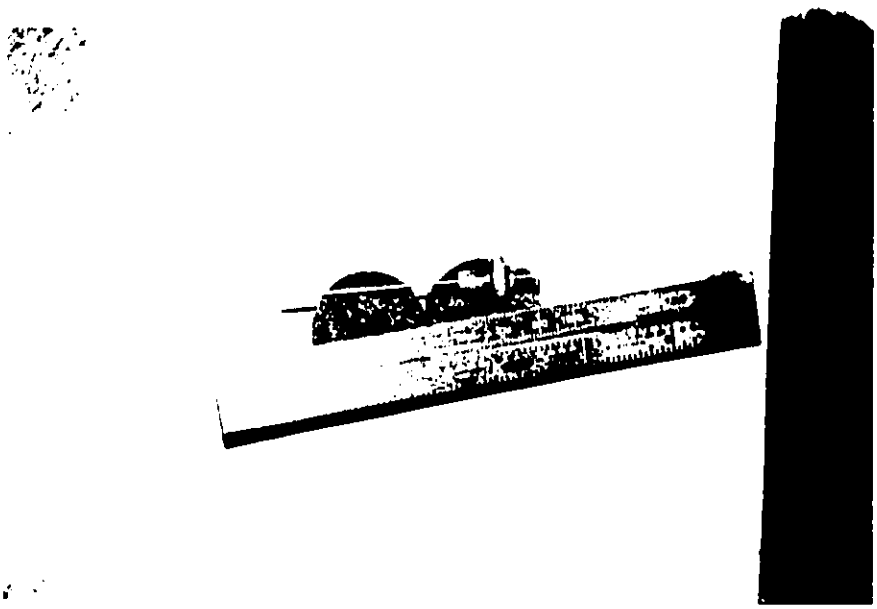

Figure 4.3 - Cross section of the S/B specimen tested for dispersibility (pinhole test). Note expansion of the 1 mm hole and the darkening around the hole.

Other than using the example of the tests performed during the experimental program, it is possible to address the problem of pore constriction considering the ideal situation presented in Figure 4.4, where a sand particle is surrounded by clay particles.

Neglecting the contact between sand particles, the approximate number of parallel clay layers surrounding each sand particle can be calculated based on the specific surface area (SSA) of bentonite (855 m^2/g) and on the average surface area

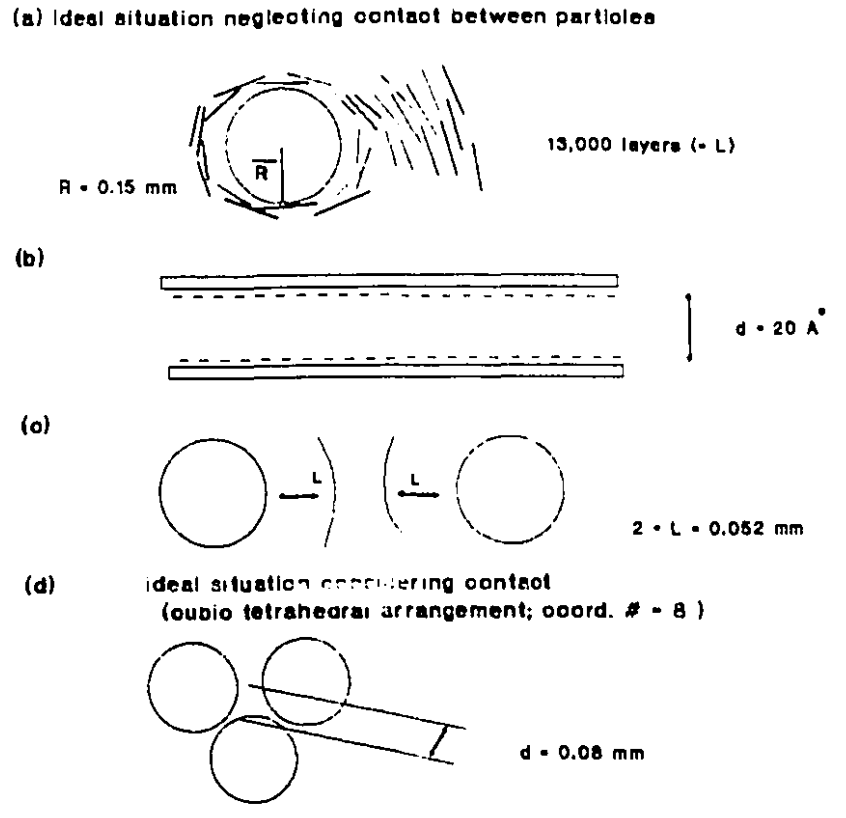

Figure 4.4 - Schematic Presentation of an Ideal Arrangement of Particles of a Sand/Bentonite Mixture.

of a sand particle. With the sand used in this study, approximately 13,000 layers of bentonite would surround each sand particle. If, in an ideal situation, total saturation is achieved, the bentonite particles will be approximately 20 Å apart (van Olphen, 1963; Yong and Warkentin, 1959) filling up almost 65% of the pore spaces (Figure 4.4). In this geometry, particle migration is not very probable because the inter-particle bond strength is several orders of magnitude greater than shear forces due to seepage (Campanella, 1965; in Mitchell and Younger, 1967). However, this is an

ideal situation where the unevenness of pore sizes is not taken into consideration. In reality, the sand particles are not perfectly uniform and of the same size, which leads to a greater degree of packing, leaving less room for the clay. With the probable formation of ultramicroscopic structures - domains - and microscopic structures - clusters or flocs - (Yong and Warkentin, 1975), amongst which bond strengths are of a lower order of magnitude than inter-particle forces, only a very small displacement of a cluster is required to cause a pore blockage.

Depending on certain conditions, some particles may be carried away over relatively long distances inside the sample and eventually be lost to the effluent, as was the case with the effluent of sample **TSBPbI3C3BP** (commented above).

The effect of possible detachment of particles under initial high gradients, or high advective velocities, raises some very interesting questions concerning the application of high hydraulic gradients (Foreman and Daniel, 1986; Bowders and Daniel, 1987; Uppot and Stephenson, 1989; Yanful et al, 1990) during tests with fine grained materials (clays). The implications arising from the results, shown in Figure 4.2, are severe. Judgement based solely on the criteria widely accepted for clay barriers, i.e.: $k < 10^{-7}$ **cm/s** (Zimmie, 1981; Eklund, 1985; Harrop-Williams, 1985), and using the results obtained with samples **TSBPbI3C3BP** or **TSBPbI3C3NB** ($k \approx 10^{-9}$ cm/s), where high initial gradients were applied ($i = 100$), would indicate that the S/B mixture tested easily qualifies as an engineered barrier material. However, if the results obtained with samples **TSBPbI1C3(3)** and **TSBPbI1C3(5)** (initial $i = 25$; $k \approx$

1.0 to 6.0 x 10^{-7} cm/s) are considered, the judgement would be highly tempered, and would perhaps lead to rejection of the material for use as a barrier material.

Effect of Saturation

The influence and importance of saturation, which is intimately related to clay-water forces (including suction), is discussed in more detail in Section 4.1.2.2. It is important to note here that despite the similarity between the k values obtained for samples **TSBPbI3C3BP** (saturated by back pressure) and **TSBPbI3C3NB** (saturated by flushing with 2 pore volumes of distilled water) - $k \approx 10^{-9}$ cm/s - the importance of saturation, which increases with increasing activity of the clay fraction of the material, should not be diminished. In the present case, the effect of a high initial gradient, eventually leading to pore constriction, possibly prevails over the effect of saturation.

Effect of Concentration

A sample was tested to evaluate the influence of a lower concentration of *Pb* (550 ppm instead of 2500 ppm) on the coefficient of hydraulic permeability. The k value obtained was in the order of 10^{-8} cm/s, as shown in Figure 4.6. This value is one order of magnitude lower than the permeabilities obtained in the test series reported in Figure 4.2 (two upper curves), for the same initial gradient of 25. **As indicated in the graph, the calculated k-value of sample TSBPbI1C1 was not**

significantly affected by an increase, and subsequent decrease, in the applied gradient (except for a minor variation possibly due to pressure adjustments following a change in i). **To confirm the results, another sample was installed in the triaxial cell, and a test with the same characteristics was performed.** The total densities of the samples were 19.1 kN/m^3, the initial water contents 18.6%, and initial void ratios 0.65.

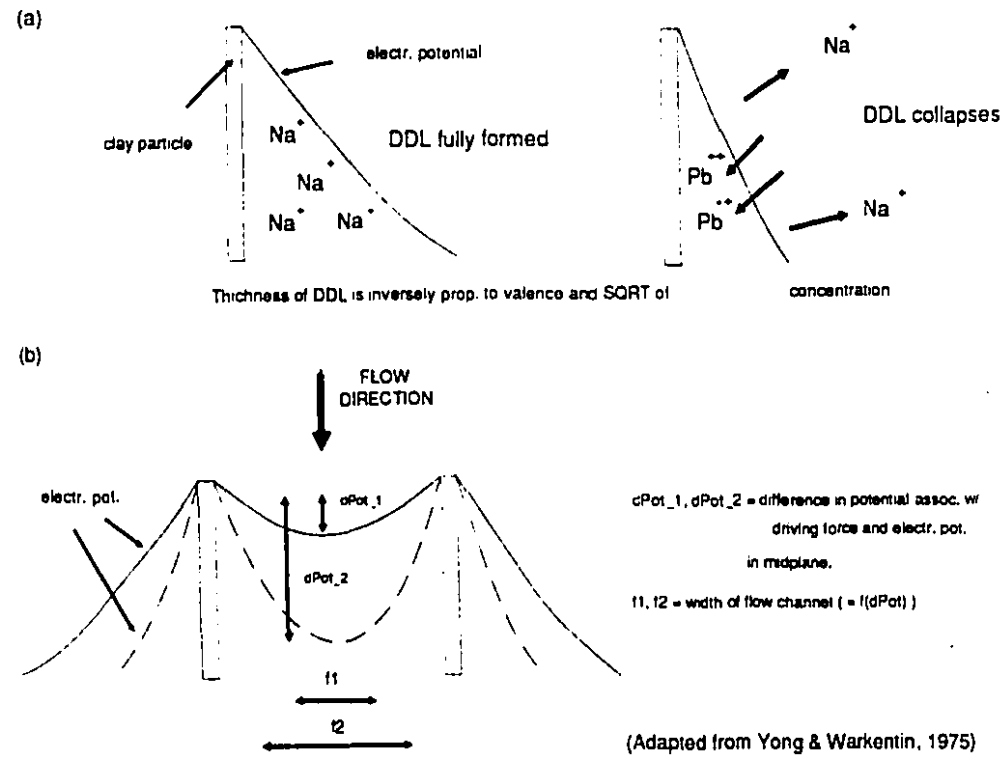

Figure 4.5 - Schematic Presentation of: a) DDL collapse due to cation exchange; b) the influence of changes in surface potential due to DDL collapse in flow characteristics.

The lower k value obtained with the lower Pb concentration is not unexpected in the light of the Gouy-Chapman diffuse double layer (**DDL**) theory (Yong and

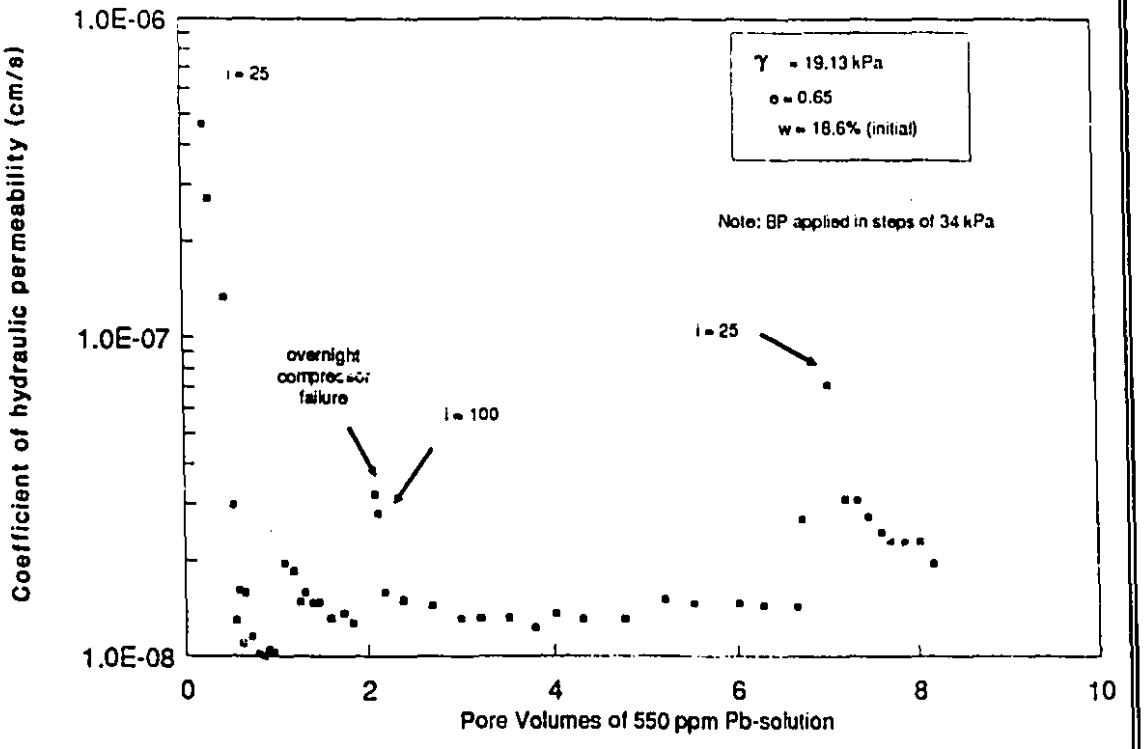

Figure 4.6 - Variation of the Coefficient of Hydraulic Conductivity of Sample **TSBPbI1C1** (Tested in the Triaxial Cell).

Warkentin, 1975; Greenland and Hayes, 1978; Sposito, 1984), which predicts that the DDL thickness (Verwey and Overbeek, 1948) is inversely proportional to the valence and to the square root of the concentration of the participating ions. The schematic diagram in Figure 4.5 shows the reduction in the DDL due to the replacement of *Na* (monovalent) by *Pb* (divalent) by effect of valence and concentration according to the Donnan principle applied to cation exchange (Greenland and Hayes, 1978). Interpenetration of the DDL, shown in the lower diagram, will produce greater or

lesser midplane (electric) potentials, depending on the species and concentration of the dissolved solutes. The magnitude of the midplane potential is indicative of the resistance to flow through the pore space between the two interacting particles (Yong and Samani, 1988). In general terms, the greater the DDL collapse, the easier the solution percolates. In the case of sample **TSBPbI1C1** (Figure 4.6), percolated with a 550 ppm lead solution, the collapse of the DDL was not as important as for samples **TSBPbI1C3(3)** and **TSBPbI1C3(5)** (Figure 4.2), percolated with a $\pm$ 2500 ppm lead solution. Thus, the calculated k of the former is expected to be lower than the k for the latter two, which was in fact observed during the tests.

This can be also visualized by the greater packing of *Pb* ions near the surface of the bentonite particles (in the Stern layer) as a result of higher concentrations of *Pb* in the contaminant solution (see Apeendix G).

The effect caused by the introduction of a contaminant can also be evidenced if the results shown above are compared with those obtained by Fernuik and Haug (1990), who tested a sand/bentonite mixture (92% Ottawa sand and 8% sodium bentonite) in a triaxial cell, under hydraulic gradients varying from 25 to 48, to obtain a permeability to **distilled water** of 4.0×10^{-9} cm/s. Despite the fact that test conditions are similar to those of samples **TSBPbI1C3(3)** and **TSBPbI1C3(5)** (Figure 4.2), their results are almost two orders of magnitude lower, indicating that the concentrated *Pb* solution used here may have affected the structure of the samples due to collapse of the DDL, as explained above.

Effect of Precontamination

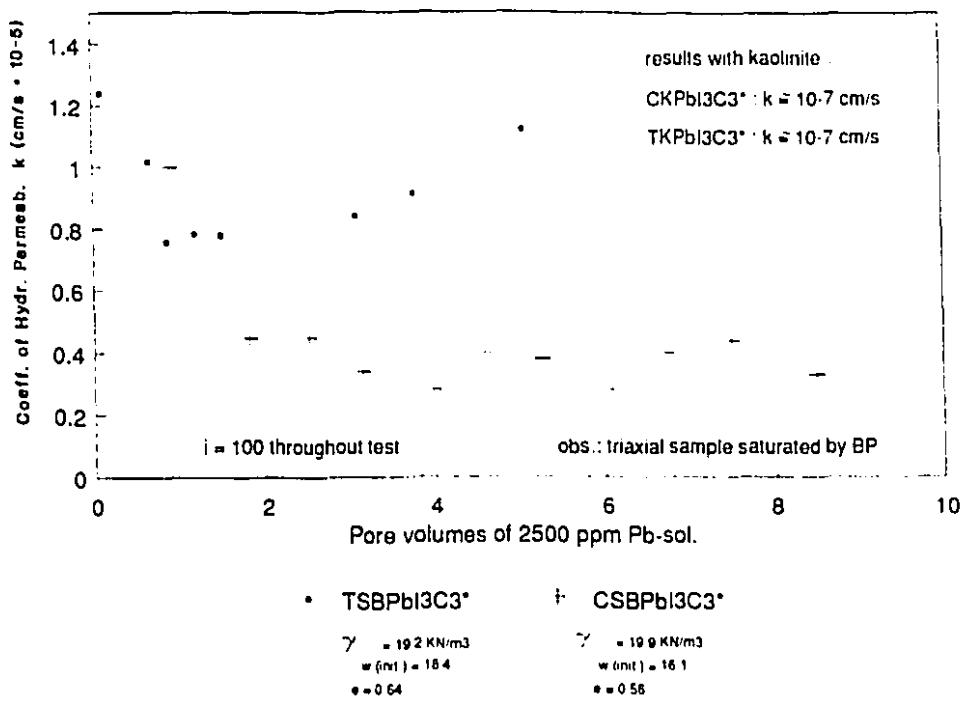

Figure 4.7 - Variation of the Coefficient of Hydraulic Conductivity of Precontaminated Samples Tested with Both Permeameters.

The effect of precontamination was also evaluated and the results of two tests, one for each permeameter, are presented in Figure 4.7. The results of similar tests performed with kaolinite samples are also shown.

Rather than mixing dry material with distilled water, a concentrated *Pb* solution (2500 ppm) was utilized. This is an intermediate situation between batch equilibrium tests, where all soil particles are in contact with the contaminant in solution and the leaching of contaminant through 'non-precontaminated' compacted samples.

Samples were compacted to virtually the same density and initial water content as the other S/B samples. A hydraulic gradient of 100 (**I3**) was then applied to a concentrated *Pb* solution (**C3** $\approx$ 2500 ppm).

The results show that the k values of the precontaminated samples were significantly greater than all other tests conducted with S/B mixtures. The apparent difference of less than one order of magnitude in k values obtained with the two permeameters, after the second pore volume was leached, may eventually be related to the greater degree of saturation of the triaxial cell sample (refer to *Effect of Saturation* in Section 4.1.2.2).

Since the soil was mixed with a *Pb* solution rather than distilled water, it was expected that the fabric produced after compaction was different, with the collapse of the DDL due to cation exchange being more effective, leading to a k quite higher than in the case of the other compacted samples.

The fact that the high initial gradients applied (**I3** = 100) did not cause pore constriction seems to indicate that precontamination lead to the formation of a different structure (macro and micro) from the other S/B samples. Unfortunately, this remains a hypothesis that could not be verified.

These tests reproduce the situation where the sand and the Na-bentonite are mixed with water containing significant concentrations of divalent cations that can cause collapse of the DDL. In this case, the k value obtained with distilled water in the laboratory becomes meaningless. These tests can also give an idea of the future behaviour of a S/B liner in the case it ever becomes overloaded with contaminant due to intense leaching over the years.

Sample Related Effects

Sample related problems may also affect k. An important one is related to differences in moisture content inside them, which is very difficult to avoid during sample preparation, mainly in the case of sand/bentonite mixtures. Non-uniformly distributed moisture zones may lead to preferential flow, thus masking the real k of the material. According to the results shown in Table 3.3, this seems not to be a problem here. Compacting wet of the Proctor optimum lessens this kind of problem (Mitchel et al, 1965; Dunn and Mitchell, 1984).

Bacterial growth may also affect flow (Gupta and Swartzendruber 1962, in Mitchell and Younger, 1967; Edil and Erickson, 1985; and references cited by the latter). Figure 4.8 presents a photograph of sample **TSBPbI1C1** after termination of test. Dark spots in the region of contact with the membrane may reveal some bacterial growth. Due to the relatively small areas occupied by these dark spots, it is not probable that bacterial growth has affected the results significantly. Nevertheless, this effect should be considered in the design of a clay barrier.

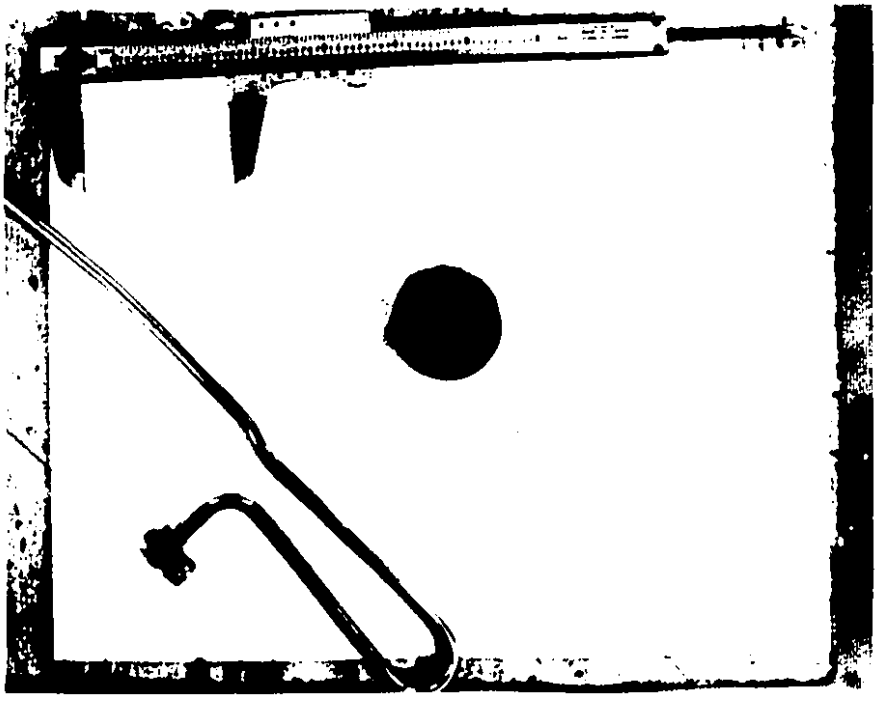

Figure 4.8 - Photograph of sample **TSBPbI1C1** after termination of a permeability test that lasted 180 days. Dark spots on the edges of the sample may reveal bacterial growth.

Effect of Type of Contaminant

A permeability test was performed with a concentrated *Zn* solution ($\approx$ 2000 ppm of *Zn*). This concentration is of the same magnitude of the highest lead solution concentration ($\approx$ 2500 ppm). The results are shown in Figure 4.9. The sample had practically the same total density (19.2 kN/m^3) and initial water content (18.3%) of the other S/B tests. The calculated initial void ratio was also the same. Saturation

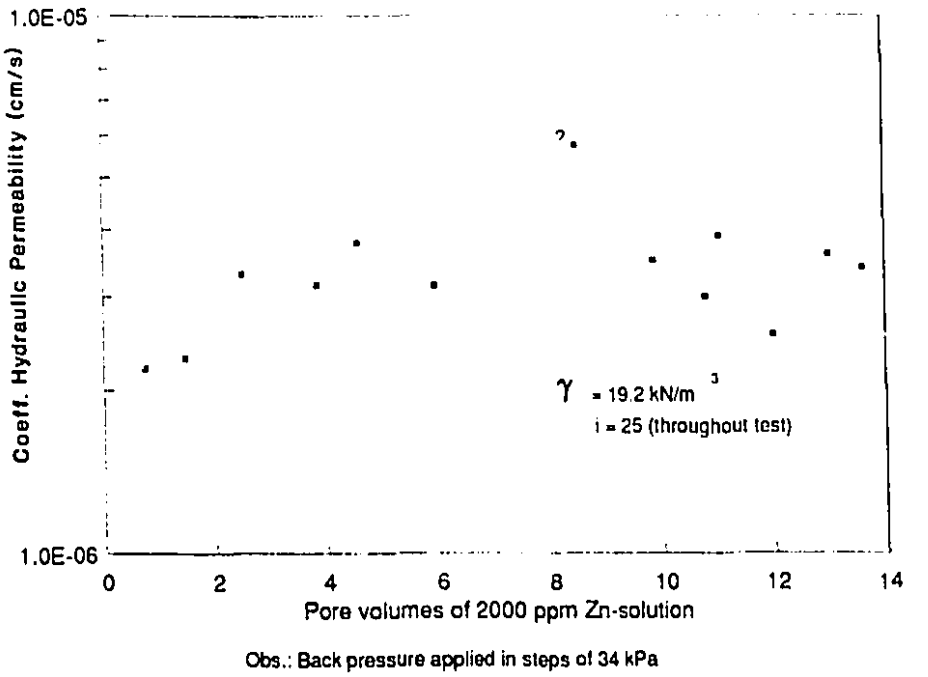

Figure 4.9 - Variation of the Coefficient of Hydraulic Conductivity of Sample **TSBZnI1C3** (Tested in the Triaxial Cell).

was performed by back pressuring, following the same procedure used for the other samples. The measured B-value in the end of the saturation phase was 0.93. The lowest gradient of the range used in this experimental work (**I1** = 25) was applied to the sample. The volume rates entering and leaving the sample, as well as the pressures applied were monitored throughout the tests. The excess chamber pressure of 13.6 kPa ensured that no leaks between the membrane and the sample could occur.

The graph in Figure 4.9 shows that the calculated coefficient of hydraulic permeability, rather than equilibrating at a lower value, increased to level off at a quite high $k \approx 3.0 \times 10^{-6}$ cm/s. In order to confirm these results, the test was repeated following exactly the same steps. A total of 4.1 pore volumes were percolated and the stabilized k was 5.7×10^{-6} cm/s.

Considering similar test conditions, i.e., **I1** = 25 and the use of very high heavy metal concentrations, the k value obtained for the *Zn* test (Figure 4.9) is one order of magnitude higher than the highest k calculated for S/B tested with *Pb* in the triaxial cell (Figure 4.2)

The higher permeability of S/B samples to concentrated *Zn* solutions can be partly explained using the Boltzmann equation and the results obtained by Alammawi (1988).

The Boltzmann equation can be written in the following way:

$$C_1 = C_2 \exp\left[\frac{(E_2 - E_1)}{kT}\right] \qquad (4.1)$$

where:

$C_1 \equiv$ concentration of cations in the inner Helmholtz plane (ions/m^3);

$C_2 \equiv$ concentration of cations in the outer Helmholtz plane[2] (ions/m^3);

$k \equiv$ Boltzmann constant (1.38×10^{-16} erg/°K);

---

[2] According to Grahame (1947), the outer Helmholtz plane defines the outer boundary of the Stern layer, where the Gouy distribution of ions begins.

$T \equiv$ temperature (°K);

$kT = 0.4 \times 10^{-20}$ J/ion at 20°C; and

$E_1, E_2 \equiv$ the potential energies of the ions in the two planes.

Alammawi (1988) calculated the difference ($E_2 - E_1$) for several elements, including *Pb* and *Zn*. According to his results, ($E_2 - E_1$) was greater for *Zn* than for *Pb*. It can be seen from the Boltzmann equation, that the greater the potential energy difference, the greater the number of ions in the inner Helmholtz plane (C_1). This means that, out of the total quantity of cations adsorbed, more are adsorbed close to the particle surface, in the Stern layer (**high affinity adsorption**), and less are in the diffuse layer. This implies a smaller DDL thickness; therefore the potential in between particles to be overcome by the percolating fluid is lower, which facilitates the flow.

The above can also be explained using the unhydrated ionic radii of *Zn* and *Pb*. Since the first is smaller than the latter (Elliott et al, 1986), there is a potential for developing a more packed arrangement of *Zn* ions very near the surface (inner Helmoltz plane) where ions lose part of their hydration shell (Grahame, 1947; Greenland and Hayes, 1978).

One can argue that the nature of the ligand[3] might have influenced the results (the *Zn* solution was prepared with $ZnSO_4 7H_2O$, whereas *Pb* solutions were prepared with $Pb(NO_3)_2$). Ligands compete with the charged surfaces for the soluble *Zn* (formation of *Zn* complexes) rendering the metal less available to adsorption (more mobile). In fact, Farrah and Pickering (1976) presented a series of results indicating that the presence and nature of the ligand caused a decrease in the *Zn* adsorbed by several types of soils, including montmorillonite. The maximum decrease occurred in the presence of chelating agents, like EDTA.

However, Elrashidi and O'Connor (1982) presented evidence that it is unlikely that complex formation cause measurable changes in *Zn* adsorption when the metal is associated with 0.005 to 0.1 M solutions of Cl^-, NO_3^-, or $SO_4^=$. A 0.1 M solution of $SO_4^=$ is equivalent to 9600 ppm, which is a much higher concentration of this ligand than used in this study.

4.1.2.2 - S/B Tested in the Consolidation Cell

Figure 4.10 presents some results of permeability tests performed with the consolidation cell. All samples were compacted to almost the same total density (between 19.7 and 19.9 kN/m^3), and saturated by flushing approximately 2.5 pore volumes of distilled water.

---

[3] Ligands are ions or molecules that act as Lewis bases, i.e., electron pair donors. Example: NO_3^-, $SO_4^=$, Cl^-, *etc.*

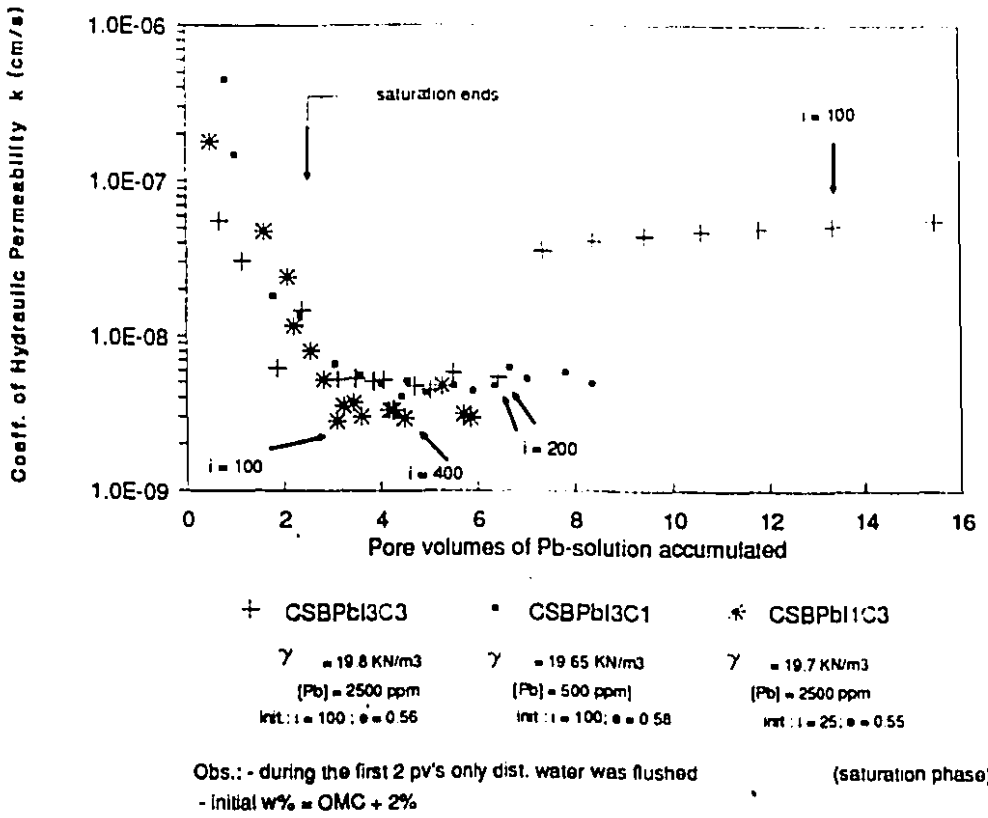

Figure 4.10 - Variation of the Coefficient of Hydraulic Conductivity of Sand/Bentonite Samples Tested in the Rigid Wall Permeameter (Consolidation Cell).

Sample **CSBPbI3C3** was percolated by a highly concentrated *Pb* solution (**C3** ≈ 2500 ppm) under an initial gradient **I3** = 100. Sample **CSBPbI3C1** was percolated by a much less concentrated *Pb* solution (**C1** ≈ 600 ppm) under the same initial gradient **I3** = 100. Finally, sample **CSBPbI1C3** was percolated with the more concentrated (**C3**) solution under a lower initial gradient **I1** = 25.

A common trend could be identified in the results of all three tests shown in Figure 4.10: the coefficient of hydraulic permeability decreased steadily during

saturation to level off at $k \approx 1.0 \times 10^{-8}$ cm/s at the end of the saturation phase. Upon permeation of the contaminant, k continued to decrease and stabilized at $\approx 5.0 \times 10^{-9}$ cm/s, for samples **CSBPbI3C3** and **CSBPbI3C1**, and at $\approx 3.0 \times 10^{-9}$ cm/s for sample **CSBPbI1C3**. These are the same k-values, for all practical purposes. An increase in the applied gradient after permeation with 4 pv's of *Pb* solution (total of 6.5 pv's) caused the k of sample **CSBPbI3C3** to increase to approximately 3×10^{-8} cm/s. For the other two samples (**CSBPbI1C3**, tested under a lower i, and **CSBPbI3C1**, tested with a less concentrated *Pb* solution than sample **CSBPbI3C3**) no changes in the calculated k were observed following increases in the applied gradient. Yong et al (1991) and Weber (1991) analyzed these tests in more detail.

Effect of Saturation on the k value

The influence of the degree of saturation on k has been investigated by several authors.

Yong and Warkentin (1975) and Elzeftawy and Cartwright (1981) find it more appropriate to relate k to the volumetric water constant (θ), because flow occurs due to the existence of a difference in soil-water potential (ψ)[4] within the soil, which in turn is a function of the soil water content (Yong and Warkentin, 1975). In

[4] ψ is a summation of several individual potentials, of which the osmotic, matric and gravitational potentials "are most often considered as being sufficient in describing ψ (Yong and Mohamed, 1991)."

unsaturated conditions, the driving forces for flow to occur must exceed the forces holding water to the soil particles (Yong and Warkentin, 1975), i.e., the clay-water forces[5]. Once the system is 'satisfied' with water, its free energy is at a minimum (Yong and Warkentin, 1975), and the internal gradients associated with suction[6] are no longer acting against the flow of water through and out from the sample.

Mitchell et al (1965) observed that "other conditions being equal [e.g.: density or void ratio], the higher the degree of saturation the greater the permeability", with higher degrees of saturation being associated with higher pore pressures. They obtained a one order of magnitude difference in k between the results of tests with and without back pressure application.

Klein et al (1983) obtained a several orders of magnitude change in the calculated k with the increase in the degree of saturation (Figure 4.11) during tests to estimate the unsaturated hydraulic conductivity of a brown sandy silt (loess) and a grey sandy clay (glacial till).

In the case of tests performed in the consolidation cell, the small differences in volume rates entering and leaving the samples indicated that saturation continued

---

5 "The presence of these forces, demonstrated in terms of double-layer and diffuse ion layer water, in effect create immobilized hydrodynamic layers of water surrounding each particle, [the thickness of which] depend on the interaction characteristics of the soil-water system [and] on the driving forces inducing flow (Yong and Warkentin, 1975)."

6 Soil suction is numerically equal to **soil water potential** with opposite algebraic sign (Yong and Warkentin, 1975). It includes matric suction and the suction due to osmotic gradients. The latter is associated with chemical potentials. "The matric suction may result from surface tension forces, from forces binding water to clay mineral surfaces, and from forces holding water to exchangeable ions (Yong and Warkentin, 1975)."

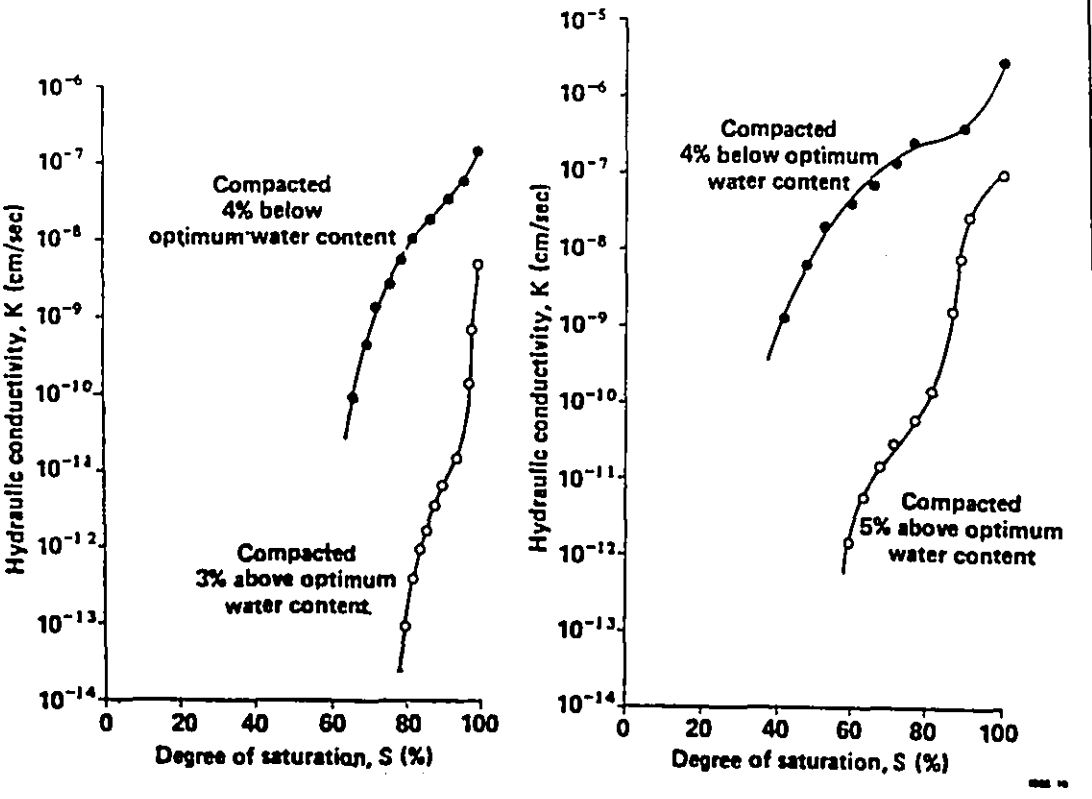

Figure 4.11 - Hydraulic Conductivity x Degree of saturation for: (a) a brown sandy silt (loess); and (b) grey sandy clay (glacial till). From Klein et al (1983).

to occur throughout the duration of all tests with S/B. It seems thus clear that the *k*-values obtained under such circumstances were not the saturated coefficients of hydraulic permeability, and that steady-state conditions were not achieved[7].

Considering the results presented in Figure 4.11, and the discussions above, it seems thus reasonable to associate the lower *k* obtained during tests with the consolidation cell with incomplete saturation of the samples.

[7] A significant amount of air was observed in the effluent lines.

Even though the calculated final degrees of saturation were very close to S = 100% (S = 74 to 79% in the beginning of tests), **B**-values could not be measured in the rigid wall permeameter to confirm the 100% saturation obtained by calculation.

In other terms, these lower *k*-values can be explained in terms of the internal gradients that develop suction forces, with higher suction associated with lower degrees of saturation (Chahal and Yong, 1965), or lower volumetric water contents (Chahal and Yong, 1965; Yong and Warkentin, 1975).

It is also expected that the flow rate during tests in the consolidation cell (unsaturated condition) should be lower than that of tests conducted in the triaxial cell (saturated), all other conditions remaining equal. Since the Darcy's velocity - thus *k* - is obtained based on the flow rate: $k_{cons.} < k_{triaxial}$.

The effective porosity - another parameter affecting permeability (Yong and Warkentin, 1975) - may have changed due to an eventual pore blockage induced by the displacement of particles or clusters, which in turn was caused by the application of high hydraulic gradients. In that case, chemico-osmotic gradients (Olsen, 1972), which are more significant for active clays like bentonite, may have had a potential influence in the low *k*-values calculated using the Darcy's law.

Combined Effects of Gradient and Concentration on k

Before increasing the hydraulic gradient of sample **CSBPbI3C3** to 200, the calculated *k* for the 3 samples shown in Figure 4.10 were very similar. Since gradient

variations with samples **CSBPbI1C3** and **CSBPbI3C1** did not lead to significant changes in the calculated *k*-value, it is possible that the combined effects of concentration and application of a very high hydraulic gradient (i=200) caused the one order of magnitude change in *k* observed during test with sample **CSBPbI3C3**.

4.1.3 - Permeameter Performance: *k*-test

Despite the same initial densities, water contents, void ratios, and hydraulic gradients applied (i=25), the final *k*-value obtained for sample **CSBPbI1C3** (Figure 4.10) differed by more than two orders of magnitude from those calculated when the triaxial cell was used, e.g.: tests with samples **TSBPbI1C3(3)** and **TSBPbI1C3(5)** (Figure 4.2). The consolidation cell sample was 'saturated' by flushing with approximately 2.5 pore volumes of distilled water, whereas the triaxial cell samples were saturated by back-pressuring. As mentioned above, unsaturated conditions prevail during tests conducted in the consolidation cell.

Based on the preceding discussions, it can be argued whether incomplete saturation of the samples - rather, the effect of suction forces - is the most reasonable cause for the persistently low *k*-values calculated in the consolidation cell for S/B samples.

In the case of tests with kaolinite, this particular effect was not as important because the suction forces (matric and osmotic) involved, are not as important as in the case of montmorillonite clays. Previous studies (e.g.: Chahal and Yong, 1965;

Yong and Warkentin, 1975) have presented sufficient data indicating that, for the same volumetric water content, higher suction are associated with smaller particle sizes.

If the worst scenario of contaminant transport is to be reproduced during laboratory permeability testing, it is highly desirable to achieve the most complete saturation possible of the barrier material being tested. In this case, back pressuring is the most convenient technique, but it cannot be used for consolidation cells without the high risk of side wall leakage (Edil and Erickson, 1985).

Advantages and Disadvantages of the Two Apparatus

Table 4.2 summarizes most of the advantages and disadvantages of the two cells.

One of the disadvantages of the flexible wall permeameter is related to the high confining pressures needed when tests are performed under high gradients (Madsen and Mitchell, 1989; Daniel et al, 1985). According to Bowders et al (1986) and Madsen and Mitchell (1989), confining pressures in excess of those expected in actual field conditions will tend to close any possible shrinkage cracks that may be developed due to clay-contaminant interactions. On the other hand, tests conditions within rigid wall permeameters are such that these cracks will not be closed, and a very large increase in the calculated k can be noticed.

	Advantages	Disadvantages
Flexible Wall (triaxial cell)	- possibility of complete saturation; - no side wall leaks; - control over total stresses.	- equipment more costly*; - longer tests unless high gradients are applied (*sic*)
Rigid Wall (consolidation cell)	- short duration of tests; - less costly equipment.	- potential for side wall leaks; - lack of provision for effective saturation; - difficulty of performing tests under low effective stresses.

* see observation by Christiansen (1985) in the end of Chapter 5.

Table 4.2 - Main Advantages and Disadvantages of the Flexible Wall and Rigid Wall Permeameters (basic ref.: Daniel et al, 1985).

It is relevant to note that shrinkage cracks have been widely reported only for tests involving interactions between clays and non-polar organic chemicals (Madsen and Mitchell, 1989; Bowders and Daniel, 1987; Brutsaert, 1987; Foreman and Daniel, 1986; Acar et al, 1985; and others). In these cases, a collapse of the DDL may occur because most organic compounds have lower dielectric constants than water (Madsen and Mitchell, 1989).

Only inorganic contaminants were used in this research work, and no shrinkage cracks were observed following visual inspection of the samples tested in the consolidation cell.

4.2 - Chemical Analyses

Following the extrusion procedure described in Section 3.5.5, samples were sectioned after termination of permeability tests. Chemical analyses were then performed with the material of the slices, the pore fluid, and the leachate collected during permeability testing.

The type of chemical analyses presented herein are fundamental in the evaluation of the compatibility between soil and permeant. They can be used as tools in the prediction of the retention capability of a soil and how the contaminants are retained.

The results of these analyses were used to: construct the profile of contamination of the samples; breakthrough curves for the material; the adsorption curves for compacted kaolinite; and to compare the performance of the two permeameters in terms of their ability to reproduce the most realistic profile of retention for the materials. The profile of contamination is important in the evaluation of the long term performance of clay barrier materials.

In order to give support to the results obtained, an ion mass balance was calculated for each test.

The appropriateness of the use of adsorption isotherm parameters in contaminant transport modelling is analyzed in light of the results obtained with compacted samples and soil suspensions.

Another relevant scientific issue was addressed: based on an adaptation of the Double layer model to account for hydration energies at small separation distances between particles (Yong and Mohamed, 1991; Alammawi, 1988), the theoretical concentrations of *Pb* adsorbed by S/B suspensions were calculated. The results were compared to the experimental results in order to evaluate the proportions of *Pb* specifically adsorbed in the Stern layer (high affinity adsorption). The occurrence of high affinity adsorption, which involves high adsorptive energies, can partly explain the differences obtained as a result of mass balance calculations (Section 4.2.5).

4.2.1 - Compacted Samples

The material from each sample slice was first washed with distilled water, in order to recuperate the contaminated pore fluid: an 'extracting' solution (ammonium acetate) was then mixed with the material in order to recuperate the adsorbed *Pb* (or *Zn*) and the remaining Na^+, K^+, Ca^{++}, Mg^{++}, and Al^{3+} (the latter for kaolinite only). The supernatant obtained after centrifugation was then analyzed by atomic absorption spectrophotometry (AAS) for Pb^{++} (or Zn^{++}), Na^+, K^+, Ca^{++}, Mg^{++}, and Al^{3+} (kaolinite only). The exchangeable-H^+ was obtained for kaolinite. The pore fluid was analyzed only for Pb^{++} (or Zn^{++}) ions. The experimental procedures were described in detail in Section 3.6.2.

The term **'adsorption characteristic of compacted materials'** is proposed as a suitable terminology to describe the curve representing the partitioning of

contaminants between the solid and liquid phases when the solid phase is not in a suspension (as is normal when partitioning studies are undertaken), but in the compacted form. In this fashion, adsorption/desorption phenomena taking place in an actual situation is more realistically reproduced.

Triplicates were made for each one of the slices of a sample. Every point in each graph represents the average of three values.

4.2.1.1 - Compacted Kaolinite

Figures 4.12 and 4.13 present the adsorption isotherms of kaolinite for tests performed in the triaxial and consolidation cell, respectively. The upper curves in each figure are the same as the isotherm presented in Figure 3.2, and were obtained by performing batch equilibrium tests (soil suspensions used). The others were constructed using the results of chemical analyses made with the compacted samples.

The equations of all curves were obtained by power curve fitting using the non-linear Freundlich model (Helfferich, 1962; Greenland and Hayes, 1978). The relatively high correlation coefficients (R^2) obtained indicate the capability of the Freundlich formulation to model the adsorption characteristics of the kaolinite used in this study. As mentioned in Section 3.1.2, this model was chosen mainly because it has been widely used in environmental geotechnology.

Adsorption curves of compacted kaolinite were constructed using *Pb* adsorption results obtained from the respective slices of the samples (refer to section

E.11 of the Appendix E for an example of calculation). The latter were designated, in the case of the triaxial cell: **T** for top, **M** for middle, **B** for bottom, and **B(s)** a very slim slice taken from the lowest part of the sample. For compacted samples tested in the consolidation cell, *Pb* adsorption was obtained for the Top and Bottom slices only, in view of the small sample thickness.

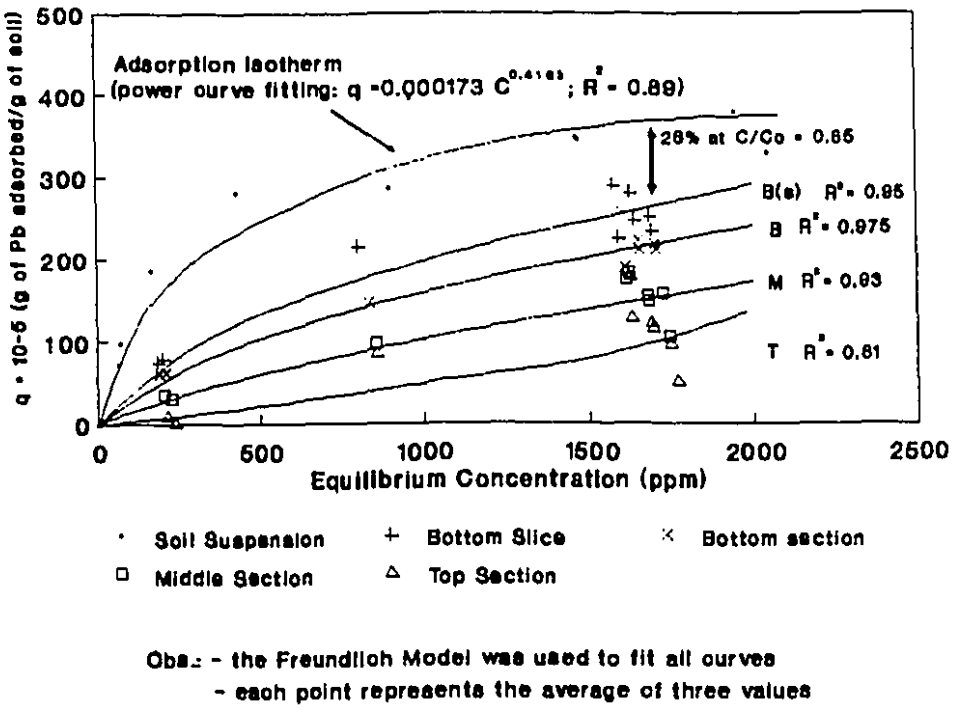

Figure 4.12 - Adsorption Characteristic Curves for Compacted Kaolinite. Tests Performed in the Flexible Wall Permeameter.

It can be seen from Figures 4.12 and 4.13 that the quantities of *Pb* adsorbed by the compacted kaolinite samples at various input permeant concentrations are less

than quantities which characterize the adsorption isotherm of the material. The differences in *Pb* adsorption are due primarily to availability of exposed clay particle surfaces. This reasoning argues that in soil suspensions, where all dispersed clay particles can contact the dissolved contaminant, accumulation processes are at its optimum. In the case of compacted materials, however, aggregate and cluster formation will considerably decrease the effective specific surface area, thus severely hampering adsorption and/or exchange. The permeant fluid will preferably flow around rather than through these clay structures (Olsen, 1962).

The effect of dissolved solutes in the compacted soil system can also be high. In the present case, the dissolved solutes are composed mainly by the exchangeable cations, whose concentrations are relatively high. These cations will compete for the excahangeable sites, resulting in lower retention of *Pb*, or a lower K_d [8].

Even in the cases where almost total breakthrough was reached, a significant difference was observed between the maximum quantities adsorbed by the compacted material (**B(s)** or **B** slices) and the soil suspension, as given by the adsorption isotherm. This is the case of sample **TKPbI3C3b**, for which $C/C_0 \approx 0.85$ after 10 pore volumes of the highest permeant concentration (**C3** $\approx$ 1750 ppm) were leached (Figure 4.15): the **B(s)** slice adsorbed 26% less than the soil in a suspension. In the case of sample **CKPbI3C3**, the **B**ottom slice adsorbed nearly 35% less than the soil in suspension after 5 pore volumes were leached to a final $C/C_0 = 0.75$ (Figure 4.15).

---

[8] This effect is particularly important in the case of S/B. The discussions that follow, as well as the conclusions of Appendix G will make it more clear.

A comparative analyses between the results obtained with the two permeameters is given in Section 4.2.2 (*Permeameter Performance: Retention*).

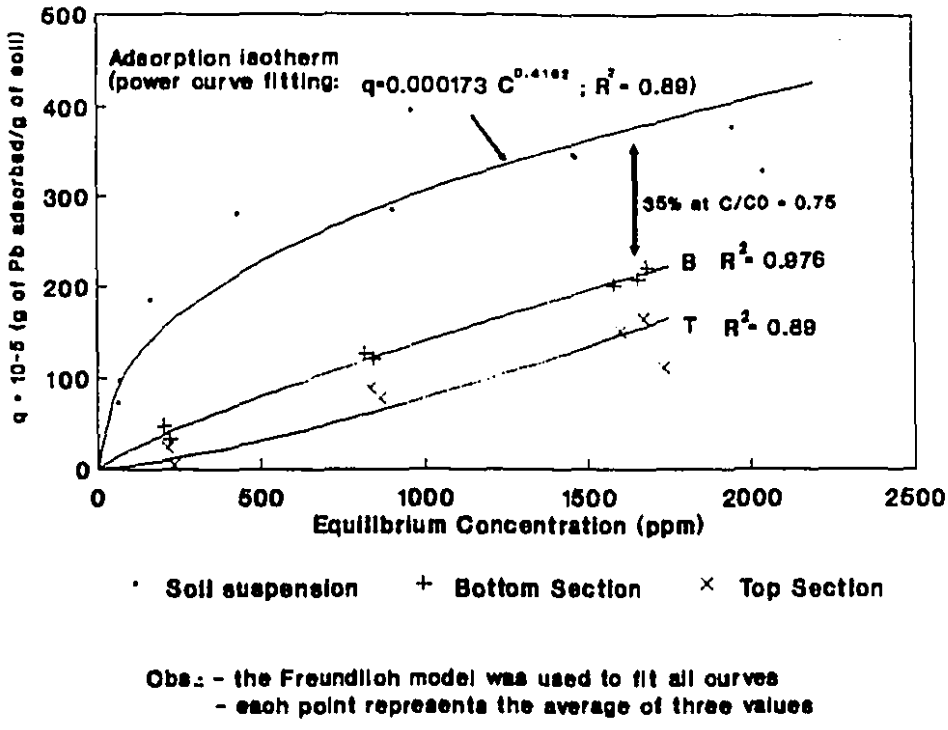

Figure 4.13 - Adsorption Characteristic Curves for Compacted Kaolinite. Tests Performed in the Rigid Wall Permeameter.

The difference between quantities retained by soil suspensions and compacted materials is even more important at low concentration levels (approximately 50% at C1 ≈ 250 ppm). It can also be noted a significant drop in the amounts of lead adsorbed along kaolinite samples. For example, in the case of the test with sample **TKPbI3C3b**, extended until almost total breakthrough was reached ($C/C_0 \approx 0.85$),

the difference in *Pb* adsorbed between the **B(s)** section, where the permeant is introduced, and the **Top** slice is quite significant (60%), reflective of the accumulation processes occurring within the sample.

The difference in quantities adsorbed between the **B(s)** layer and the **Bottom** sections (in g_{ads}/g_{soil}, to account for size differences) is also noticeable; this confirms the results obtained by Warith (1987), Griffin et al (1976), among others, who observed that heavy metals are retained in the first centimetres of clay barrier materials.

4.2.1.2 - Compacted Sand/Bentonite

The Freundlich model was also found to fit the adsorption isotherm for the S/B mixture, as can be seen in Figure 4.14 (the curve is the same presented in Figure 3.3). The experimental program with this material was not as extensive as that of kaolinite, because of the time requirement to perform permeability tests with S/B. Consequently, the results of tests involving both permeameters were condensed in Figure 4.14. An adsorption curve for the compacted material was not constructed due to the limited amount of data available.

Similarly to the results obtained for kaolinite, the compacted S/B samples adsorbed less lead than the quantities which characterize the material's adsorption isotherm. For example, the **Bottom** slice of sample **TSBPbI1C3(3)** - a test conducted until $C/C_0 = 0.7$ in the triaxial cell (Figure 4.16, presented later) - retained 20% less

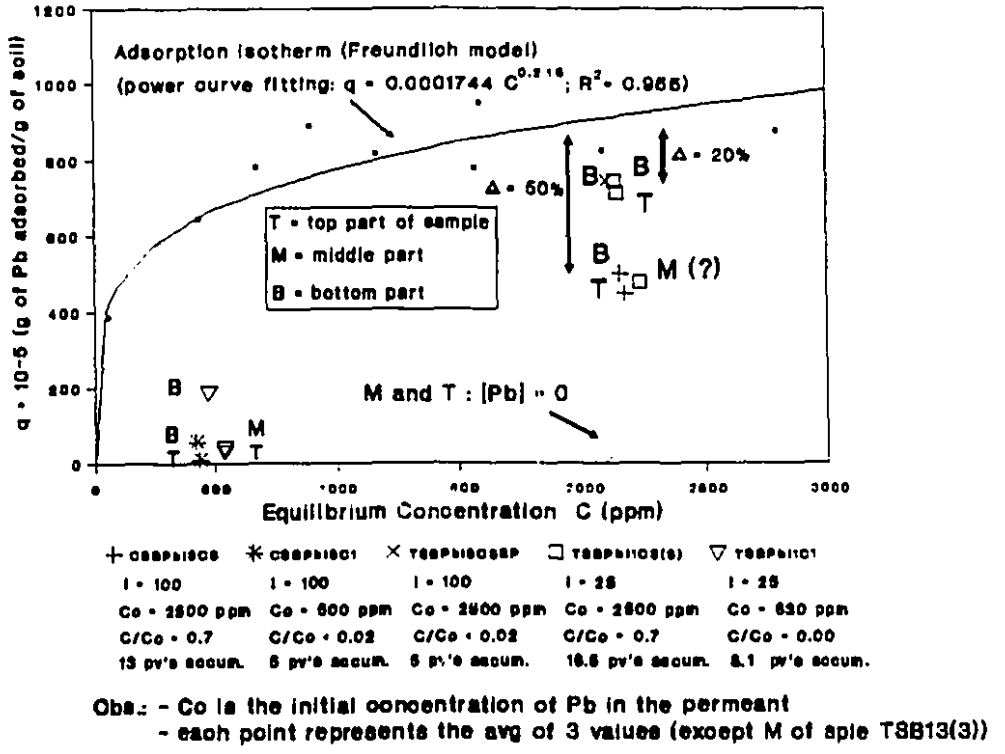

Figure 4.14 - Adsorption of Lead by Sand/Bentonite (90%/10%).

than the amount adsorbed by the soil in a suspension. The Top retained 23% less. In the case of sample **CSBPbI3C3**, tested in the consolidation cell, the Bottom slice adsorbed almost 50% less than the soil in a suspension, after $C/C_0 = 0.7$ and 13 pore volumes had been percolated (Figure 4.16).

As for kaolinite, the differences in amounts adsorbed by compacted material and soil suspension are partly due the total exposed surface of clay particles, which is reduced by aggregate and cluster formation.

Another possible explanation for the observed difference refers to high affinity adsorption in the Stern layer (see Appendix G). In this case, part of the adsorbed *Pb* may not be 100% desorbed (or 'extracted') by the ammonium acetate due to the high energy level of adsorption involved: specific adsorbed *Pb* ions may not be displaced by NH_4^+ ions of the extracting solution. As a consequence, the remaining *Pb* ions are not found in the supernatant obtained after extraction procedure, and a lower concentration of *Pb* is obtained by AAS. Farrah and Pickering (1978) presented results indicating that ammonium acetate (at pH =7.0) was not able to extract all the lead adsorbed on montmorillonite in the case adsorption occurred at a pH near 7.0 (see also ***Pb* Mass Balance** in Section 4.2.5).

The contrast between adsorption of *Pb* by S/B suspension and compacted S/B samples is more significant at low concentration levels, as is the case for kaolinite. However, there seems to have a less marked drop in the amounts retained along the profile of S/B samples than in the case of kaolinite samples, as indicated by the adsorption patterns of samples **TSBPbI1C3(3)** and **CSBPbI3C3**. These tests continued until $C/C_0 = 0.7$ (Figure 4.14). The quantities retained in the **T**op portion of the samples are not very different from those adsorbed in the **B**ottom, possibly because S/B samples are shorter than kaolinite samples. The **T**op and **M**id slices of sample **TSBPbI3C3BP** did not adsorb any lead; all the lead was detected in the **B**ottom slice.

Although composed of only 10% of bentonite, S/B samples adsorbed significantly more *Pb* than kaolinite in absolute terms, i.e., in g_{ads}/g_{soil}. This can be partly attributed to the higher: a) cation exchange capacity (CEC); and b) specific surface area (SSA) of bentonite.

The CEC of bentonite is 109.0 meq/100g (Table 3.2); thus, in 100 g of the mixture the CEC is 10.9 meq (the contribution of the fine sand is negligible), which is more than 50 % greater than the CEC of the kaolinite.

The bentonite used has a SSA of approximately 855 m^2/g; thus 1.0 g of the mixture contains 0.1 g of bentonite and a total exposed surface of 85 m^2 (exposed surface of sand is negligible), against only 24 m^2 for 1 g of kaolinite - a ratio of approximately 3.5.

4.2.2 - Permeameter Performance: Retention

From the results presented in Figures 4.12 , 4.13 and 4.14, it seems that soils tested in the triaxial cell tend to adsorb more - in absolute terms, i.e., in g_{ads}/g_{soil} - than those tested in the consolidation cell . The verification is valid if one compares, for example, the quantities adsorbed by the bottom slices of consolidation cell samples with the bottom slices of triaxial cell samples, for tests with similar characteristics (gradient, concentration of *Pb* permeant, final C/C_0, etc.). The normalization needed to account for differences in length of flow (height of the slices) and cross-sectional areas is implicitly considered because the results are presented in terms of total mass

of solids used for the chemical analyses.

This difference in performance can be related to the fact that consolidation cell samples are not fully saturated. In an unsaturated condition, the electric double layer may not be fully developed, and the adsorbed cations (with their associated anions) "are **tightly** held by the negative charged clay surfaces" as salt precipitates (Mitchell, 1976), rendering exchange (e.g.: with Pb^{++}) more difficult.

It can be observed in Figures 4.12 and 4.14 that, for the highest concentration of *Pb*, the differences between the amounts adsorbed by soil suspensions (upper curves) and the bottom slices of samples tested in the **triaxial cell** did not change significantly, irrespective of the material tested (Δ_{kao} = 26%; $\Delta_{S/B}$ = 20%). The same cannot be said about samples tested in the **consolidation cell.** From 35% for tests with kaolinite (Figure 4.13), the difference increased to 50% for a test with S/B (Figure 4.14).

As evidenced by the much higher heat-of-wetting associated with smectites (Grim, 1968)[9], saturation affects S/B more than kaolinite. Also, part of the exchange capacity of smectites is located in the interlayer region (Grim, 1968; Mitchell, 1976); if saturation is not complete, the interlayer exchangeable cations are not easily accessible. This can also be explained in terms of the greater swelling pressures associated with high swelling clays like bentonite (Yong and Mohamed, 1991; Yong and Warkentin, 1975; Mitchell, 1976).

---

[9] The higher heat-of-wetting is in turn associated with the greater surface area of smectites, which, in simple terms, need more water than kaolinite to fully develop the DDL.

4.2.3 - Leachate Collected

The procedure for chemical analysis of the leachate collected during permeability tests was described in Section 3.6.1. The leachate collected was acidified and the concentration of *Pb* (or *Zn*) was obtained by atomic adsorption. The results were then plotted against the number of pore volumes collected.

4.2.3.1 - Effluent of Kaolinite Tests

It can be observed in the results of Figure 4.15 that *Pb* was identified in the leachate only after 2 to 3 pore volumes of highly concentrated permeant (**C3**) had been collected. As mentioned before, this shows that, despite the low buffering capacity of kaolinite (Yong et al., 1990; Phadungchewit, 1990), *Pb* retention by kaolinite does occur.

The pH of the leachate did not change much during the test, remaining below approximately 4.4. These results are analyzed in further detail further in the text (*Retention Modes - Section 4.2.6*).

4.2.3.2 - Effluent of S/B Tests

The breakthrough curves for three S/B tests are presented in Figure 4.16.

A greater number of pore volumes were necessary in order to identify any *Pb*

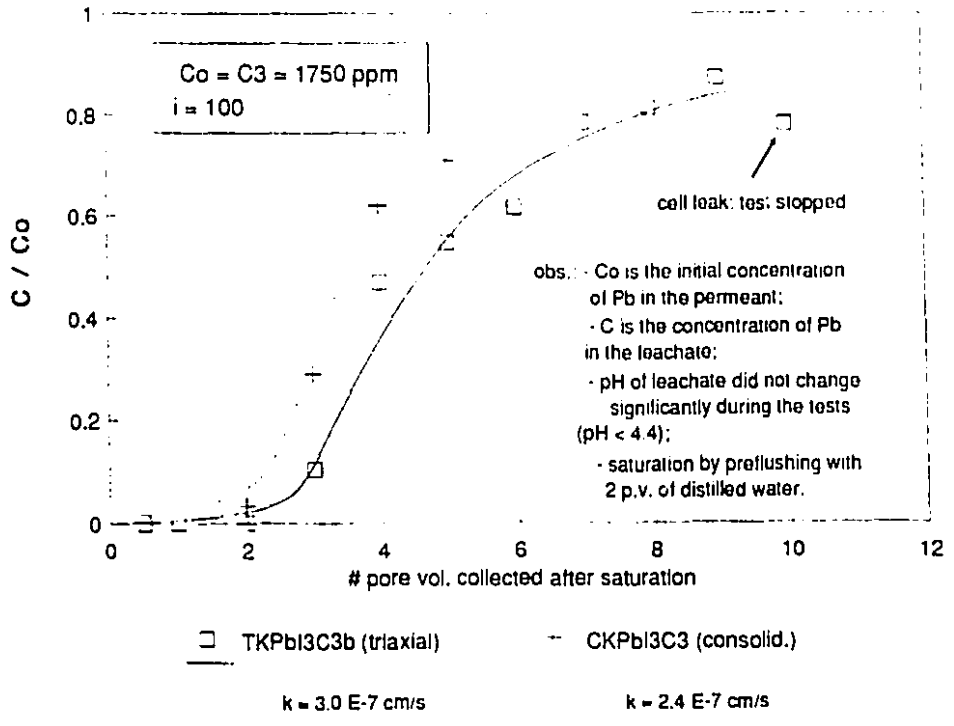

Figure 4.15 - Breakthrough Curves for Two Representative Tests with Kaolinite Samples.

in the leachate of S/B tests, 4 to 5, against 2 to 3 for kaolinite samples. This supports the remark made previously in this text that S/B samples, although composed of only 10% of bentonite retained more lead than kaolinite, or that *Pb* is not very mobile in the presence of bentonite (Warith, 1987).

The fact that zinc was detected earlier than lead in the leachate collected indicates that *Zn* is more mobile than *Pb*. This agrees with the findings of several authors, e.g.: Farrah and Pickering (1977); Phadungchewit (1990); etc. The greater

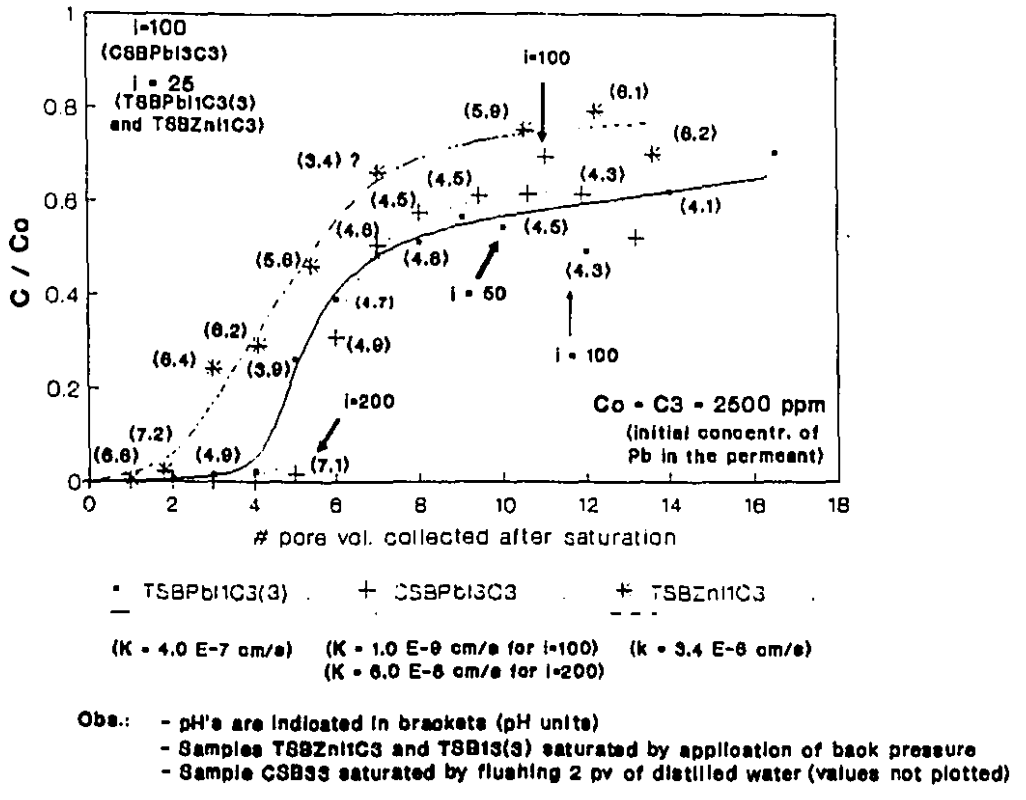

Figure 4.16 - Breakthrough Curves for Three Representative Tests with Sand/Bentonite.

mobility (or lower selectivity) of *Zn* is discussed in further detail in Section 4.2.5.2.

The pH of each leachate collected is indicated in brackets in Figure 4.16. It is interesting to note that the drop in pH is inversely proportional to the intensity of the increase in the *Pb* concentration measured. For the test with sample **CSBPbI3C3** the pH drops abruptly from 7.1 after approximately 5 pore volumes were collected, to 4.6 after 7 pore volumes accumulated. Concomitantly, C/C_0 rises from only 0.01 to 0.5 (breakthrough point). This shows that the pH of the leachate might be an

indicator of the evolution of the contamination front. Yong et al (1990) associated pH reductions of soil solutions with competition of *Pb* ions species and H^+ for adsorption sites. Since *Pb* has a higher affinity than H^+ (Bohn et al, 1985) it leads to a higher concentration of H^+ in the solution.

In the case of sample **TSBPbI1C3(3)**, however, the pH decreased faster, reaching the acidic range much before the breakthrough point. Thus, no definite conclusions can be made concerning the use of pH as an indicator of the evolution of the contaminant front, based on these limited tests with S/B.

Further related studies, e.g.: Yong et al (1990), who carried out a research on the buffering capacity of clay soils and its relation to heavy metal retention, can eventually cast more light on this particular problem.

4.2.4 - Comments on Adsorption by Compacted Clays

From the results of chemical analyses performed with the effluent collected during some tests with kaolinite, including the two shown in Figure 4.15, the retardation factor, **R**, which represents the retardation of the front of contamination relative to the bulk flow of water (Freeze and Cherry, 1979), can be obtained by a simple set of calculations, using the equation below (Freeze and Cherry, 1979) :

$$R = \frac{\bar{v}_l}{\bar{v}_c} = 1 + \frac{\rho_b}{n} \cdot K_d \qquad (4.2)$$

where:

v is the average linear velocity of the solution along the flow line;

v_c is the velocity of the $C/C_0 = 0.5$ point on the concentration profile of the retarded constituent;

ρ_b is the dry density of the porous medium;

n is the porosity; and

K_d is the distribution (or partitioning) coefficient, which represents the partitioning of the constituent between the solution and the soil particles ($\partial \mathbf{q}/\partial \mathbf{C}$).

As can be seen, different K_d's may be obtained, depending on:

1 - the curve selected: (a) adsorption isotherm (upper curve on Figure 4.12 or 4.13); (b) one of the adsorption characteristic curves for the compacted material (other curves);

2 - the level of equilibrium concentration (**C**) at which the K_d is measured (K_d is the tangent to the curves).

Here are some examples of different K_d's (and retardation factors **R**) that can be obtained based on Equation (4.2), depending on the 'choices' made:

1 - **curve**: adsorption isotherm (upper curve on Figure 4.12);

tangent taken at: the initial 'linear' portion (secant) => $K_d \approx 10$ ml/g;

R ≈ 27;

note: this is the common 'choice' in Environmental Geotechnology practice (Freeze and Cherry, 1979; Bowders et al., 1986; EPA, 1987; Rowe, 1988; Barone et al, 1989; National Research Council (U.S.), 1990);

2 - **curve**: adsorption characteristic curve for **B(s)** (second curve from the top in Figure 4.12);

tangent taken at: the initial 'linear' portion (secant); => $K_d \approx 3.4$ ml/g; **R** ≈ 10;

3 - **curve**: same as above;

tangent taken at: the region where **C** ≈ 1700 ppm;

=> $K_d \approx 0.9$ ml/g; **R** ≈ 3.5;

note: at the level of concentration selected all curves for compacted kaolinite are rather parallel, i.e., approximately the same K_d can be obtained independently of the curve chosen;

4 - **curve**: adsorption characteristic curve for **B** (consolidation cell Figure 4.13);

tangent taken at: the region where **C** ≈ 1700 ppm;

=> $K_d \approx 1.11$ ml/g; **R** ≈ 3.9.

For comparison, it is possible to calculate **R** expressing the velocities in terms of the total volume collected at breakthrough point ($C/C_0 = 0.5$), V_p, and the volume of voids of the sample, V_v. **R** is obtained by dividing V_p by V_v. In other words, it

consists of the number of pore volumes needed to achieve $C/C_0 = 0.5$. In this case, it is necessary to assume that the breakthrough curve obeys the mathematical solution of the longitudinal dispersion equation in granular medium (error function model), as presented by Ogata and Banks (1961) and later adapted by Ogata (1970) to account for adsorption processes. **For the kaolinite test TKPBI3C3b, shown in Figure 4.15, R = 4.5.**

From the above calculations, it becomes evident that the most reasonable retardation factor for kaolinite was obtained by taking the tangent to the adsorption characteristic curve of compacted kaolinite at the level of concentration actually used during the permeability test, i.e., the 3rd and 4th 'choices' above.

Making the same assumptions and the same set of calculations for S/B samples, the retardation factor, **R**, was obtained based on Equation (4.2) ($\mathbf{R} = V_p/V_v$ at $C/C_0 = 0.5$) and found to be approximately 7 for test **CSBPbI3C3**, and 7.6 for test **TSBPbI1C3(3)**. On the other hand, if the approximately linear portion of the material's adsorption isotherm ($\mathbf{C} \leq 100$ ppm) is taken, $K_d \approx 60$ ml/g and **R** = 273 !

Unfortunately, due to the limited amount of data, it was not possible to calculate **R** using the K_d obtained from adsorption characteristic curves for compacted S/B.

This seems to indicate that: a) as far as modelling of contaminant transport is concerned, the adsorption characteristics of compacted samples may yield more reasonable values than isotherms constructed with soil suspensions; and b) K_d must be obtained from the tangent of the adsorption characteristic curve at the level of

concentration to be found in an actual problem.

The present results and comments (for both kaolinite and S/B) raise some very interesting points about the widespread use of constant partitioning coefficients (Freeze and Cherry, 1979; Bowders et al, 1986; EPA, 1987; Rowe, 1988; Barone et al, 1989; National Research Council (U.S.), 1990), often obtained from 'linear' adsorption isotherms (e.g.: Freeze and Cherry, 1979; Bowders et al, 1986; National Research Council (U.S.), 1990; ASTM ES-10-85 and D4319), in contaminant transport modelling[10].

The fact that several different K_d's may be obtained, depending on the isotherm selected (adsorption isotherm or the adsorption characteristic curves of compacted materials) and where the tangent is taken, have severe implications in the prediction of contaminant transport. For example, the simplification[11]:

$$\partial S/\partial C = \text{constant (linear isotherms)}$$

may lead to an improper evaluation of the adsorption/desorption component to be used in the advection/dispersion models (Equations (1.2) and (1.3)). $\partial S/\partial C$ =

---

10 Only recently non-linear adsorption isotherms were reported in the geotechnical literature (Shakelford and Daniel, 1991). The authors obtained curvilinear isotherms for the adsorption of *Zn*, *Cd*, and *K* onto kaolinite.

11 According to the nomenclature employed here, $\partial q/\partial C$ should be used. **q** is the amount adsorbed in grams per grams of soil.

constant does not apply in all cases and depends on the nature of both the charged surface and the contaminant itself.

The fact that the amounts retained by compacted materials are lower than those adsorbed by soil suspensions, as suggested by the results obtained with kaolinite and the S/B mixture, shows that, by using adsorption isotherms, adsorption and accumulation processes can be overestimated. This is of key importance in the evaluation of the capability of a protection barrier to contain heavy metals over its expected lifespan.

When adsorption characteristic curves are used, the effects of precipitation, dissolution from the solid surface, effective exposed surface area, cluster, and ped, as well as particle migration are taken into consideration. This does not hold when soil suspensions are used, since the solid:liquid ratio does not reflect the reality of a compacted clay barrier.

For example, the pH of an acid *Pb*-solution will not be altered as dramatically when in contact with a few grams of S/B as it will when it is percolated through the compacted S/B material. In the latter case, the precipitation level is more intense, thus it is expected that the partitioning between the two phases will be dictated by the compounding effects of cation exchange and precipitation. Also, aggregate and cluster formation, as discussed before, cause a decrease in the exposed surface area, thus lowering the exchange capacity of the soil, which may not be the case with soil suspensions.

Considering the above, non-linear adsorption characteristic curves of compacted materials seem to be more appropriate to represent the partitioning of contaminants between the solid phase and the percolating liquid.

Finally, curve fitting is also of fundamental importance, and the type of model chosen (Freundlich, Langmuir, B.E.T., etc.) will dictate the quality of the correlation. In the present case, the non-linear Freundlich model was used with success.

4.2.5 - Ion Mass Balances

Upon termination of chemical analyses, lead mass balances were calculated for most samples, following the procedure outlined in the Appendix E.

The limitations associated with mass balance calculations are described concomitantly with the presentation of results.

4.2.5.1 - *Pb* Mass Balance

Tables 4.3 and 4.4 present the mass balances for kaolinite samples tested with the triaxial and the consolidation cells, respectively. Tables 4.5 and 4.6 present the mass balance results for S/B samples tested in the triaxial and the consolidation cells, respectively. Values in grams represent the summation over the quantities found for each individual slice, except for the total *Pb* input.

Basically, the amount of lead introduced in the system was compared to the

Test (C_0 in ppm; final C/C_0; tot # pv's)	Pb input (g)	Pb adsorbed (g) (% tot)	Pb in pores (g) (% tot)	Pb in leachate (g) (% tot)	Total (g)	Δ
TKPbI2C1 i = 50 C_0 = 250 C/C_0 = 0.00 5 pv's	0.044	0.040 (85%)	0.007 (15%)	0.000	0.047	7%
TKPbI3C1 i = 100 C_0 = 250 C/C_0 = 0.00 5 pv's	0.037	0.031 (66%)	0.016(?) (34%)	0.000	0.047	27%
TKPbI3C2 i = 100 C_0 = 850 C/C_0 = 0.17 5 pv's	0.165	0.105 (78%)	0.024 (18%)	0.006 (4%)	0.135	18%
TKPbI1C3 i = 25 C_0 = 1750 C/C_0 = 0.02 5 pv's	0.300	0.147 (49%)	0.077 (26%)	0.076 (25%)	0.298	2%
TKPbI3C3b i = 100 C_0 = 1750 C/C_0 = 0.85 10 pv's	0.601	0.187 (33%)	0.078 (14%)	0.302 (53%)	0.567	6%

Note: quantities in grams were obtained by adding the amounts of each individual slice (except for *Pb* input). Δ = discrepancy between Pb input and total identified in the system.

Table 4.3 - Lead Mass Balance Results for Kaolinite (Triaxial Cell).

sum of amounts found in the adsorbed form, in the pore fluid, and in the leachate collected.

Test (C in ppm; final C/C_0; tot # pv's)	Pb input (g)	Pb adsorbed (g) (% tot)	Pb in pores (g) (% tot)	Pb in leachate (g) (% tot)	Total (g)	Δ
CKPbI1C3 i = 25 C ≈ 1750 C/C_0 = 0.63 5 pv's	0.250	0.131 (52%)	0.059 (24%)	0.064 (26%)	0.254	2%
CKPbI2C1 i = 50 C ≈ 250 C/C_0 = 0.00 3 pv's	0.019	0.015 (80%)	0.002 (11%)	0.000	0.018	9%
CKPbI2C2 i = 50 C ≈ 850 C/C_0 = 0.10 4 pv's	0.096	0.063 (66%)	0.003 (3%)	0.003 (3%)	0.069	28%
CKPbI2C3 i = 50 C ≈ 1750 C/C_0 = 0.03 4 pv's	0.196	0.100	not measur.	0.002	0.102	48%
CKPbI3C1 i = 100 C ≈ 250 C/C_0 = 0.00 5 pv's	0.033	0.022 (60%)	0.004 (14%)	0.000	0.026	20%
CKPbI3C2 i = 100 C ≈ 850 C/C_0 =0.24 5 pv's	0.130	0.078 (60%)	0.024 (19%)	0.013 (10%)	0.115	11%
CKPbI3C3 i = 100 C ≈ 1750 C/C_0 = 0.74 5 pv's	0.290	0.125 (43%)	0.065 (22%)	0.109 (37%)	0.299	2%

Note: quantities in grams were obtained by adding the amounts of each individual slice (except for *Pb* input). Δ = discrepancy between Pb input and total recuperated in the system.

Table 4.4 - Lead Mass Balance Results for Kaolinite (Consolidation Cell).

As shown in Tables 4.3 to 4.6, the greatest percentage of lead was always found in the adsorbed form, with the **B**ottom slices adsorbing more *Pb* than the **M**iddle and **T**op slices (Figures 4.12 to 4.14). This confirms the results obtained by Yong et al (1987), who observed that heavy metals are retained in the initial sections (in the present case, the bottom part) of soil samples.

Test (C in ppm: final C/C_0; tot # pv's)	Pb input (g)	Pb adsorbed (g) (% tot)	Pb in pores (g) (% tot)	Pb in leachate (g) (% tot)	Total (g)	Δ
TSBPbI1C3_3 i = 25 C ≈ 2500 C/C_0 = 0.70 16.5 pv's	0.657	0.431 (61%)	0.010 (1%)	0.268 (38%)	0.709	8%
TSBPbI3C3BP i = 100 C ≈ 2500 C/C_0 ≈ 0.00 5 pv's	0.188	0.168 (97%)	0.005 (3%)	0.000	0.173	8%
TSBPbI1C1 i = 25 C ≈ 600 C/C_0 ≈ 0.00 8 pv's	0.069	0.048 (70%)	N.A.	8.0 E-3 (12%)	0.056	18%
TSBPbI1C3_5	mass balance not calculated					

Note: quantities in grams were obtained by adding the amounts of each individual slice (except for *Pb* input); bdl = below detectable limits. Δ = discrepancy between Pb input and total identified in the system.

Table 4.5 - Lead Mass Balance Results for Sand/Bentonite (Triaxial Cell).

The small discrepancies between the quantities introduced and identified in the system can be attributed both to the fact that ammonium acetate may not be able to extract 100% of the adsorbed (specifically or not) *Pb* (Karamanos et al, 1976; Farrah and Pickering, 1978; see also the Appendix G), and to experimental errors. Concerning the latter, dilutions of highly concentrated solutions are very delicate: a simple spike more, or less, can lead to erroneous results.

Another possible source of these small discrepancies, in the case of S/B tests, may be associated with the presence of colloids in the supernatant. Gschwend and Wu (1985) and Servos and Muir (1989) used much higher centrifugal forces and longer centrifugation periods than those used in this research and still identified colloids in their supernatant. In the present case, some of the heavy metals (ionic species) 'extracted' when the **acidified** ammonium acetate solution was mixed with the soil can eventually be adsorbed onto these colloids and will not be detected by AAS.

Large discrepancies were normally associated with cell leaks (e.g.: **CKPbI2C3**, Table 4.4), and to contamination of test tubes or glassware (e.g.: sample **TKPbI3C1**, Table 4.3).

4.2.5.2 - *Zn* Mass Balance

The results of the mass balance calculated for the sample percolated with *Zn* solution (shown in Table 4.6) did not show a pattern similar to those obtained for tests with *Pb*. The concentration of *Zn* is uniformly distributed along the sample (the

Test (C in ppm; final C/C_0; tot # pv's)	Pb input (g)	Pb adsorbed (g) (% tot)	Pb in pores (g) (% tot)	Pb in leachate (g) (% tot)	Total (g)	Δ
CSBPbI3C1 i = 100 C = 500 C/C_0 = 0.02 6 pv's	0.058	0.019 (33%)	0.002 (3%)	0.000	0.021	64%
CSBPbI3C3 i = 100 C = 2500 C/C_0 = 0.70 13 pv's	0.662	0.470 (71%)	0.033 (5%)	0.223 (34%)	0.726	10%

Note: quantities in grams were obtained by adding the amounts of each individual slice (except for *Pb* input). Δ = discrepancy between Pb input and total recuperated in the system.

Table 4.6 - Lead Mass Balance Results for Sand/Bentonite (Consolidation Cell). Top, Middle and Bottom sections adsorbed practically the same amounts of *Zn*), and most of the ions were identified in the leachate (68%), whereas only 28% was in the adsorbed form. Moreover, *Zn* was detected in the leachate collected much earlier than *Pb*, for tests with similar characteristics (Figure 4.16).

This can be mainly associated with the lower selectivity (or higher mobility) of *Zn* as compared to *Pb* for most clays and oxides, at various system pH (Farrah and Pickering, 1977; Phadungchewit, 1990). Selectivity, in turn, can be explained by the ionic size (Elliott et al, 1986). According to Bohn et al (1985) "the ease of exchange or the strength with which cations of equal charge are held is generally inversely proportional to the hydrated radii, or proportional to the unhydrated radii" (in Phadungchewit, 1990).

Test (C in ppm; final C/C_0; tot # pv's)	Zn input (g)	Zn adsorbed (g) (% tot)	Zn in pores (g) (% tot)	Zn in leachate (g) (% tot)	Total (g)	Δ
TSBZnI1C3 i = 25 C = 2000 C/C_0 = 0.79 13.6 pv's	0.438	0.093 (28%)	0.015 (4%)	0.232 (68%)	0.340	22%

Note: quantities in grams were obtained by adding the amounts of each individual slice (except for *Zn* input). Δ = discrepancy between Pb input and total identified in the system.

Table 4.7 - Zinc Mass Balance Results for Sand/Bentonite (triaxial cell).

The greater mobility of ionic *Zn* can be also explained in terms of the greater activity of *Zn* and based on the standard Gibbs free energy ($\Delta G°$) of the system, defined as (Sawyer et McCarty, 1978; Bohn et al, 1985)[12]:

$$\Delta G° = -RT \ln K \qquad (4.3)$$

where: R ≡ universal gas constant;

T ≡ absolute temperature in °K; and

K ≡ equilibrium constant of the reaction describing the exchange phenomena.

12 The negative sign means that energy is released and the system becomes more stable. The higher the absolute value, the more 'spontaneous' is the reaction (Bohn et al, 1985).

If only ionized or ionizable species are involved, and assuming that only two cations are involved in the process, the exchange reaction can be written as (adapted from Schweich and Sardin, 1986):

$$wHM^{++} + 2EC^{w+}\text{-}clay \rightleftarrows 2EC^{w+} + wHM^{++}\text{-}clay \qquad (4.4)$$

where: HM^{++} ≡ divalent heavy metal (*Pb* or *Zn*); and

EC ≡ exchangeable cation of valence *w*.

Considering the exchange of Pb^{++} (or Zn^{++}) for Na^{+}, the equation constant (**K**) may be described as (Krishnamoorthy and Overstreet, 1949):

$$K = \frac{[Pb^{++}]_{ads}\,(Na^{+})^2}{(Pb^{++})_{sol}\,[Na^{+}]^2} \qquad (4.5)$$

in which the brackets refer to the concentrations present in the exchange phase (**ads**orbed) as exchangeable ions, and the parenthesis denote the activities of the ions in the equilibrium **sol**ution.

According to Schweich and Sardin (1986), the equilibrium law associated with the reaction given by Equation (4.4) is described by the selectivity coefficient **D**. Thus, Equation (4.3) can be written as follows:

$$\Delta G^\circ = -RT \ln D \qquad (4.6)$$

Since the selectivity of *Pb* is higher than that of *Zn* (Farrah and Pickering, 1977; Phadungchewit, 1990):

$$\Delta G^\circ_{Pb} < \Delta G^\circ_{Zn} \text{ or } |\Delta G^\circ_{Pb}| > |\Delta G^\circ_{Zn}|$$

A positive variation of the free energy can be also related to the **activity** (**a**) of the solute according to Equation (4.7):

$$\Delta G = RT \ln a \qquad (4.7)$$

thus, $\mathbf{a}_{Zn} > \mathbf{a}_{Pb}$ or $(Zn)_{sol} > (Pb)_{sol}$

Comparing the two selectivity coefficients:

$$D_{Pb} = \frac{[Pb]\ (Na)^2}{(Pb)\ [Na]^2} > D_{Zn} = \frac{[Zn]\ (Na)^2}{(Pb)\ [Na]^2}$$

and given that the exchangeable system is the same:

$$D_{Pb} = \frac{[Pb]_{ads}}{(Pb)_{sol}} > D_{Zn} = \frac{[Zn]_{ads}}{(Zn)_{sol}}$$

It can be seen that the above relation will hold only if $[Pb]_{ads} > [Zn]_{ads}$, **which corresponds to the results obtained in this research.**

It is important to note that the high flow rate of the test with *Zn* (as compared to those with *Pb*) may have had some influence on the adsorption of this ion by bentonite surfaces.

Since precipitation of *Zn* (or *Pb*) could occur due to the high pH of the soil mixture, "the affinity of the heavy metal to be retained in soils could then be related to the **pK** of the first hydrolysis product of the metals ..." (Phadungchewit, 1990), with the pK of *Pb* being higher than that of *Zn* both for illite and montmorillonite (Baes and Messner, 1976; in Phadungchewit, 1990; Elliott et al, 1986).

The difference in amounts of *Zn* introduced in the system and recuperated during chemical analysis (Δ = 22%) can be partly attributed to experimental errors (many dilutions were necessary in order to obtain the degree of accuracy needed for atomic absorption analysis). It can also be explained by the occurrence of high affinity adsorption of *Zn* onto the bentonite surface (refer to *Effect of Type of Contaminant* in Section 4.1.2.1). In this case, the concentrated ammonium acetate solution may not be capable of 'extracting' all the *Zn* from the particle surface (Farrah and Pickering, 1978), as is the case with *Pb*.

4.2.5.3 - Total Ion Mass Balance

Another form of cross checking (or ion mass balance) was tried by comparing the total quantity of Pb^{++} adsorbed by the clay particles to the total amount of Na^{+}, K^{+}, Ca^{++}, Mg^{++}, AL^{3+} (kaolinite only), and H^{+} (kaolinite only) exchanged by Pb^{++}. This was done by calculating the differences between the contributions of each individual ion to the total CEC of the material and their concentration in the supernatant obtained from the 'extraction' phase; these differences were summed up over all index cations and compared to the total concentration of Pb^{++} in the same supernatant. This can be better visualized with the following equation:

$$(CEC_{Na} - [Na]_{rem}) + (CEC_{Ca} - [Ca]_{rem}) + \ldots = [Pb]_{super}$$

where:

CEC_M = contribution of ion M to the total CEC;

$[M]_{rem}$ = amount of M remaining on particle surface after exchange reactions have taken place, i.e, after termination of test; or $[M]_{rem}$ = the concentration of M (ionic form) in the supernatant after 'extraction' with acidified (pH = 3.6) ammonium acetate (4 g in 40 ml);

$[Pb]_{super}$ = concentration of *ionic* Pb^{++} (Figure 3.4) in the acidic supernatant (pH $\approx$ 3.6) after exchange by NH_4^+ ions ('extraction'); i.e, it represents the amounts of *Pb* that actually 'extracted' the other ions.

Unfortunately, this cross checking was not successful in most cases (especially for S/B), because it cannot be guaranteed that the full CEC of the materials were actually 'available' for exchange with the percolating *Pb* solution: some particles did not participate in the exchange process due to particle agglomeration. The formation of clusters and other micro and ultra-microscopic structures are very difficult to control and the structure changes from sample to sample despite the good repeatability of the static compaction procedure (Dunn and Mitchell, 1984).

Other concurrent phenomena may also render the total ion mass balance very difficult to calculate and interpret, e.g.: the dissolution of aluminum from the crystal structure of kaolinite at low pH, and subsequent replacement of index cations on the exchange sites by the dissolved *Al* ions (Duquette and Hendershot, 1987; Boland et al, 1980). The rate of dissolution, and the intensity of this type of exchange are very difficult to evaluate, and they vary significantly from system to system. Thus, changes in the system during lead percolation are very different from those which occurred when the CEC of the material was obtained, rendering the total ion mass balance rather inaccurate.

It may be observed that, although the affinity of clay minerals for aluminum is higher than that of lead due to the higher valence of *Al* (Scheffer and Schachtschabel, 1966; in Forstner and Wittmann, 1981), *Pb* can 'extract' the *Al* from exchange sites by effect of concentration, according to the Donnan principle applied to cation exchange. In fact, in quite a few cases of mass balance calculation for kaolinite samples, it was observed that, some Al^{3+} was exchanged by Pb^{++}.

4.2.6 - Retention Modes

4.2.6.1 - Retention of Pb by Kaolinite

The exchange capacity of kaolinite is mainly due to broken bonds at the edges of the clay minerals (Grim, 1968), and is recognized to be low compared to almost all other types of clay minerals. The results presented in this chapter show that kaolinite is able to adsorb lead despite:

a) its low buffering capacity (Yong et al, 1990; Phadungchewit, 1990);

b) the fact that at pH's lower than 4.5 - the approximate isoelectric point of kaolinite (Yong and Ohtsubo, 1987) - kaolinite develops a net positive surface charge.

It is not very probable that significant precipitation of *Pb* occurred inside kaolinite samples, due to the low pH of the kaolinitic clay (pH = 4.3 - 4.7) and of the *Pb* solution introduced (pH = 3.6). In the low pH range, *Pb* is normally found as a dissolved species (Figure 3.4), or ions, that can readily displace other ions in the diffuse double layer by effect of concentration and valence, according to the Donnan principle applied to cation exchange (Greenland and Hayes, 1978).

It can thus be concluded that the prevailing retention phenomena in this case is **physisorption** (cation exchange) to kaolinite edges (mainly) and surfaces (Yong et

al, 1990). Physisorption, or nonspecific adsorption, is a particular case of adsorption involving only electrostatic forces. According to Sposito (1984), physisorption is the chief mechanism governing the adsorption of metal ions.

4.2.6.2 - Retention of Pb by Sand/Bentonite

Significant precipitation must have occurred due to the high pH (8.6 to 8.8) existing inside S/B samples in the beginning of the tests[13]. This is partly responsible for the higher retention of *Pb* by S/B as compared to kaolinite. In this particular case, lead may have precipitated as hydrous metallic oxides species (lead hydroxide - $Pb(OH)_2$, as shown in Figure 3.6), or as lead nitrate ($Pb(NO_3)_2$) itself.

The precipitate may coat fabric units (Yong et al, 1979; Wang, 1990) and interact with the clay by: electrostatic attraction (coulombic) forces; cation bridging; hydrogen bonding; water bridging; and van der Waals forces (Wang, 1990).

As evidenced by the results presented in this study (e.g.: adsorption characteristic of compacted soils, mass balances, etc.), *Pb* is still found as a dissolved species, or ions, that can readily displace other ions in the diffuse double layer.

The results of mass balance calculations and the theoretical calculations made in Appendix G suggest that high affinity adsorption may also occur when bentonite interacts with solutions containing lead ions.

---

[13] In some tests, the pH dropped to the acidic range after a few pore volumes had been leached (see, for example, the results presented in Figure 4.16 in Section 4.2.3.2). For others it remained relatively high (pH $\approx$ 7.0).

In view of the above, and due to the very high: CEC, specific surface area, and high pH of bentonite (Tables 3.1 and 3.2), it can be postulated that adsorption as ionic species (physisorption), precipitation, and high affinity adsorption are the prevailing retention modes for *Pb*, in the case of the sand/bentonite mixture. This is in agreement with observations made by Harter (1983) concerning retention of *Pb* by montmorillonite.

The precise proportions of each (precipitate, physisorbed, and specifically adsorbed), can be assessed experimentally by using the sequential extraction technique, which was employed by Phadungchewit (1990), among others. Unfortunately, a thorough evaluation of these proportions could not be made within the scope of the present experimental program. A partial evaluation (precipitation phenomena excluded) was made using the double layer theory and the results of tests with soil suspensions (Appendix G). In the case of compacted clays, further investigations would be needed.

Finally, the minor quantities of *Pb* identified in the leachate (refer to ***Pb* mass balance** in Section 4.2.5) indicate that *Pb* was not very mobile in the S/B system.

4.2.6.3 - Retention of Zn by Sand/Bentonite

As discussed previously in Section 4.1.2.1 (**effect of type of contaminant**), *Zn* can be adsorbed in the Stern layer, where the energy of adsorption is higher than in the diffuse layer (physisorption). Based on his own results and other data from

literature, Harter (1983) observed that "it is probable that *Zn* is primarily retained on some portion of the exchange complex...", although the retention of *Zn* by precipitation cannot be discarded due to the high pH of the soil mixture.

As revealed by the mass balance calculation for the *Zn* test (Section 4.2.5), a great proportion of the *Zn* was detected in the leachate. This seems to indicate that the transport of this heavy metal can be much more important than in the case of lead, which confirms the affinity order - *Pb* > *Zn* - obtained by several researchers, e.g.: Forbes et al (1976; in Nriagu, 1978), Farrah and Pickering (1977), Harter (1983), Phadungchewit (1990), etc.. Due to the high flow velocities associated with high hydraulic conductivities, it is also possible that precipitate species may be carried out of the sample to be collected in the leachate.

The precise proportions of *Zn* adsorbed as ionic species, as precipitate, and transported as complexes or in the precipitate form was not evaluated in this study and are beyond its scope.

4.2.7 - Summary of Results

The results presented in this chapter are summarized in Figures 4.17 and 4.18.

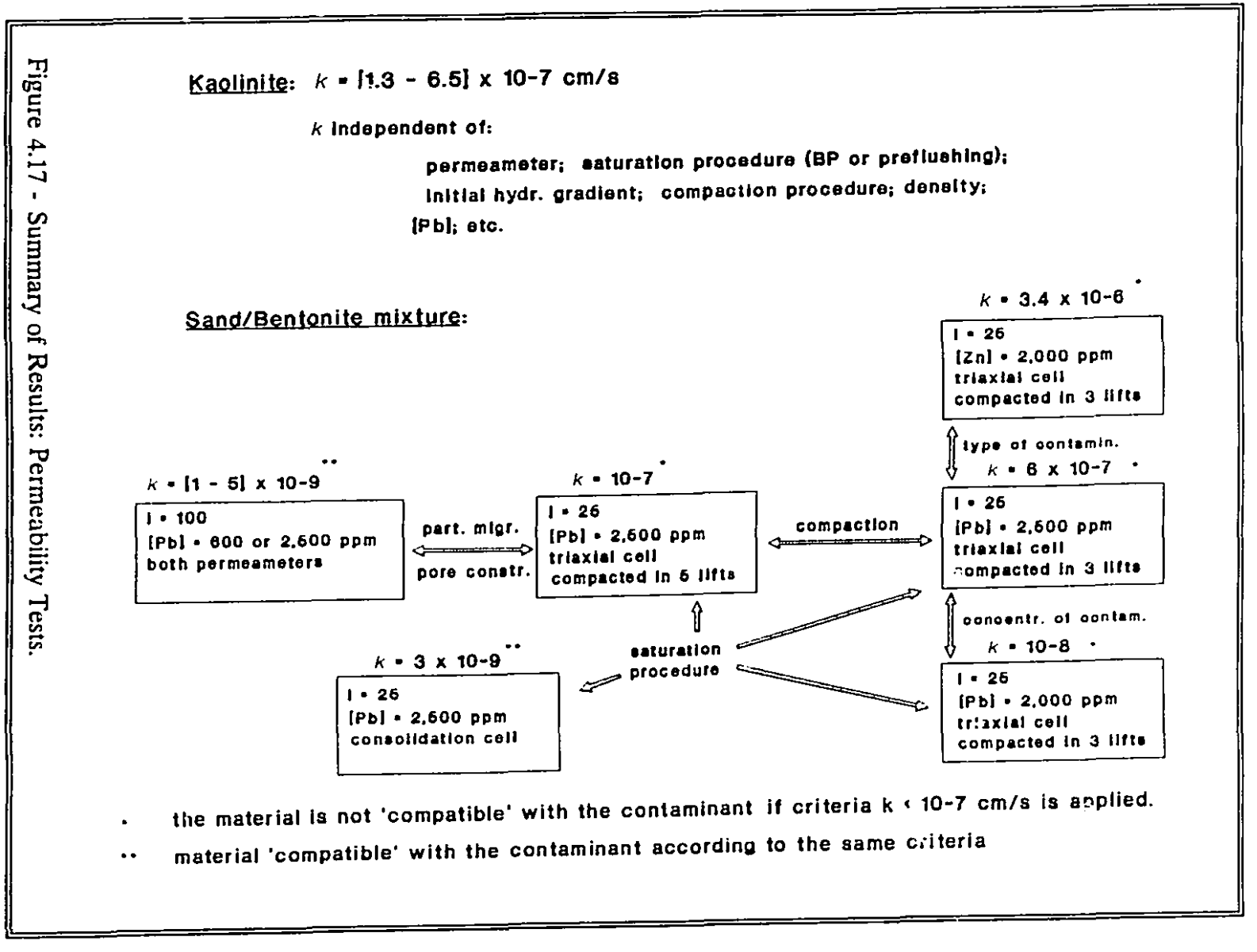

Figure 4.17 - Summary of Results: Permeability Tests.

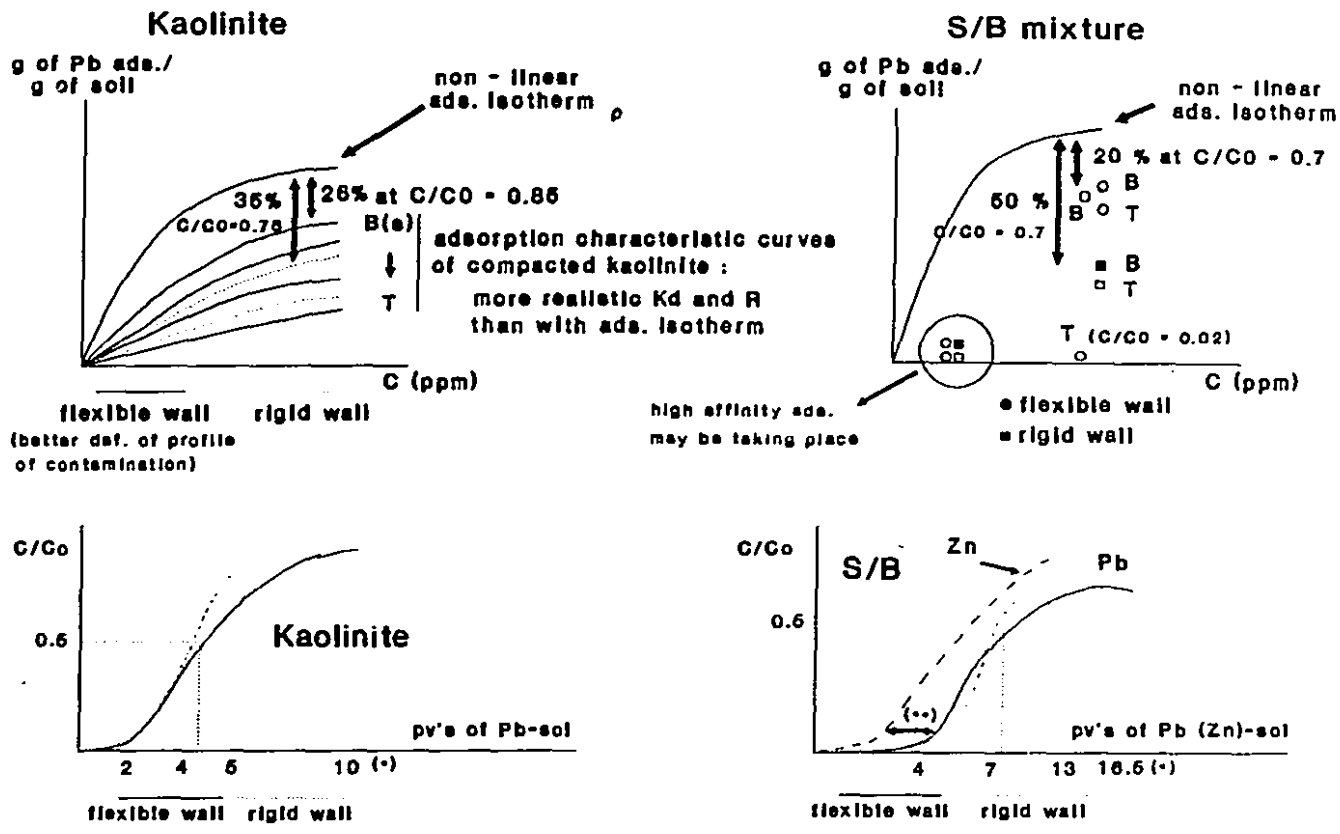

Figure 4.18 - Summary of Results : Chemical Analyses.

(•) assessment of the long term performance of the materials
(••) Zn less adsorbed than Pb: more mobile (lower selectivity)

- mass balance calculation: a) cross check ; b) helped identifying retention modes other than physisorption or precipitation (e.g.: high affinity adsorption in the Stern layer)

CHAPTER 5

CONCLUSIONS

5.1 - General

This research work has focused on some important aspects of compatibility studies involving heavy metals and clay soils.

Compatibility was analyzed in terms of changes in the coefficient of hydraulic permeability of the two clay soils, due to percolation of concentrated heavy metal solutions, and in terms of the capacity of **compacted** clays to retain heavy metals. The use of adsorption characteristic curves of compacted material, instead of adsorption isotherms, was introduced as a more realistic approach to the description of the partitioning of heavy metals between compacted clays and the liquid phase.

5.2 - Permeability Tests

Several *k*-tests were performed with the two materials. Some lasted for only a few weeks, others several months, depending on test conditions. The response to changes in the fabric/structure arrangement observed during *k* tests were interpreted

based on the fundamentals of soil-contaminant interactions. The main conclusions are as follows.

5.2.1 - k-tests with Kaolinite

The results of laboratory permeability tests agree with previous experience with kaolinite in regard to the relative 'insensitivity' of the clay to pore-water chemistry changes, as far as the coefficient of hydraulic permeability is concerned. They indicated that little or no differences exist between the *k*-values obtained for kaolinite samples tested in either permeameter - flexible-wall or rigid-wall. This has also been confirmed by other researchers and testifies to the relatively "inactive" nature of kaolinite, as compared to active clays like bentonite.

5.2.2 - k-tests with S/B

The results of permeability testing with S/B in the **triaxial cell** showed a clear dependency on (refer to Figure 4.2): a) the initial hydraulic gradient applied; b) the saturation procedure chosen; c) the concentration of the percolating solution; d) the type of contaminant; e) the compaction energy applied to prepare the samples; and f) the type of apparatus used.

a) The application of high initial hydraulic gradients to S/B samples led to particle migration and consequent pore constriction (or pore blockage). Pore blockage causes a reduction in the effective porosity - another parameter affecting permeability - of the samples, constituting another possible cause for the significant drop in the calculated coefficient of hydraulic permeability obtained when high hydraulic gradients were applied (lower curves in Figure 4.2).

The implications arising from this observation are severe. If the criteria widely accepted - $k < 10^{-7}$ cm/s (Zimmie, 1981; Harrop-Williams, 1985; etc.) - is used, the low k-value ($k \approx 10^{-9}$ cm/s) obtained with S/B samples tested under an initial gradient of 100 (Figure 4.2) would qualify the S/B to be employed in an engineered barrier (as far as the parameter 'permeability' is concerned). However, the high k-value ($k > 10^{-7}$ cm/s) obtained for the other two triaxial samples (upper curves in Figure 4.2), tested under a much lower gradient, would lead to the rejection of the material for use as an 'impermeable' barrier. In this case, relatively mobile contaminants (e.g.: *Zn*) may reach the ground water at concentrations higher than those accepted by water quality legislation.

According to the results obtained, once the permeability (k-value) has stabilized, the sample (i.e.: its fabric/structure arrangement) seems to be less vulnerable to the effects of changes in the applied hydraulic gradient. Mitchell and Younger (1967) attributed this fact to the "formation of a stable structure". A slight hydraulic gradient path dependency was observed in one S/B sample tested in the consolidation cell (Fig. 4.10).

b) The effect of sample saturation is illustrated by comparing the results of two S/B tests performed in the triaxial cell, submitted to a hydraulic gradient of 25 (Figure 4.2), with a test performed in the consolidation cell under the same gradient (Figure 4.10). The final low k-value calculated for the consolidation cell test - more than two orders of magnitude lower than those conducted in the triaxial cell - was mainly related to incomplete saturation of the sample, and the consequent higher suction forces due to osmotic and matric potentials (Section 4.1.2.2).

In the case of kaolinite, suction forces are not as important. As a consequence, incomplete saturation of consolidation cell samples did not lead to significant differences in the calculated coefficient of hydraulic permeability of the material, as compared with those obtained as a result of tests with the flexible wall permeameter (Table 4.1).

c) It was verified that the higher the concentration of *Pb* in the solution, the higher the k-value. This was explained using the DDL theory, which predicts that the higher the concentration - and the valence - of the contaminant in the pore fluid, the greater the collapse of the double layer, which facilitates percolation (*Effect of Concentration* in Section 4.1.2).

d) k calculated during the test with a concentrated *Zn* solution was almost one order of magnitude higher than the highest k obtained for a S/B sample tested for *Pb* in the triaxial cell. This was explained in terms of the DDL thickness and high

affinity adsorption in the Stern layer (*Effect of Type of Contaminant* in Section 4.1.2.1), and/or in terms of a more packed arrangement of ions near the surface of a particle due to the lower ionic radius of *Zn* ions. The more packed the DDL, the easier the percolating solution flows through. The higher mobility of *Zn* is discussed further in this chapter.

e) The results obtained for samples **TSBPbI1C3_3** and **TSBPbI1C3_5**[14] (Fig. 4.2) indicated that the methodology to prepare samples must be chosen carefully if actual field conditions are to be reproduced in the laboratory. Depending on the compaction energy applied, different fabric/ structure arrangements are obtained, with major implications in the final coefficient of hydraulic permeability calculated.

f) Finally, it was observed that regardless of the initial gradient applied, or the concentration of the contaminant in the percolating solution, the coefficients of hydraulic permeability obtained with the **consolidation cell** were two orders of magnitude lower than those obtained with the flexible wall permeameter (Figure 4.10). It seems that insufficient saturation prior to leaching of the contaminant (refer to **b** above) is the controlling factor leading to this difference.

---

[14] **S/B** samples tested in the **T**riaxial cell, under an initial hydraulic gradient **I1** = 25, and a concentration of ***Pb*** solution **C3** ≈ 2500 ppm. The first was compacted in three **(3)** lifts, whereas the second in five **(5)**.

For the two S/B tests performed in the rigid wall cell under higher hydraulic gradients ($i = 100$), the effect of saturation could not be interpreted independently from the effects of concentration and pore blockage.

5.3 - Chemical Analyses

From the chemical analyses with: the compacted materials, the pore fluid, and the leachate collected, it was possible to draw the following conclusions.

5.3.1 - Kaolinite

Despite its low buffering capacity, *Pb* retention by kaolinite does occur. In terms of percentages of the total input, most *Pb* was found in the adsorbed form, with some found in the pore fluid, and negligible amounts found in the leachate collected after 4 to 5 pore volumes had been leached (Tables 4.3 and 4.4). Evidently, for the two tests designed to last until high concentrations of the contaminant were detected in the leachate collected (C/C_0 close to unity), the proportions of *Pb* in the leachate were higher.

Compacted kaolinite did not adsorb as much *Pb* (in grams adsorbed per grams of soil) as the soil suspensions, even for the tests that lasted longer. This was interpreted in terms of the availability of exposed clay particle surface (cluster

formation). The difference increased with decreasing solution equilibrium concentration (Figure 4.12).

The bottom sections of kaolinite samples (where the contaminant was introduced) adsorbed significantly more *Pb* than the top sections, a reflection of the accumulation process occurring inside the material. This was more evident at low concentration levels, because the bottom part had not been 'satisfied' yet, i.e., it still had the capacity to retain *Pb*.

Due to the low pH of both the soil and the contaminant solution, and based on the results of *Pb* mass balance calculations, it could be concluded that low affinity physi-sorption is the main retention mode in kaolinite/*Pb*-solution systems. Precipitation was minimized by keeping the pH of the system low. The possibility of some high affinity adsorption is not excluded, and could explain the small discrepancies in the mass balances calculations (Tables 4.3 and 4.4). Unfortunately, this could not be verified for kaolinite in the present study.

5.3.2 - Sand/Bentonite Mixture

As in the case of kaolinite, compacted S/B adsorbed less *Pb* than soil suspensions (Figure 4.14), and this difference was also explained in terms of a lower 'effective' exposed surface area (cluster formation). The difference between amounts adsorbed by compacted material and soil suspensions was also greater at lower heavy metal concentration levels.

Besides experimental errors, the small discrepancies in the *Pb* mass balance calculations (Tables 4.5 and 4.6) can be attributed to the occurrence of high affinity adsorption. In such cases, the ammonium ions of the 'extracting' solution are not able to displace the *Pb* ions that are situated in the Stern layer because of the high energy level necessary for the exchange to occur. In order to support this suggestion, the theoretical concentrations of *Pb* adsorbed (high and low affinity types of adsorption) onto clay particles of a soil suspension were calculated and compared to experimental values (Appendix G). An adaptation of the DLVO theory (DDL model) was employed (Alammawi, 1988; Yong and Mohamed, 1991).

Other *Pb* retention modes of importance for S/B were precipitation and low affinity physisorption. The first is due to the high pH of the mixture, which causes the *Pb* to precipitate as $Pb(OH)_2$ species (Figure 3.6), and the second is due to simple replacement of the exchangeable cations by *Pb* by effect of valence and concentration, as predicted by the double layer theory (also evaluated for soil suspensions in the Appendix G).

Zinc was found to be more mobile than *Pb* which agrees with the selectivity order of heavy metal retention in soils found by several authors (e.g.: Farrah and Pickering, 1977; Galvez, 1989; Phadungchewit, 1990). The breakthrough point for tests with *Zn* not only occurred earlier than all other tests using *Pb*, but the percentage of *Zn* found in the leachate was higher than that of *Pb* for a test which was performed under similar boundary conditions and a similar final C/C_0 (Figure 4.16).

5.3.3 - Other Remarks about Retention by Compacted Materials

The fact that the adsorption by compacted materials is lower than the adsorption by soil suspensions is fundamental when selecting the appropriate formulation to represent the partitioning of a contaminant between the solid and liquid phases in models describing the advective-dispersive transport of retarded species through porous media. **Irrespective of the model chosen, the differences between the compacted soil system and soil suspensions must be respected.**

The use of non-linear adsorption characteristic curves, instead of linear adsorption isotherms obtained from batch equilibrium tests, must be encouraged as a more realistic approach to clay-contaminant partitioning in clay barrier design.

As demonstrated in this study, the indiscriminate use of linear adsorption isotherms in all cases, or more precisely: the assumption of a constant distribution coefficient K_d may lead to an imprecise evaluation of the adsorption capability of the compacted soil.

The appropriate equation to describe the adsorption curve itself is also of concern. In this study, the non-linear Freundlich model was used with success to describe the adsorption isotherms of both materials, and the adsorption characteristic curve of compacted kaolinite. However, this particular model may not be the most appropriate for all systems.

5.4 - Permeameter Efficiency

The efficiency of the two permeameters was evaluated considering: a) its sensitivity to detect fabric/structure changes due to clay-contaminant interactions during leaching; b) its performance in measuring the coefficient of hydraulic permeability of the materials; and c) its ability to reproduce the accumulation process occurring inside the barrier material.

5.4.1 - *k* - tests

The basic difference in terms of the ability of the two permeameters to measure the laboratory coefficient of hydraulic permeability of clay soils was related to the efficiency to saturate the sample. Since the application of back pressure is not recommended for rigid wall permeameters (the risk of side-wall leakage increases), suction forces due to osmotic and matric potentials may induce lower flow rates coming out of the samples, i.e., lower calculated *k*-values (Section 4.1.2.2).

As mentioned previously, the effects of saturation on the coefficient of hydraulic permeability obtained from tests performed in the rigid wall permeameter may have overshadowed the effect of varying the concentration of *Pb* in the contaminant solution. The latter effect was identified very clearly during the experimental program with the flexible wall permeameter.

Considering the above, and if proper saturation is desired to reproduce the worst scenario of contamination, the choice of efficient saturation procedures (e.g.: back pressuring) is inevitable. The results presented have suggested that flushing the sample with distilled water prior to percolation of the contaminant solution is not an efficient saturation procedure. As a consequence, the use of triaxial cells - or other adaptations of flexible wall permeameters, are recommended for the permeability phase of a compatibility study. The use of the rigid wall cell is nonetheless advisable as an additional information, especially when performing compatibility studies involving clay soils and organic contaminants of low dielectric constants. The interaction between organic contaminants and compacted clay samples may lead to the formation of cracks (Acar et al, 1985; Mitchell and Madsen, 1989), which are better identified in the rigid wall cell.

5.4.2 - Retention

In the *Pb* retention analyses, it was seen that the amounts of *Pb* adsorbed per gram of soil for both kaolinite and S/B samples were greater as a result of tests with the triaxial cell. This was related to the higher degree of saturation of triaxial cell samples (Section 4.2.2).

For the high level of concentration (**C3**), the difference between *Pb* adsorption by compacted material and soil suspensions did not change significantly as a result of triaxial cell tests with either kaolinite or S/B. However, the results of tests

conducted in the rigid wall permeameter showed an increase from 35% (kaolinite) to 50% (S/B). This was interpreted in terms of the greater sensibility of S/B to the effect of saturation (Section 4.2.2).

5.5 - Suggestions for Further Studies

Permeability testing is far from being a closed issue. Many improvements can still be made at various levels: equipment, saturation procedure, sample preparation (a study of the most effective means to prepare sand/bentonite mixtures at various percentages of bentonite is in order), compaction, etc.

The development of an experimental procedure to test the permeability of clay soils under controlled swell is certainly a very challenging subject. Various types of contaminants can be leached through the samples, including heavy metals and polar and non polar organic contaminants, with low or high dielectric constants. Such a study can make a significant contribution to the present knowledge of the behaviour (geotechnical and physico-chemical) of engineered landfill covers and liners made of clay materials.

Flow characteristics in unsaturated porous media have been the subject of several theses and papers. It is nonetheless another open issue in environmental geotechnology. The development of new in-situ or laboratory techniques to obtain the unsaturated permeability of clay soils is needed. Becoming acquainted with

already existing techniques can also be a very interesting subject for a Masters program.

Some procedural details described by Warith (1987) can be combined with the experimental procedure proposed here to create a very efficient means of describing the evolution of the contamination front in systems where either diffusion or advection predominates. In this case, a flexible wall permeameter (triaxial cell) would be employed. In systems where diffusion predominates, diffusion coefficients can be obtained, using the model proposed by Warith (1987), with increased efficiency.

Further investigation with compacted clays would possibly facilitate the development of a correlation between the amounts of lead adsorbed by compacted samples and soil suspensions using the "effective" exposed surface area as input. This can be quite relevant in the evaluation of the adsorption capacity of a (compacted) barrier material in the field. Also, the results of batch equilibrium tests could be used with more accuracy.

Further studies on the evaluation of the amounts of various contaminants adsorbed in the Stern layer (high affinity adsorption) is also of great importance. The work developed here and those of Alammawi (1988) and Yong and Mohamed (1991), as well as several important references on double layer theory (e.g.: Kruyt, 1952; Grahame, 1947; van Olphen, 1963; Yarif and Cross, 1979; Sposito, 1984; etc) can be of great help.

Besides adsorption, other retention phenomena must be accounted for in contaminant migration studies. A speciation study (Phadungchewit, 1990; Yong et al, 1990) can complement the compatibility study by indicating the amounts adsorbed, precipitated, complexed, etc. Speciation may be a very effective means of evaluating the mobility of heavy metals in compacted materials with time.

5.6 - Personal Statement

Before finalizing the text of this thesis, I would like to express some personal ideas (opinions) about the global problem of ground water protection in engineered landfill sites. These ideas were developed during the period I have been in contact with this extremely serious problem, which is sometimes treated as a simple engineering (geotechnical) problem.

A remark made by J.F. Christiansen (in the discussions of a paper from Daniel et al (1985), which I came across in the early stages of my work) was perhaps the starting point of a series of fruitful discussions I have had with Dr. Yong and some graduate student colleagues, about the philosophy of the work we have been trying to develop. It seems appropriate to reproduce that remark here:

"Over the years, it has been distressing to see purportedly serious research conducted with apparatus priding itself in simplicity and ease of operation, and

then being applied to one of the most complex and potentially serious problems we have, that is, the containment of hazardous waste.

Our primary objective must be to achieve increased accuracy in predicting seepage quantities and rates of plume advancement.

So, in developing apparatus and test procedures, let us concentrate on reducing the magnitude of the many errors which can be introduced in the laboratory."

Indeed, an engineered barrier is something like the impervious core of a large earth dam; if it does not perform properly, piping may develop, eventually causing the total rupture of the dam. There is no need to discuss the cost - in terms of lives and money - associated with such a catastrophe. In the case of a barrier, no apparent (or evident to the eyes) rupture occurs, but the threat is immense in terms of ground water pollution.

Before construction of an earth dam begins, many years are needed for the research of the appropriate borrow materials - among many other design details. Their geotechnical properties must be very well known; there is no such a thing as a quick two month period of tests in this type of construction.

I believe that protection liners should receive the same kind of treatment. In fact, many years are needed before a site is approved for landfilling (as much as 10 years in the Toronto area, for example). This seems more than sufficient for government authorities, or the private sector, interested in the economical exploration of the landfill, to develop the necessary characterization of the site and of the con-

struction materials: hydrogeological conditions, amounts and quality of the borrow materials available, extensive in situ and laboratory permeability tests with all possible materials that can be employed in the protection barrier, thorough compatibility analyses, determination of diffusion parameters, etc.

There should be very limited compromise in terms of the costs and time-requirement for the completion of these necessary tests because, as Christiansen (1985) insists, "[we are dealing with] one of the most complex and potentially serious problem we have, that is, the containment of hazardous waste."

The bottom line of all this is simple: there is still a lot of room for the development of techniques to evaluate the quality of potential barrier materials in landfill sites, not to mention the place reserved for the development of the scientific background related to the problem of ground water protection. As stated above, only very limited compromise must be made in terms of the costs involved in the performance of these tests.

We can pride ourselves on our ability to develop sophisticated models to describe contaminant transport and retention, but if the parameters that feed these models are not well understood and technically well determined, the models will be anything but useful.

BIBLIOGRAPHY

Acar, Y.B., Hamidon, A., Field, S.D., and Scott, L. (1985). 'The Effect of Organic Fluids on Hydraulic Conductivity of Compacted Kaolinite'. *Hydraulic Barriers in soil and Rock*. Editors: Johnson, A.I., Frobel, R.K., Cavalli, N.J., and Pettersson, C.B., ASTM STP 874, pp. 171-187.

Alammawi, A.M. (1988). *Some Aspects of Hydration and Interaction Energies of Montmorillonite Clay*. Ph. D. thesis dissertation, McGill University, Montreal, 279 pp.

Alther, G., Evans, J.C., Fang, H.-Y., and Witmer, K. (1985). 'Influence of Inorganic Permeants upon the Permeability of Bentonite'. *Hydraulic Barriers in soil and Rock*. Editors: Johnson, A.I., Frobel, R.K., Cavalli, N.J., and Pettersson, C.B., ASTM STP 874, pp. 64-74.

Anderson,D.C., Crawley, W., and Zabcik, J.D. (1985). 'Effects of Various Liquids on Clay Soil:Bentonite Slurry Mixtures'. *Hydraulic Barriers in soil and Rock*. Editors: Johnson, A.I., Frobel, R.K., Cavalli, N.J., and Pettersson, C.B., ASTM STP 874, pp. 93-106.

Barone, F.S., Yanful, E.K., Quigley, R.M., and Rowe, R.K. (1989). 'Effect of Multiple Contaminant Migration on Diffusion and Adsorption of Some Domestic Waste Contaminants in a Natural Clayey Soil'. *Can. Geotech. J.*, Vol. 26, pp. 189-198.

Barrow, N.J. (1985). 'Reactions of Anions and Cations with Variable-Charge Soils'. *Advances in Agronomy*, Vol. 38, pp. 183-230.

Benson, C.H., and Daniel, D.E. (1990). 'Influence of Clods on Hydraulic Conductivity of Compacted Clay' *J. Geotech. Eng.*, ASCE, Vol. 116, No. 8, pp. 1231-1248.

Boast, C.W. (1973). 'Modeling the Movement of Chemicals in Soil by Water', *Soil Sci.*, Vol. 115, No.3.

Bohn, H.L., McNeal, B.L., and O'Connor, G.A. (1985), *Soil Chemistry*. Wiley, N.Y., 341 pp.

Boland, M.D.A., Posner, A.M., and Quirk, J.P. (1980). 'pH-Independent and pH-Dependent Surface Charges on Kaolinite'. *Clays and Clay Minerals*, Vol. 28, No.6, pp. 412-418.

Bolt, G.H. (1956). 'Physico-chemical Analysis of Compressibility of Pure Clays', *Géotechnique*, Vol. 6, No. 2, pp. 86-93.

Bowders, J.J., Daniel, D.E., Broderick, G.P., and Liljestrand, H.M. (1986). 'Methods for Testing Compatibility of Clay Liners with Landfill Leachate'. *Hazardous and Industrial Solid Waste Testing*. Editors: Petros, J.K., Lacy, W.J., and Conway, R.A., ASTM STP 886, pp.223-250.

Bowders, J.J., and Daniel, D.E. (1987). 'Hydraulic Conductivity of Compacted Clay to Dilute Organic Chemicals'. *J. Geotech. Eng.*, ASCE, Vol. 113, No. 12, pp. 1432-1448.

Boynton, S.S., and Daniel, D.E. (1986). 'Hydraulic Conductivity Tests on Compacted Clay'. *J. Geotech. Eng.*, Vol. 111, No. 4, pp. 465-477.

Brutsaert, W.F. (1987). 'Suitability of Marine Clays as Hazardous Waste Site Liners'. *J. Envir. Eng.*, ASCE, Vol. 113, No. 5, pp. 1141-1148.

Budhu, M., Giese, R.F., Campbell, G., and Baumgrass, L. (1991). *Can. Geotech. J.*, Vol. 28, pp. 140-147.

Cartwright, K. (1984). 'Shallow Land Burial of Municipal Wastes'. *Groundwater Contamination*. National Academy Press, Washington.

Chahal, R.S., and Yong, R.N. (1965). 'Validity of the Soil Water Characteristics Determined with the Pressurized Apparatus'. Soil Sci., Vol. 99, No.2, pp. 98-103.

Chapuis, R.P. (1990). 'Sand-Bentonite Liners: Predicting Permeability from Laboratory Tests, *Can. Geotech. J.*, Vol. 27, pp. 47-57.

Cheung, S.C.H., Gray, M.N., Dixxon, D.A. (1985). 'Hydraulic and Ionic Diffusion Properties of Bentonite-sand Buffer Materials'. *Proc. Intern. Conf. on Coupled Proc. Assoc. with a Nuclear Waste Repository*, U. California. Berkeley.

Chhabra, R., Pleysier, J., and Cremers, A. (1975). 'The Measurement of the Cation Exchange Capacity and Exchangeable Cations in Soils: A New Method'. *Proc. Intern. Clay Conf.*, Wilmette, Illinois, pp. 439-449.

Clark, T.M., and Piskin, R. (1977). 'Chemical Quality and Indicator Parameter for Monitoring Landfill Leachate'. *Environ. Geology*, Vol. 1, pp. 329-340.

Daniel, D.E., and Benson, C.H. (1990). 'Water Content-Density Criteria for Compacted Soil Liners'. *J. Geotech. Eng.*, ASCE, Vol. 116, No.12, pp. 1811-1830.

Daniel, D.E., Anderson, D.C., and Boynton, S.S. (1985). 'Fixed-Wall Versus Flexible-Wall Permeameters'. *Hydraulic Barriers in soil and Rock*. Editors: Johnson, A.I., Frobel, R.K., Cavalli, N.J., and Pettersson, C.B., ASTM STP 874, pp. 107-126.

Daniel, D.E. (1984). 'Predicting Hydraulic Conductivity of Clay Liners'. *J. Geotech. Eng.*, ASCE, Vol. 110, No.2, pp. 285-300.

Day, S.R., and Daniel, D.E. (1985). 'Hydraulic Conductivity of Two Prototype Clay Liners'. *J. Geotech. Eng.*, ASCE, Vol. 111, No.8, pp. 957-970.

Desaulniers, D.E., Cherry, J.A., and Gilham, R.W. (1984). 'Hydrogeologic Analysis of Long Term Solute Migration in Thick Clayey Quaternary Deposits'. *Proc. Intern. Symp. on Groundwater Resour. Utilization and Contaminant Hydrogeology*. International Association of Hydrogologists, pp. 349-356.

Desaulniers, D.E., Kaufman, R.S., Cherry, J.A., and Bentley, H.W. (1986). '^{37}Cl-^{35}Cl Variations in a Diffusion-Controlled Groundwater System', *Geochimica et Cosmochimica Acta*, Vol. 50, No. 8, pp. 1757-1764.

Desaulniers, D.E., Cherry, J.A., and Fritz, P. (1981). 'Origin, Age and Movement of Pore Water in Argillaceous Quaternary Deposits at Four Sites in Southwstern Ontario'. *J. of Hydrology*, Vol. 50, pp. 231-257.

Dunn, R.J, and Mitchell, J.K. (1984). 'Fluid Conductivity Testing of Fine-Grained Soils'. *J. Geotech. Eng.*, ASCE, Vol. 110, No. 11, pp. 1648-1665.

Dunn, R.J. (1983). *Hydraulic Conductivity of Soils in Relation to Subsurface Movement of Hazardous Wastes*. Ph. D. thesis dissertation, University of California, Berkeley, 338 pp.

Duquette, M., and Hendershot, W.H. (1987). 'Contribution of Exchangeable Aluminum to Cation Exchange Capacity at Low pH'. *Can. J. Soil Sci.*, Vol. 67, pp. 175-185.

Eklund, A.G. (1985). 'A Laboratory Comparison of the Effects of Water and Waste Leachate on the Performance of Soil Liners'. *Hydraulic Barriers in soil and Rock*. Editors: Johnson, A.I., Frobel, R.K., Cavalli, N.J., and Pettersson, C.B., ASTM STP 874, pp. 188-202.

Elliott, H.A., Liberati, M.R., and Huang, C.P. (1986). 'Competitive Adsorption of Heavy Metals by Soils'. *J. Environ. Qual.*, Vol. 15, No. 3, pp. 214-219.

Elrashidi, M.A., and O'Connor, G.A. (1982). 'Influence of Solution Composition on sorption of Zinc by Soils'. *Soil Sci. Soc. Am. J.*, Vol. 46, pp. 1153-1158.

Elzeftawy, A., and Cartwright, K. (1981). 'Evaluating the Saturated and Unsaturated Hydraulic Conductivity of Soils'. *Permeability and Groundwater Contaminant Transport*. Editors: Zimmie, T.F., and Riggs, C.O., ASTM STP 746, pp. 168-181.

EPA (1987). 'Batch Type Adsorption Procedures for Estimating Soil Attenuation of Chemicals'. Office of Solid Waste and Emergency Response, U.S. Environmental Protection Agency, Washington, D.C., EPA/530-SW-87-006.

EPA (1986). 'Cation Exchange capacity of Soils (Ammonium Acetate)'. Method 9080. U.S. ammonium acetate method 9080. Environmental Protection Agency, Washington, D.C.

Farley, K.J., Dzombak, D.A. and Morel, F.M.M. (1985). 'A Surface Precipitation Model for the Sorption of Cations on Metal Oxides'. *J. Colloid and Interface Sci.*, Vol. 106, No. 1.

Farrah, H., and Pickering, W.F. (1978). 'Extraction of Heavy Metal Ions Sorbed on Clays'. *Water, Air, and Soil Poll.*, Vol. 9, pp. 491-498.

Farrah, H., and Pickering, W.F. (1979). 'pH Effects in the Adsorption of Heavy Metal Ions by Clays'. *Chemical Geology*, Vol. 25, pp. 317-326.

Farrah, H., and Pickering, W.F. (1977). 'Influence of Clay-Solute Interactions on Heavy Metal Ion Levels'. *Water, Air, and Soil Poll.*, Vol. 8, pp. 189-197.

Fernuik, N., and Haug, M. (1990). 'Evaluation of In-Situ Permeability Test Methods'. *J. Geotech. Eng.*, ASCE, Vol. 116, No. 2, pp. 297-311.

Finno, R.J, and Schubert, W.R. (1986). 'Clay Liner Compatibility in waste Disposal Practice'. *J. Environ. Eng.*, Vol. 112, No 6., pp. 1070-1084.

Foreman, D.E. and Daniel, D.E. (1986). 'Permeation of Compacted Clays with Organic Chemicals'. *J. Geotech. Eng.*, ASCE, Vol. 112, No. 7, pp. 669-681.

Forstner, U., and Wittmann, G.T.W. (1981, revised ed., 1983). *Metal Pollution in the Aquatic Environment*. Springer-Verlag, N.Y., 486 pp.

Freeze, R.A., and Cherry, J.A. (1979). *Groundwater*. Prentice-Hall, N.J., 604 pp.

Fried, J.J. (1975). '*Groundwater Pollution*'. Elsevier, Amsterdam, 330 pp.

Galvez, R. (1989). *Clay Suspension as a Buffering System for Accumulation of Lead as a Soil Pollutant*. M. Eng. thesis dissertation, McGill Univeristy, Montreal, 116 pp.

Goodall, D.C. (1975). *Pollutant Migration from Sanitary Landfill Sites, Sarnia, Ontario*. M.E.Sc. thesis dissertation, University of Western Ontario, London, 135 pp.

Gore & Storrie, Limited (1982). *Canadian Inventory of Hazardous Waste. Report prepared for Environment Canada.*

Grahame, D.C. (1947). 'The Electrical Double Layer and The Theory of Electrocapillarity'. Chemical Reviews, Vol. 41, pp. 441-501.

Green, R.E., and Corey, J.C. (1971). 'Calculation of Hydraulic Conductivity: A Further Evaluation of Some Predictive Methods'. *Soil Sc. of America, proc.*, 35:3-8.

Greenland, D.J., and Hayes, M.H.B., editors (1978). *The Chemistry of soil Constituents*. Wiley, N.Y., 469 pp.

Gregg, S.J., and Sing, K.S.W. (1982). *Adsorption, Surface Area, and Porosity*. Academic Press, N.Y., 303 pp.

Griffin, R.A., and Shimp,N.F. (1976). 'Effect of pH on Exchange-Adsorption or Precipitation of Lead from Landfill Leachate by Clay Minerals'. *Environ. Sci. and Tech.*, Vol. 10, No. 13, 1262-1268.

Griffin, R.A., Shimp, N.F., Steele, J.D., Ruch, R.R., White, W.A., and Hughes, G.M. (1976). 'Attenuation of Pollutants in Municipal Landfill Leachate by Passage Through Clay'. *Environ. Sci. and Tech.*, Vol. 10, No.13, 1262-1268.

Grim, R.E., and Güven, N. (1978). *Bentonites*. Elsevier, N.Y., 256 pp.

Grim, R.E. (1968). *Clay Mineralogy*. 2nd ed., McGraw-Hill, N.Y., 596.

Gschwend,P.M., and Wu, S-c. (1985). 'On the Constancy of Sediment-Water Partition Coefficients of Hydrophobic Organic Pollutants'. *Environ. Sci. and Tech.*, Vol. 19, No.1, pp. 90-96.

Hahne, H.C.H., and Kroontje, W. (1973). 'Significance of pH and Chloride Concentration on Behaviour of Heavy Metal Pollutants: Mercury (II), Cadmium (II), Zinc (II), and Lead (II)'. *J. Environ. Qual., Vol. 2, No. 4, pp. 444-450.*

Hamilton, J.M., Daniel, D.E., and Olson, R.E. (1981). 'Measurement of Hydraulic Conductivity of Partially Saturated Soils'. Permeability and Groundwater Contaminant Transport. Editors: Zimmie, T.F., and Riggs, C.O., ASTM STP 746, pp. 182-196.

Harrop-Williams, K. (1985). 'Clay Liner Permeability: Evaluation and Variation'. *J. Geotech. Eng.*, ASCE, Vol. 111, No. 10, pp. 1211-1225.

Harter, R.D., ed. (1986). *Adsorption Phenomena*. van Nostrand-Reinhold, N.Y., 379 pp.

Harter, R.D. (1983) 'Effect of Soil pH on Adsorption of Lead, Copper, Zinc,and Nickel'. *Soil Soc. Am. J.*, Vol. 47, pp. 47-51.

Hayward, D.O., and Trapnell, B.M.W. (1964). *Chemisorption*. Butterworth, London, 323 pp.

Helfferich, F. (1962). *Ion Exchange*. McGraw-Hill, N.Y., 624 pp.

Israelachvili, J.M. (1982). 'Forces Between Surfaces in Liquids'. *Advances in Colloid and Interface Science*, Vol. 16, pp. 31-47.

Jackson, M.L. (1967). *Soil Chemical Analysis*. Prentice-Hall, New Delhi, 498 pp.

Karamanos, R.E., Bettany, J.R., and Rennie, D.A. (1976). 'Extractability of Added Lead in Soils Using Lead-210'. *Can. J. of Sci.*, Vol. 56, pp. 37-42.

Kipling, J.J. (1965). *Adsorption from solutions of Non-Electrolytes*. Academic Press, N.Y., 328 pp.

Klein, S. Johnson, T.M., and Cartwright, K. (1983). 'Moisture Characteristics of Compacted Soils for Use in trench Covers'. *'Role of the Unsaturated Zone in radioactive and Hazardous Waste Disposal'*. Editors: Mercer, J.W., Rao, P.S.C., and Marine, I.W., Ann Arbor Science, Ann Arbor, pp. 101-111.

Krishnamoorthy, C. and Overstreet, R. (1949). 'Theory of Ion Exchange Relationships'. *Soil Sci.* 68, pp. 307-315.

Kruyt, H.R. (1952). *Colloid Science*. Elsevier, New York.

Lambe, T.W. (1958). 'The Engineering Behavior of Compacted Clay'. *J. of the Soil Mech. Found. Div.*, ASCE (May), paper 1655.

Lentz, R.W., Horst, W.D., Uppot, J.O. (1985). 'The Permeability of Clay to Acidic and Caustic Permeants'. *'Hydraulic Barriers in soil and Rock'*. Editors: Johnson, A.I., Frobel, R.K., Cavalli, N.J., and Pettersson, C.B., ASTM STP 874, pp. 127-139.

Lundgren, T.A. (1981). 'Some Bentonite Sealants in Soil Mixed Blankets'. *Proc. 10th Int. Conf. Soil Mech. Found. Eng.*, Stockholm, Vol. pp. 349-354.

Madsen, F.T., and Mitchell, J.K. (1989). 'Chemical Effects on Clay Hydraulic Conductivity and Their Determination'. Special Presentation to the Zurich Tech. Inst., Zurich, 66 pp.

Maguire, M., Janece, S., Vimpany, I., Higginson, F.R., and Pickering, W.F. (1981). *Austr. J. Soil Res.*, Vol. 19.

Mangold, D.C., and Tsang, C-F. (1991). 'A Summary of Subsurface Hydrological and Hydrochemical Models'. *Reviews of Geophysics*, Vol. 29, pp. 51-79.

Mitchell, J.K. (1976). *Fundamentals of Soil Behavior*. Wiley, N.Y., 422 pp.

Mitchell. J.K., and Younger, J.S. (1967). 'Abnormalities in Hydraulic Flow Through Fine-Grained Soils'. Coefficient of Hydraulic Permeability and Capillarity of Soils. ASTM STP 417, pp. 106-139.

Mitchell, J.K., Hooper, D.R., and Campanella, R.G. (1965). 'Permeability of Compacted Clays'. *J. Soil Mech. Found. Div.*, ASCE, Vol. 91, No. SM4 (July), pp. 41-65.

Moore, J.N., and Luoma, S.N. (1990). 'Hazardous Waste from Large Scale Metal Extraction'. *Environ. Sci. and Tech.*, Vol. 24, No. 9.

Molinari, J. (1986). 'Consideration by the IAEA of the Problems Involved in Quantifying Solid-Liquid Interactions'. *Application of Distribution Coefficients to Radiological Assessment Models*. Editors: Sybley, T.H., and Myttenaere, C., Elsevier, N.Y., pp. 401-404.

National Research Council, U.S. (1990). *Ground Water Models. Scientific and Regulatory Applications*. Edited by the Comm. on Ground Water Modeling Assess., F.W.Schwartz, chairman. National Academy Press, Washington, 303 pp.

Nobre, M.M.M. (1987). *Estudo Experimental do Transporte de Polluentes*. M. Sc. thesis dissertation, Civil Eng. Dept., Pontificia Univ. Catolica, Rio de Janeiro, 214 pp.

Norrish, K. (1954). 'The Swelling of Montmorillonite'. *Disc. Faraday Soc., Vol. 18, pp. 120-134.*

Nriagu, J.O., ed. (1978). *The Biogeochemistry of Lead in the Environment (vol. 1 of 2)*. Elsevier, N.Y.

Ogata, A. (1970). 'Theory of Dispersion in a Granular Medium'. U.S. Geological Survey Proffessional Paper 411-I, Washington, 34 pp.

Ogata, A., and Banks, R.B. (1961). 'A Solution of the Differential Equation of Longitudinal Dispersion in Porous Media'. U.S. Geological survey Proffessional Paper 411-A, Washington, 7 pp.

Olsen, H.W. (1962). 'Hydraulic Flow Through Saturated Clays'. *Clays and clay Minerals*. Vol. 9, Pergamon Press.

Olsen, H.W. (1972). 'Liquid Movement Through Kaolinite Under Hydraulic, Electric, and Osmotic Gradients'. *The Am. Ass. of Petroleum Geol. Bull.*, Vol. 56, No.10, pp. 2022-2028.

Ottewill, R.H. (1977). 'Stability and Instability in Disperse Systems'. *J. Colloid and Interface Sci.*, Vol. 58, No.2, pp. 357-373.

Pashley, R.M. (1981). 'DLVO and Hydration Forces Between Mica Surfaces in Li^+, Na^+, K^+, and Cs^+ Electrolyte Solutions: A Correlation of Double Layer and Hydration Forces with Surface Cation Exchange Properties'. *J. Colloid and Interface Sci.*, Vol. 83, No. 2, pp. 531-546.

Patterson, J.W. (1989). 'Industrial Waste Reduction'. *Environ. Sci. Tech.*, Vol. 23, No. 9, pp. 1032-1038.

Peirce, J.J., Sallfords, G., Peel, T.A., and Witter, K.A. (1987). 'Effects of Selected Inorganic Leachates on Clay Permeability'. *J. Geotech. Eng.*, ASCE, Vol. 113, No. 8, pp. 915-920.

Peirce, J.J., and Witter, K.A. (1986). 'Termination Criteria for Clay Permeability Testing'. *J. Geotech. Eng.*, ASCE, Vol. 112, No. 9, pp. 841-854.

Peirce, J.J., Sallfords, G., and Murray, L. (1986). 'Overburden Pressures Exerted on Clay Liners'. *J. Environ. Eng.*, Vol. 112, No.2, pp. 280-290.

Phadungshewit, Y. (1990). *The role of pH and Buffer Capacity in Heavy Metal Retention in Clay Soils*. Ph. D. thesis dissertation, McGill University, Montreal, 180 pp.

Push, R. (1982). 'Mineral-water interactions and their Influence on the Physical Behaviour of Highly Compacted Na-bentonite.', *Can. Geotech. J.*, Vol 19, pp. 381-387.

Quigley, R. M., Fernandez, F., and Lowe, R.K. (1988). 'Clayey Barrier Assessment for Impoundment of Domestic Waste Leachate (Southern Ontario) Including Clay-Leachate Compatibility by Hydraulic Conductivity Testing'. *Can. Geotech. J.*, Vol. 25, pp. 574-581.

Quigley, R.M., Fernandez, F., Yanful, E.K., Helgason, T., and Margaritis, A. (1987a). 'Hydraulic Conductivity of Contaminated Natural Clay Directly Below a Domestic Landfill'. *Can. Geotech. J.*, Vol. 24, pp. 377-383.

Quigley, R.M., Yanful, E.K., and Fernandez, F. (1987b). 'Ion Transfer by Diffusion Through Clayey Barriers'. *Geotechnical Practice for Waste Disposal*. Editor: R.D. Woods, Special Publ. No. 13, ASCE, N.Y., 137-158.

Rowe, R.K., Caers, C.J., and Barone, F. (1988). 'Laboratory Determination of Diffusion and Distribution Coefficients of Contaminants Using Undisturbed Clayey Soil'. *Can. Geotech. J.*, Vol. 25, pp. 108-118.

Rowe, R.K. (1988). 'Eleventh Canadian Geotechnical Colloquium: Contaminant Migration Through Groundwater - The role of Modelling in the Design of Barriers'. *Can. Geotech. J.*, Vol. 25, pp. 779-798.

Schweich, D., and Sardin, M. (1986). 'Methodology for Determining Distribution Coefficients amd Alternative Description of the Sorption Process'. *Application of Distribution Coefficients to Radiological Assessment Models*. Editors: Sibley, T.H., and Myttenaere, C., Elsevier, N.Y., pp. 15-24.

Servos, M.R., and Muir, D.C.G. (1989). 'Effect of Suspended Sediment Concentration on the Sediement to Water Partition Coefficient for 1,3,6,8-Tetrachlorodibenzo-*p*-dioxin'. *Environ. Sci. and Tech.*, Vol. 23, No.10, pp. 1302-1306.

Shakelford, C.D. (1988). *Diffusion of Inorganic Chemical Wastes in Compacted Clay*. Ph. D. thesis dissertation, Univ. of Texas, Austin. Publ. by U.M.I Diss. Inform. Serv., Ann Arbor, 449 pp.

Shakelford, C.D., and Daniel, D.E. (1991). 'Diffusion in Saturated Soil. I: Background'. *J. Geotech. Eng.*, ASCE, Vol. 117, No. 3, pp. 467-484.

Sherard et al. (1976) - 'Pinhole Test for Identifying Dispersive Soils', *J. Geotech. Eng. Div.*, Vol. GT1, Jan., pp. 69-85.

Skempton, A.W. (1954). 'The Pore-Pressure Coefficients *A* and *B*'. *Géotechnique*, Vol. 4, pp. 143-147.

Slater, R.W. (1982). 'Chemical Control in the 80's in Canada'. *New-Chemicals Workshop*. Environment Canada, EPS 3-EP-83-4, pp. 1-6.

Sposito, G. (1984). *The Surface Chemistry of Soils*. Oxford University Press, N.Y., 234 pp.

Storey,J.M.E., and Peirce, J.J. (1989). 'Influence of Changes in Methanol Concentration on Clay Particle Interactions'. *Can. Geot. J.*, Vol. 26, pp. 57-63.

Sweeney, M.W., Melville, W.A., Trgovcich, B., and Leslie Grady, C.P. (1982). 'Adsorption Isotherm Parameter Estimation'. *J. Environ. Eng. Div.*, ASCE, Vol. 108, No. EE5, 913-923.

Singh, U.P., Emenhiser, T.C., Garcia-Bengochea, J.I., and Orban, J.E. (1984). 'Cleanup of Miami Drum Hazardous Waste Site'. *J. Environ. Eng.*, Vol. 110, No.2, pp. 343-355.

Uehara, G., and Gillman, G. (1981). *The Mineralogy, Chemistry, and Physics of Tropical Soils with Variable Charge Clays*. Westview Press, Boulder, 170 pp.

Uppot, G., and Stephenson, R.W. (1989). 'Permeability of Clays Under Organic Permeants'. *J. Geotech. Eng.*, ASCE, Vol. 115, No. 1, pp. 115-131.

U.S. National Academy of Science (1984). 'Toxicity Testing: Strategies to Determine Needs and Priorities'. National Research Council, National Academy Press, Washington, D.C.

van Olphen, H. (1963). *An Introduction to Clay Colloid Chemistry*. Wiley, 2nd ed., N.Y., 318 pp.

van Genuchten, M.Th. (1978). 'Simulation Models and Their Application to Landfill Disposal Siting: A Review of Proceedings of the Four Annual Research Symposium'. U.S. Environmental Protection Agency, EPA-600/9-78-016.

Verwey, E.J.W., and Overbeek, J.Th. G. (1948). *Theory of the Stability of Lyophobic Colloids*. Elsevier, Amsterdam.

Wang, B-W. (1990). *A Study of the Role and Contribution of Amorphous Materials in Marine Soils of Eastern Canada*. Ph. D. thesis dissertation, McGill University, Montreal, 193 pp.

Warith, M.A. (1987). *Migration of Leachate Solution Through Clay Soil*. Ph. D. thesis dissertation, McGill University, Montreal, 340 pp.

Warkentin, B.P., and Schofield, R.K. (1962). 'Swelling Pressure of Na-montmorillonite in NaCl solutions'. *J. of Soil Science*, Vol. 13, No. 1, pp. 98-105.

Weber, L.M. (1991). *The Permeability and Absorption Capability of Kaolinite and Bentonite Clays Under Heavy Metal Leaching*. M. Sc. thesis dissertation, McGill University, Montreal, 108 pp.

Yanful, E.K., Haug, M.D., and Wong, L.C. (1990). 'The Impact of Synthetic Leachate on the Hydraulic Conductivity of a Smectitic Till Underlying a Landfill Near Saskatoon, Saskatchewan'. *Can. Geotech. J.*, Vol. 27, pp. 507-519.

Yanful, E.K., Nesbitt, H.W., and Quigley, R.M. (1988a). 'Heavy Metal Migration at a Landfill Site, Sarnia, Ontario, Canada.-I: Thermodynamic Assessment and Chemical Interpretations'. *Applied Geochemistry*, Vol. 3, pp. 523-533.

Yanful, E.K., Quigley, R.M., and Nesbitt, H.W. (1988b). 'Heavy Metal Migration at a Landfill Site, Sarnia, Ontario, Canada.-2.: Metal Partitioning and Geotechnical Implications'. *Applied Geochemistry*, Vol. 3, pp. 623-629.

Yariv, S., and Cross, H. (1979). *Geochemistry of Colloid Systems*. Springer-Verlag, N.Y., 447 pp.

Yong, R.N., and Mohamed, A.M.O. (1991). 'A Study of Particle Interaction Energies in Wetting of Unsaturated Expansive Clays'. *Proc. of Workshop on Stress Partitioning in Engineered Clay Barriers*. Durham, N.C., May.

Yong, R.N., and Ohtsubo, M. (1987). 'Interparticle Action and Rheology of Kaolinite-Amorphous Iron Hydroxide (Ferrihydrite) Complexes'. *Applied Clay Science*, Vol. 2, pp. 63-81.

Yong, R.N., and Samani, H.M.V. (1987). 'Modelling of Contaminant Transport in clays via Irreversible Thermodynamics'. *Geotechnical Practice for Waste Disposal.*

ASCE-GT Specialty Conference, ASCE Geotech. Spec. Pub. 13:846-860, Ann Arbor, Michigan.

Yong, R.N., and Samani, H.M.V. (1988). 'Effect of Adsorption on Prediction of Pollutant Migration in a Clay Soil'. *Proc. Joint CSCE-ASCE National Conference on Envir. Eng.*, Vancouver.

Yong, R.N., and Warkentin, B.P. (1959). 'Physico-Chemical Analysis of High Swelling Clays Subject to Loading'. *Proc. 1st Pan Am. Cong. Mecanica de Suelos y Cimentaciones*, Vol. II, Mexico.

Yong, R.N., and Warkentin, B.P. (1975). *Soil Properties and Behaviour.* Elsevier, N.Y., 449 pp.

Yong, R.N., Cabral, A.R., and Weber, L.M. (1991). 'Evaluation of Clay Compatibility to Heavy Metal Transport and Containment: Permeability and Retention'. *First Canadian Conf. Envir. Geotech.* Editors: Chapuis, R.P., Aubertin, M., Canadian Geotechnical Society, May, Montreal, pp. 314-321.

Yong, R.N., Elmonayeri, D.S., and Chong, T.S. (1985). 'The Effect of Leaching of Leaching on the Integrity of a Natural Clay'. *Eng. Geology*, Vol. 21, pp. 279-299.

Yong, R.N., Sethi, A.J., and LaRochelle, P. (1979). 'Significance of Amorphous Material Relative to Sensitivity in Some Champlain Clays'. *Can. Geotech. J.*, Vol. 16, pp. 511-520.

Yong, R.N., Warith, M.A., and Boonsinsuk, P. (1987). 'Migration of Leachate Solution Through Clay Liner and Substrate'. *Hazardous and Industrial Solid Waste*

Testing and Disposal: Sixth Volume. Editors: Lorenzen, D., Conway, R.A., Jackson, L.P., Hamza, A., Perket, C.L., and Lacy, W.J., ASTM STP 933, pp. 208-225.

Yong, R.N., Warith, M.A., and Boonsinsuk, P. (1986). 'Attenuation of Landfill Leachate Contamination by Clay Soil: A Comparative Laboratory and Field Study'. *Proc. Intern. Conf. on Environ. Geotechnology*, Vol. II.

Yong, R.N., Warkentin, B.P, Phadungchewit, Y., Galvez, R. (1990). 'Buffer Capacity and Lead Retention in Some Clay Materials'. *Water, Air, and Soil Poll.* Vol. 53, pp. 53-67.

Zimmie, T.F. (1981). 'Geotechnical Testing Considerations in the Determination of Laboratory Permeability for Hazardous Waste Disposal Siting'. *Hazardous Solid Waste Testing: First Conference*. Editors: Conway, R.A., and Malloy, B.C., ASTM STP 760, pp. 293-304.

Appendix A - Mineralogical Characteristics

A.1 - Kaolinite

The mineralogical characteristics of the kaolinite was obtained by diffraction analysis with a Siemens diffractometer with copper radiation. Previous experience with this material has indicated that no smectite should be present in the kaolinite, which simplified sample preparation.

Some material was ground with a mortar and pestle, and 100 mg were placed in a 10 ml volumetric flask. Approximately 5 ml of distilled water were added, and the flask was placed in an ultrasonic bath for 5 minutes to allow for dispersion. The flask was then filled to the mark with distilled water. From this mixture, 4 ml were pipetted onto two glass slides (4 cm x 4 cm) and allowed to air dry.

A special slide was prepared to confirm the presence of kaolinite. The slide was heated to 550 °C in a muffle furnace for 30 to 40 minutes. At this temperature all kaolinite peaks are 'destroyed', i.e., kaolinite becomes amorphous to X-ray (Tan, 1982).

The results are presented in Figure A.1. The samples showed the distinctive kaolinite peaks at 7.2 and 3.6 Å. The heated sample displayed no peaks, thereby confirming the presence of kaolinite.

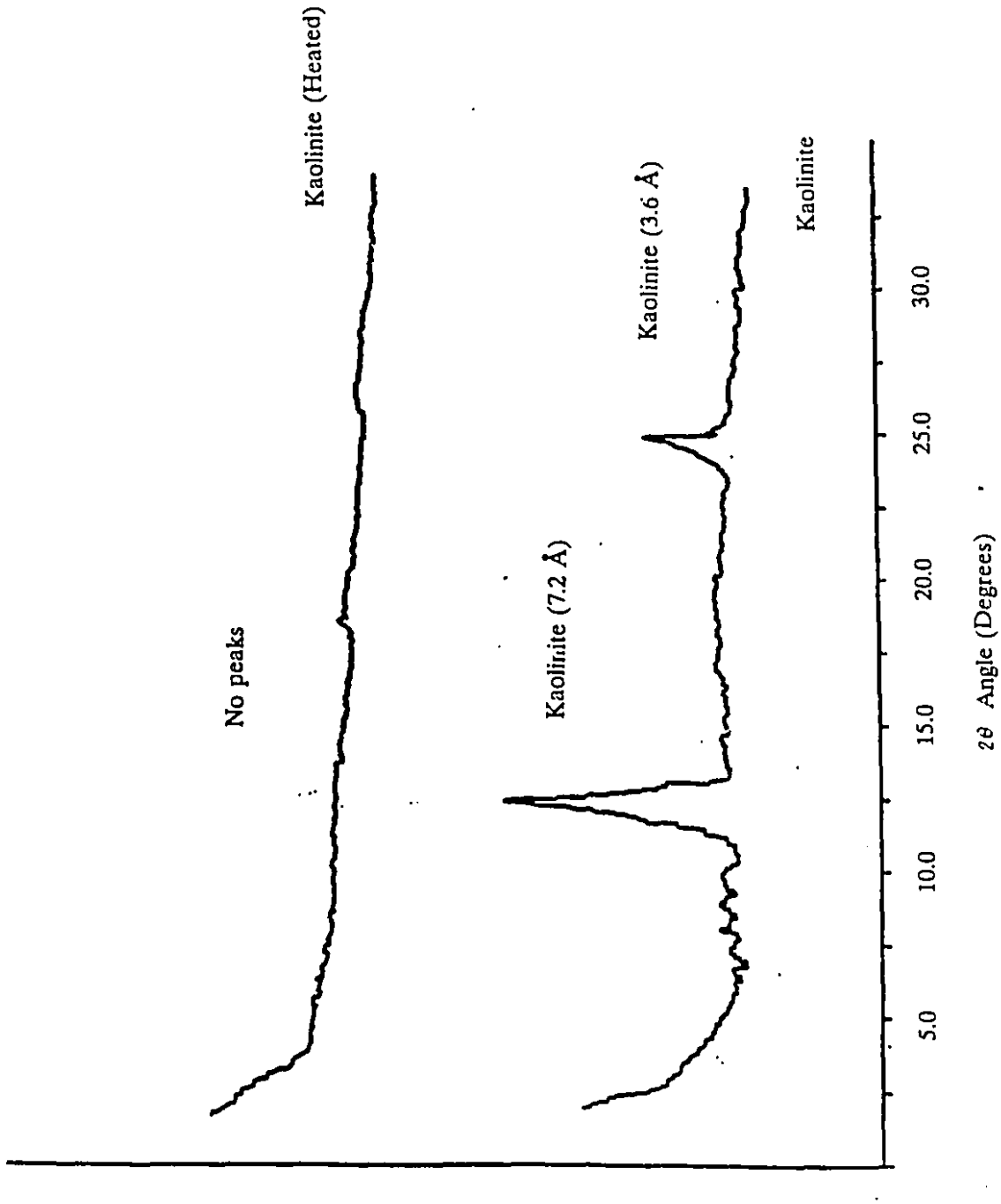

Figure A.1 - X-ray Diffraction Patterns for Kaolinite

A.2 - Bentonite

A Phillips APD 1710 X-ray diffractometer with copper radiation was used to perform the X-ray analysis of the bentonite used in to make the sand/bentonite mixture. The procedure for sample preparation was identical to that of kaolinite, with the addition of a supplementary slide: once the dry slide had been analyzed, a 10% glycerol solution was sprayed on the sample to shift the peak value.

The X-ray patterns are presented in Figure A.2. The air dry samples shows a peak at 12.8 Å, a value that indicates the presence of sodium bentonite. The glycerol treated sample shows a peak shift to 18 Å, as well as a minor peak at 8.9 Å.

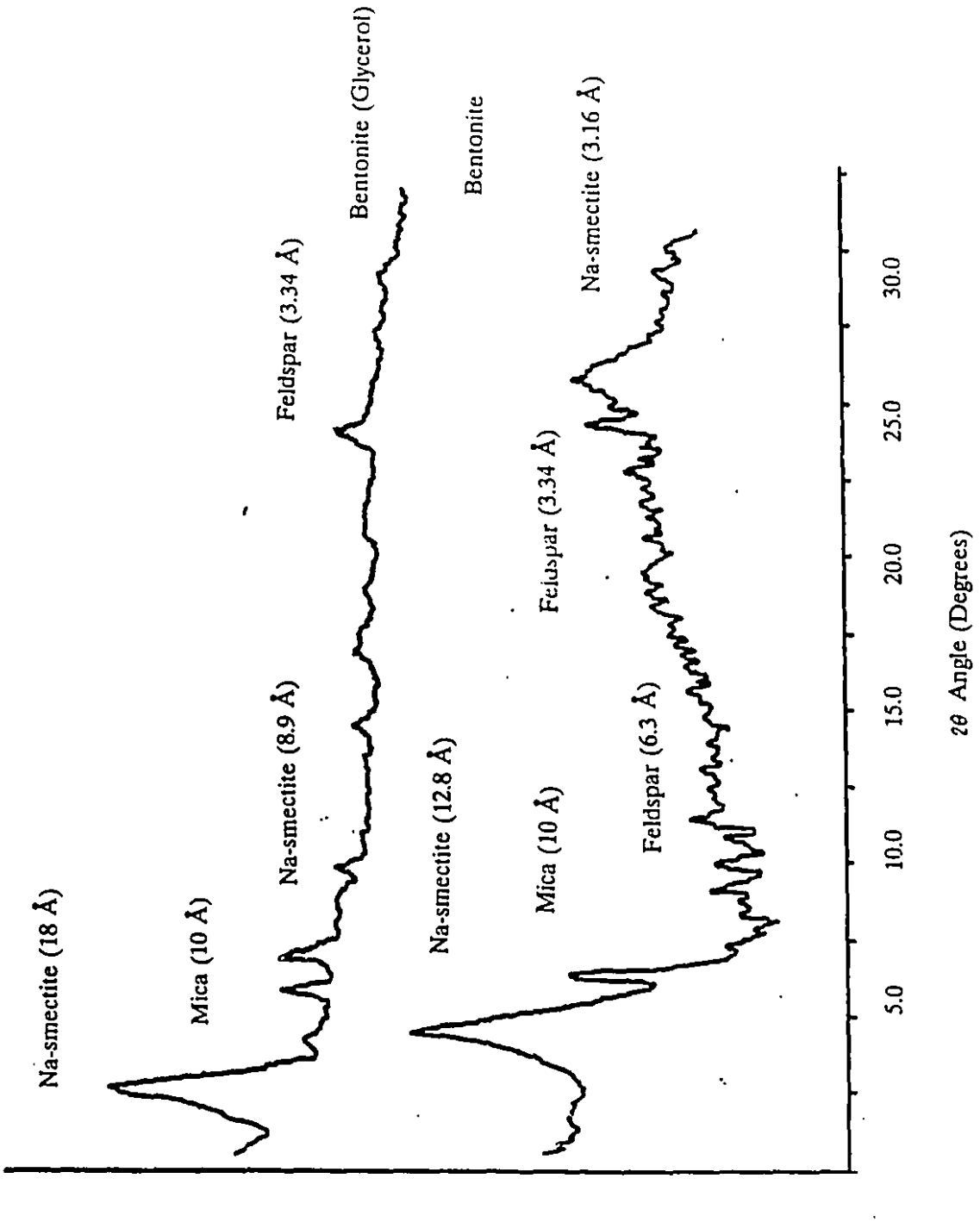

Figure A.2 - X-ray Diffraction Patterns for Bentonite

Appendix B - Geotechnical Test Results with Both Materials

B.1 - Kaolinite Hydrite PX

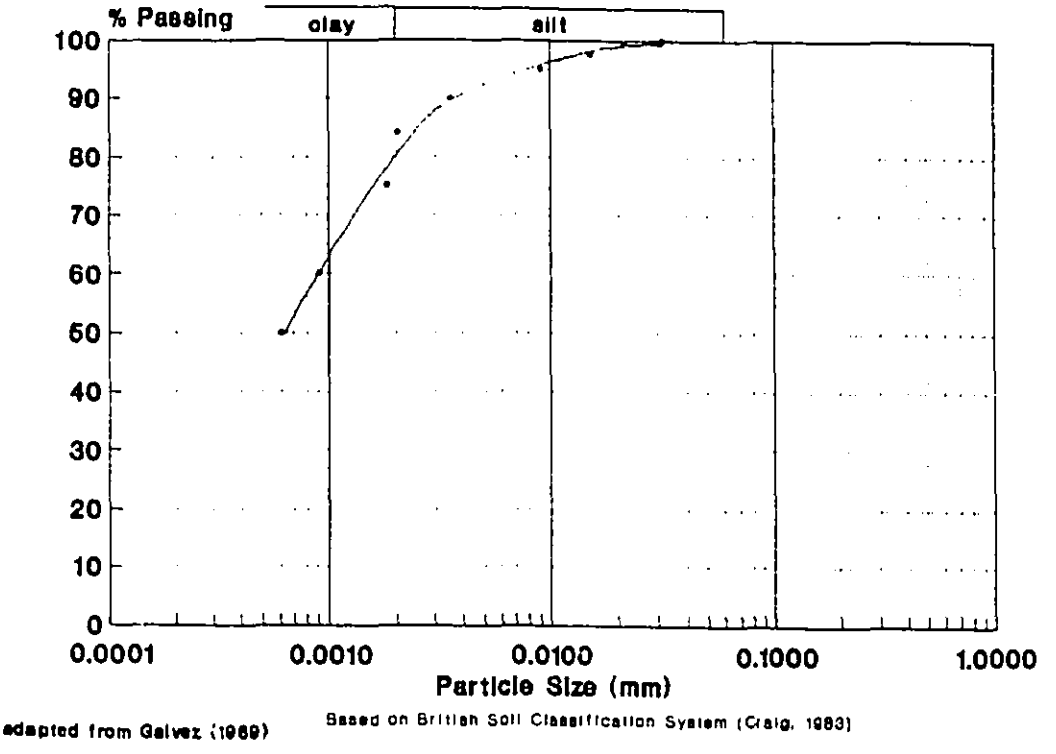

Figure B.1 - Grain size Distribution Curve for the Hydrite PX Kaolinite.

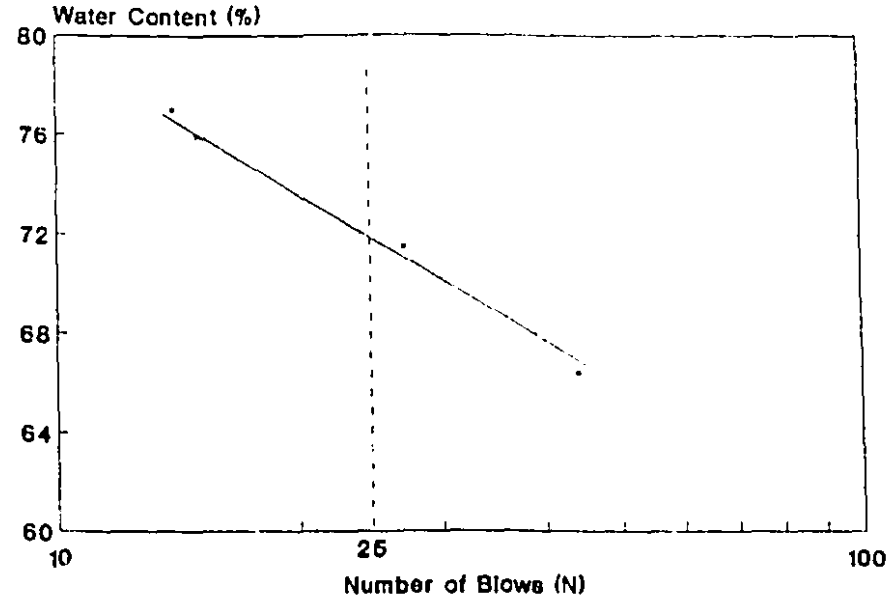

Figure B.2 - Liquid Limit for Kaolinite Hydrite PX.

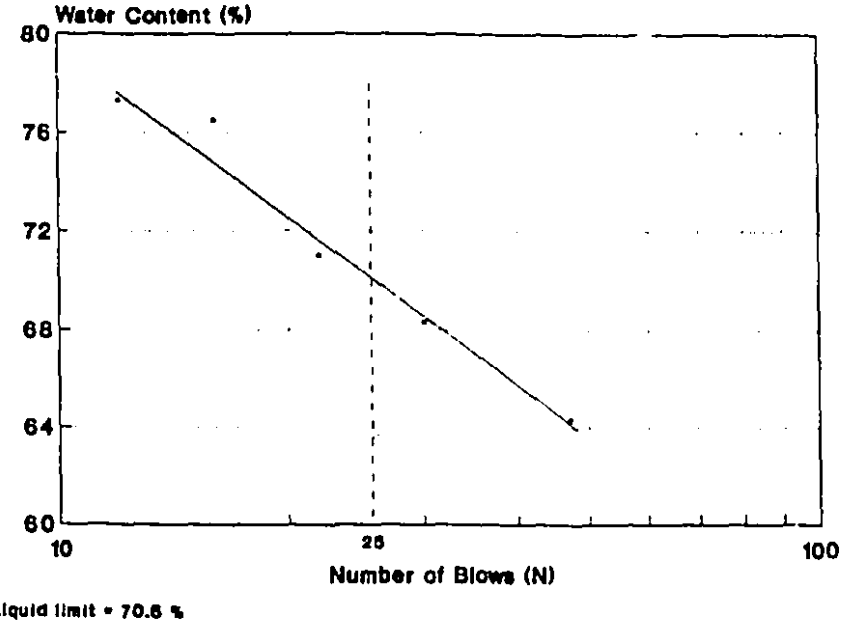

Figure B.3 - Liquid Limit for Kaolinite Hydrite PX Obtained with a 250 ppm *Pb*-solution.

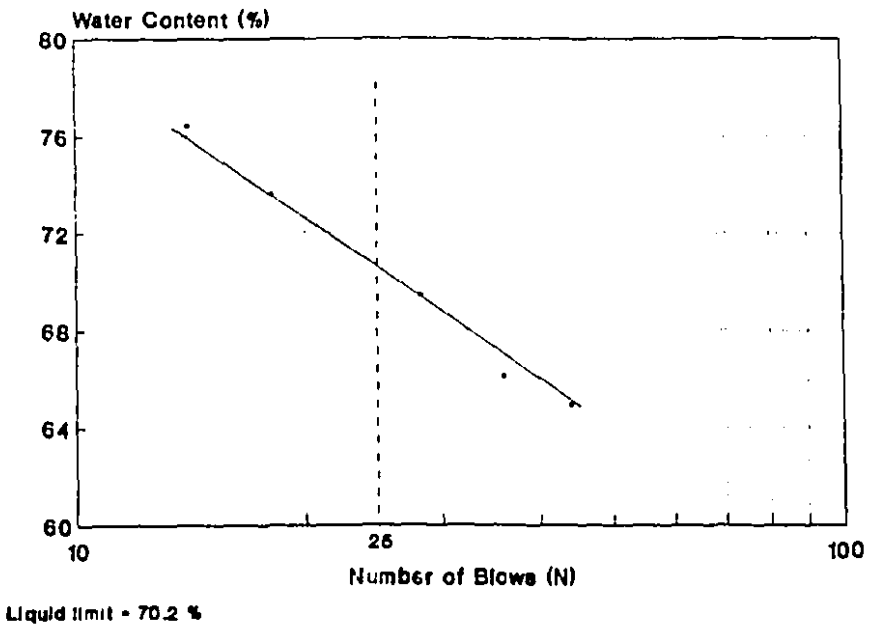

Figure B.4 - Liquid Limit for the Kaolinite Hydrite PX Obtained with a 1750 ppm *Pb*-solution.

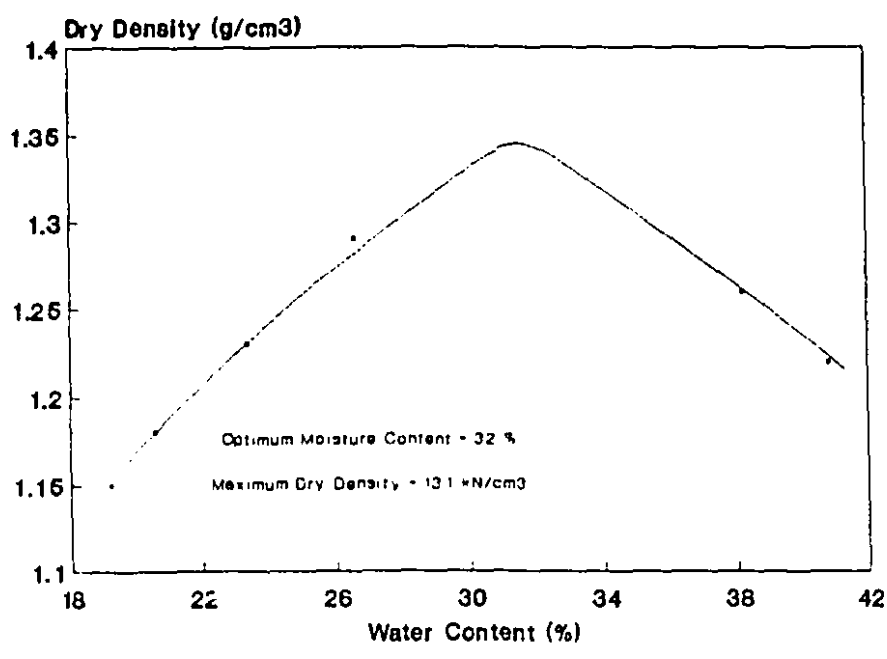

Figure B.5 - Compaction Test with the Kaolinite Hydrite PX.

B.2 - Silica 40 Sand (90%) / Bentonite (10%)

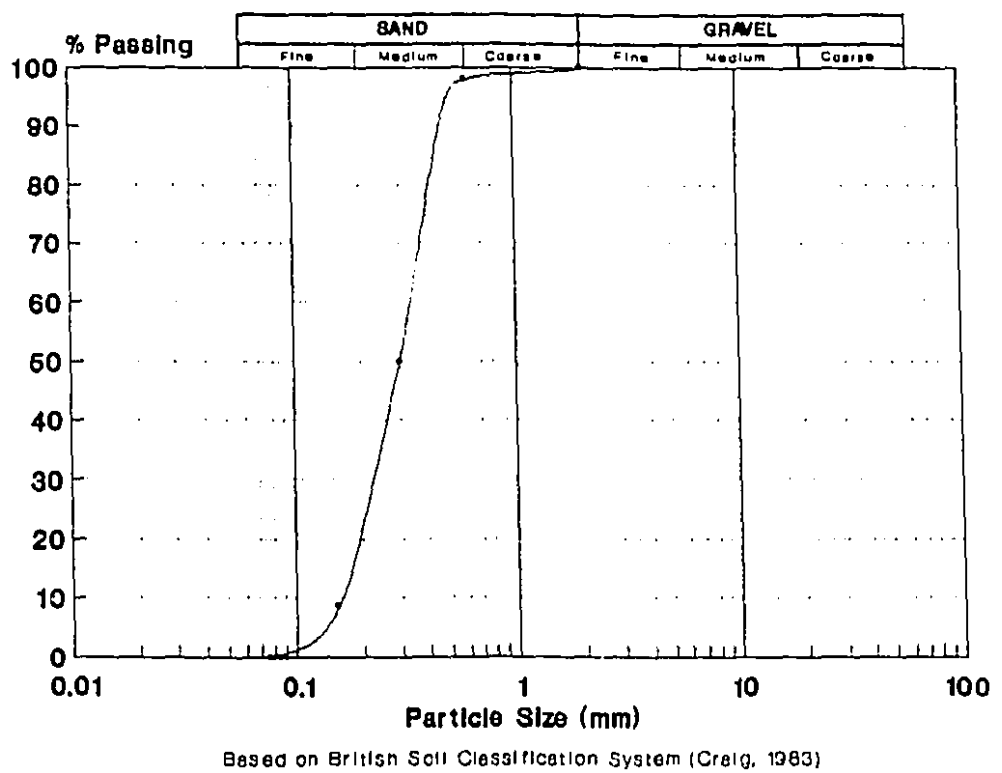

Figure B.6 - Grain size Distribution Curve for the Silica 40 Sand.

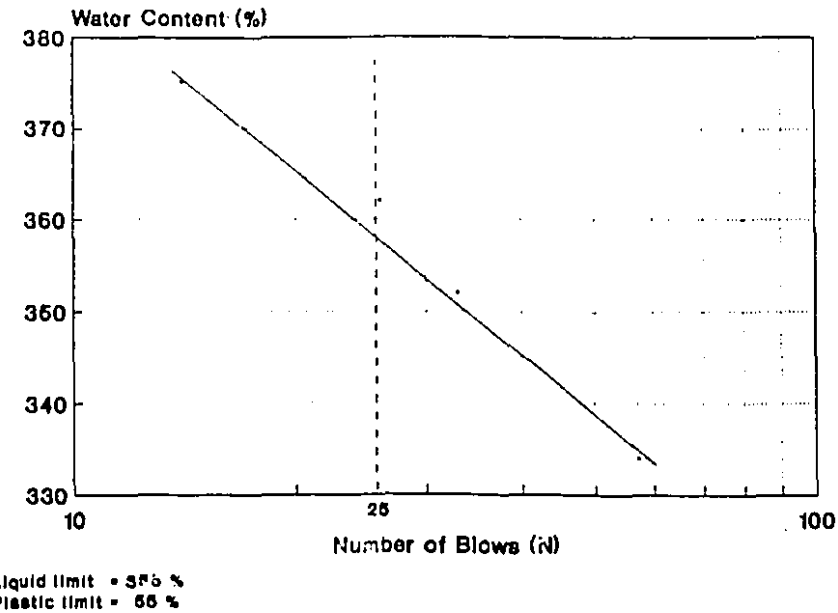

Figure B.7 - Liquid Limit for the Bentonite Clay.

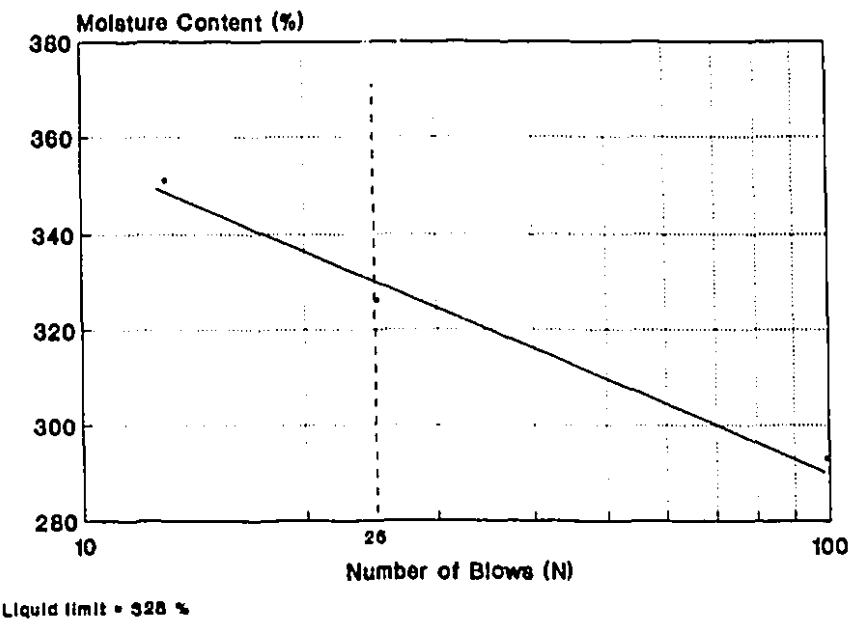

Figure B.8 - Liquid Limit for the Bentonite Clay Obtained with a 500 ppm *Pb*-solution.

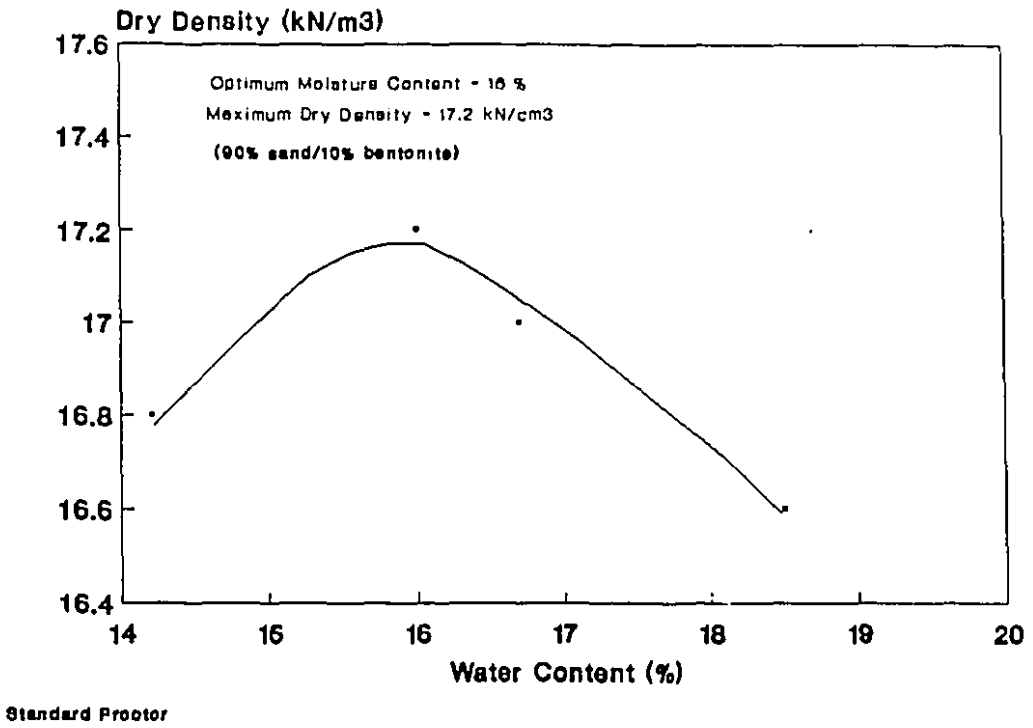

Figure B.9 - Compaction Test with the Sand/Bentonite Mixture (90%/10%).

Appendix C - CEC Determination

The Cation Exchange Capacity (CEC) was determined using an adaptation of the ammonium acetate method described by Black (1965; in Chhabra et al, 1975).

C.1 - The ammonium acetate solution was prepared under a fumehood by adding 57 ml concentrated acetic acid and 68 ml concentrated ammonium hydroxide to 700 ml distilled water. Since the desired pH of the solution was 3.6[1], acetic acid was added to bring the pH down;

C.2 - Four grams of soil (kaolinite or bentonite) were carefully weighed into a plastic 40 ml centrifuge tube (Nalgene). Triplicates were prepared, so a total of 12 grams of soil was needed. ;

C.3 - To each of the three centrifuge tubes, 33 ml of the ammonium acetate solution was added. The tubes were then placed in a mechanical shaker for approximately 2 hours;

---

[1] In order to create an acidic condition; see explanation in the text of Chapter ?.

C.4 - Following shaking, the tubes were placed in a high speed Damon IEC HT centrifuge for approximately 10 minutes (30 minutes for S/B mixture). The supernatant was then decanted into a 100 ml container;

C.5 - Steps C.3 and C.4, D.3.5 were repeated two more times to make a total of 100 ml of supernatant collected;

C.6 - The supernatant was then analyzed for *Na*, *K*, *Mg*, *Ca*, and *Al* (kaolinite only) using a GBC 902 double beam atomic absorption spectrophotometer. In some cases dilutions may be needed in order to keep the atomic absorption reading in the most accurate range. The analysis involved measuring the concentrations (in **ppm**) of all cations in the supernatant, as well as their background concentrations both in the ammonium acetate solution and in the distilled water used for dilutions. These background concentrations must be subtracted from the average concentrations (from triplicates) to give the final concentration of each ion;

C.7 - To convert from **ppm** to **meq/100 g**, the formula below (C.1) was used:

$$meq/100g = \frac{[g/L] \times 100ml \times 100g \times 1000}{1000ml \times 4g \times equ.weight\,of\,cation} \qquad (C.1)$$

where: [g/L] ≡ concentration of the ion in grams per litre;

100 ml -> amount of ammonium acetate;

1000 ml -> 1000 ml in 1 litre;

4 g -> amount of dry soil; and

1000 -> to convert from equivalents to miliequivalents.

C.8 - The value in meq/100 g for each of the cations was summed up to determine the **CEC** of the material.

C.9 - Since kaolinite is a variable charge type of mineral, it is important to consider the pH of the system. In the present case, not only the kaolinitic clay is acidic, but the ammonium acetate solution was prepared at pH = 3.6. Thus, the exchangeable H^+ (see procedure below) and Al^{+++} have to be included in the total CEC (see discussion in Chapter ?).

C.10 - In the case of bentonite, the exchangeable H^+ and Al^{+++} are not considered in the total CEC.

C.11 - Determination of the Exchangeable-H^+ (adapted from Jackson, 1967):

2.5 g of kaolinite were mixed with 25 ml of ammonium acetate solution. The pH of the solution was nearly neutral, and was recorded before

addition of the clay (pH_0). The mixture was shaken intermittently over a one hour time span. After one hour, the pH of the mixture was measured (pH_1). The exchangeable-H^+ content, in meq/100g, was calculated according to the Formula :

$$exch.\ hydr.\ (meq/100g) = (pH_0 - pH_1) \times 22 \qquad (C.2)$$

Appendix D - Sample Preparation for Chemical Analyses

D.1 - Preliminary Observations

D.1.1 - This procedure is used to evaluate the adsorption capability of clay samples which have been percolated by heavy metal solutions. In the case trace metal concentrations are used, this procedure may have to be slightly changed (use of super-quality distilled water, use of a graphite furnace instead of flame atomic spectrometry, greater care during washing of the glassware, etc.);

D.1.2 - This procedure may not be the ideal when more than one contaminant species are being tested;

D.1.3 - This procedure applies to samples extruded from most types of permeameters. In some specific cases, e.g.: samples tested in double-ring permeameters (Anderson et al, 1985), a different procedure may be required.

D.1.4 - For a given: a) diameter; b) specific weight of the material; and c) compacted density, each slice must be thick enough, so that triplicates can be made of them. Each one of the triplicates has to weigh 4 g when dry, in order to keep the liquid:solid ratio of 1:10 (EPA, 1987)

during the extraction procedure. Example of calculation of the minimum weight of a slice:

given that the final water content of the slice is $w_f\% = 24\%$ and that $\pm$ 2.0 g will be used for water content determination:

W_s = [4.0 g x 3 (triplicates) $\pm$ 2] x 1.24 = 17.4 g,

say: 20.0 g, for eventual losses;

D.1.5 - When testing kaolinite for acidic contaminant solutions (see Section 3.1.1), 2.5 g per slice have to be added. This material is used to determine the amount of exchangeable-H^+ (see the procedure described by Jackson (1967) in the Appendix C). If bacteriological analyses are in demand, the samples may have to be prepared with more material.

D.2 - Preliminary Procedures

D.2.1 - Extrude sample, weigh it and measure diameter and height. Carefully wrap it up in plastic film in between steps 1 and 2;

D.2.2 - Slice it to the number of sections desired. In this procedure, we will be referring to 3 slices;

D.2.3 - Weigh each section;

D.2.4 - Spare some soil from each section for water content (w%) measurement;

D.2.5 - Keep the material of each slice in a separate plastic bag. Label the bags with the designated name of the slice (e.g.: **B** for bottom). If not proceeding immediately to the next step, gather them in another bag, tight it and store it in a humid room. If bacteriological analyses are to be executed, store it in a freezer.

D.3 - Washing Procedure

D.3.1 - Label nine 40 ml centrifuge Nalgene tubes (or equivalent), 3 for each slice (e.g.: B1, B2, ...T2, and T1), and three 250 ml (or more) glass bottles (e.g.: T, M, and B). For kaolinite, a 10^{th} tube is necessary in order to obtain the exchangeable-H^+.

D.3.2 - If the final water content of a slice is, for example, 24%, pour 4.0 x 1.24 = 4.96 g into each of the 3 Nalgene tubes relative to that slice. Repeat the same calculation and procedure to the other slices;

D.3.3 - Add 40 ml of distilled water to each tube;

D.3.4 - Allow them to shake for 1 hour on a end-to-end mechanical shaker;

D.3.5 - Centrifuge them for 30 min at 10,000 g. This Δt and centrifuge force are sufficient to settle the bentonite (or to have clear supernatants),

according to our experience. The Δt and the centrifuge force can be reduced to 10 min and 1000 g in the case of kaolinite;

D.3.6 - Carefully empty the contents of the three tubes of each slice in the same glass bottle (T1, T2 and T3 -> T, ...) without losing any of the soil. The supernatant of the 10th tube (the material for calculation of the exchangeable-H^+) may be discarded;

D.3.7 - Repeat steps D.3.3 through D.3.6 once again. At the end of the washing procedure, each one of the 3 glass bottles will have **240 ml** of diluted **pore fluid** (40 ml x 3 (triplicates) x 2 (repetition));

D.3.8 - The diluted pore fluid is then analyzed for the specific contaminant by AAS. In certain cases, further dilution may be required in order to achieve the degree of accuracy of the AAS apparatus;

D.3.9 - Do not dispose of the soil in the tubes. The material of the 10th tube is dried and used for the evaluation of the exchangeable-H^+, following the procedure described by Jackson (1967).

D.4 - Extraction Procedure

D.4.1 - Label nine 100 ml Nalgene bottles: T1, T2, ..., B2 and B3;

D.4.2 - Prepare 3 (triplicates) x 3 (slices) x 100 ml = 900 ml (say 1 l) of ammonium acetate ('extractant') by adding 81 ml of concentrated

acetic acid and 97 ml of concentrated ammonium hydroxide, and completing it to 1 litre;

D.4.3 - In the present research, the pH of the ammonium acetate was lowered to 3.6 for reasons given in the text. In this case, concentrated acetic acid was added until the pH reached the desired 3.6;

D.4.4 - The same 9 tubes with the washed out soil will be employed here;

D.4.5 - Add 34 ml of the extractant to each tube;

D.4.6 - Execute the same procedure as those of steps D.3.4 and C.4, D.3.5;

D.4.7 - Pour the contents of each centrifuge tube in a separate bottle (T1 in T1, T2 in T2, ...);

D.4.8 - Repeat steps D.4.5 through D.4.7 two more times (add 33 ml, instead of 34 ml of extractant);

D.4.9 - In the end of the extraction procedure, each one of the 9 bottles will have 100 ml of the supernatant. In some cases, dilution is required, in order to evaluate the concentrations of the specific contaminant in these supernatants.

Appendix E - Pb Mass Balance Calculation

E.1 - For a better understanding of the procedure described in this appendix, it is recommended the reading of Appendix D.

E.2 - The actual procedure used to calculate mass balances with kaolinite samples was slightly different, but the one described below can be perfectly applied;

E.3 - After the sample preparation phase, there are 3 bottles containing the pore fluid (**T**, **M**, and **B**), 9 bottles containing the supernatant from the 'extraction' phase (triplicates for **T**, **M**, and **B**), and several tubes containing the leachate collected during permeability testing. The concentration of *Pb* in each one, and in the *Pb*-solution introduced are obtained by AAS. For accuracy, the concentration of *Pb* in the acidified distilled water used for dilutions and in the ammonium acetate solution ('extraction' phase) were also obtained ('background' concentrations);

E.4 - The average concentration in the supernatants - in **g/L** - was used in the following steps;

E.5 - The first step in the mass balance calculation involved the determination of the input quantity of lead: the actual concentration in the *Pb*-solution obtained from AAS was multiplied by the size of one pore volume (volume of voids of the sample);

E.6 - The amount of lead adsorbed by the clay was obtained for each one of the slices using the formula (E.1):

$$mass\,of\,Pb\,(g) = \frac{[g/L] \times WDS \times 100ml}{1000ml \times 4g} \qquad \text{(E.1)}$$

where: [g/L] ≡ average concentration of lead in the supernatant;

WDS ≡ total weight of dry soil for the slice;

100 ml ≡ amount of ammonium acetate added ('extraction' phase);

1000 ml in 1 L;

4 g ≡ weight of dry soil used during the 'extraction' phase;

E.7 - The amount of lead found in the pores of each slice was obtained using the formula (E.2) :

$$mass\,of\,Pb\,(g/L) = \frac{[g/L]_w \times WDS \times 240ml}{WDS_w \times 1000ml} \qquad \text{(E.2)}$$

where: [g/L] ≡ concentration of *Pb* in the pore fluid;

WDS ≡ as above (formula (E.1));

240 ml ≡ volume of distilled water used during the 'washing';

WDS_w ≡ 4 g (weight of dry soil used) x 3 (triplicates) = 12 g;

1000 ml in 1 L;

E.8 - The amount of *Pb* found in the leachate collected was calculated by simply multiplying the concentration in ppm obtained by AAS for each tube, by its respective volume. The total *Pb* in the leachate is the summation of all individual values;

E.9 - The final mass balance equation is:

$$Pb_{introduced} = Pb_{adsorbed} + Pb_{pores} + Pb_{leachate} \qquad (E.3)$$

The causes of discrepancies between the amounts introduced and identified in the system were discussed in Chapter 4.

E.10 - Example of mass balance calculation (sample **TSBPbI1C3_3**):

E.10.1 - Preliminary data:

T : AVG [g/L] = 0.287; AVG $[g/L]_w$ = 0.0094;

M : AVG [g/L] = 0.190; AVG $[g/L]_w$ = 0.0025;

B : AVG [g/L] = 0.295; AVG $[g/L]_w$ = 0.0107;

T : Weight = 35.36 g; w% = 23.2% => WDS = 28.70 g;

M : Weight = 29.67 g; w% = 22.3% => WDS = 24.26 g;

B : Weight = 18.55 g; w% = 24.7% => WDS = 14.88 g;

E.10.2 - Amount introduced:

16.45 pv's collected. 1 pv (V_v) = 16.5 ml (calculated)

[blank] = 2419 ppm = 2.419 g/L

=> 2.419 g/L * 0.01645 l * 16.5 = 0.657 g introduced;

E.10.3 - amount adsorbed:

T : (0.287 * 28.70 * 100)/(1000 * 4) = 0.2059 g

M : (0.190 * 24.26 * 100)/(1000 * 4) = 0.1152 g

B : (0.295 * 14.88 * 100)/(1000 * 4) = 0.1097 g

total adsorbed = 0.4308 g

E.10.4 - amount in the pores:

T : (0.0094 * 28.70 * 240)/(12 * 1000) = 0.0054 g

M : (0.0025 * 24.26 * 160[2])/(8 * 1000) = 0.0012 g

B : (0.0107 * 14.88 * 240)/(12 * 1000) = 0.0032 g

total in pores = 0.0098 g

E.10.5 - amount in the leachate:

pv #1 : 0.0015 g/L * 0.0165 L = $2.5 * 10^{-5}$ g;

... pv#14, and

pv #16.45 : 1.7 g/L * (0.0165 L * 2.45) = 0.0687 g

total in leachate = 0.2682 g

E.10.6 - total amount found in the system:

total *Pb* = 0.2682 (leach.) + 0.0098 (pores) + 0.4308 (ads)

total *Pb* = 0.7088 g

E.10.7 - discrepancy : [(0.7088/0.657) - 1] * 100 ≈ 8%

E.11 - The amounts of lead found in the adsorbed form, shown in the preliminary data of the example above, were plotted in the same graph as the

---

[2] only duplicates were prepared for the Mid section

adsorption isotherm. In the case of kaolinite, the number of values plotted was sufficient to draw a curve linking the amounts adsorbed by the **B(s)**, **B**, **M**, and **T** slices of the various samples. This curves were named "adsorption characteristics of compacted material".

Before plotting, it is necessary to convert the values to grams of *Pb* adsorbed/grams of soil (Y-axis of the adsorption isotherm graph) using the formula (E.4) :

$$q = \frac{(C_0 - C) \times V}{M} \qquad \text{(E.4)}$$

where: $(C_0\text{-}C)$ ≡ concentration of *Pb* in the supernatant;

V = volume of ammonium acetate (= 100 ml); and

M = mass of soil used during the 'extraction' phase = 4 g;

Here is one example with the **B**ottom slice of sample **TSBPbI1C3_3**:

$(C_0\text{-}C)$ = AVG [g/L] = 0.295 = $2.95 * 10^{-4}$ g/ml;

V/M = 25 ml/g;

=> value in g/g = $25 * 2.95 * 10^{-4} = 7.4 * 10^{-3}$ g/g.

Appendix F - Data Results of Triaxial Cell Tests

F.1 - Sample Characteristics Before Permeability Testing

SAMPLE_ID	H (cm)	AREA (cm2)	W_TOT (g)	W_T (g)	W_M (g)	W_B (g)	W_BS (g)	w T (%)	w M (%)	w B (%)	e_f AVG	S AVG (%)
TKPbI2C3	7.30	9.65	127.85	0.00	0.00	0.00	0.00	41.4	42.5	43.4	1.04	100.0
TKPbI2C1	7.30	10.26	133.99	44.00	0.00	0.00	0.00	40.6	0.0	0.0	1.04	100.0
TKPbI1C3	6.54	11.22	128.47	41.00	41.22	38.54	7.61	41.3	45.5	46.4	1.06	100.0
TKPbI3C1	6.92	10.29	129.62	45.06	42.51	35.34	6.53	35.2	41.0	41.1	0.96	100.0
THIXO	6.90	10.00	125.97	0.00	0.00	0.00	0.00	40.4	0.0	0.0	0.98	100.0
TKPbI3C3*	0.00	0.00	0.00	0.00	0.00	0.00	0.00	45.0	0.0	0.0	0.00	0.0
TKPbI3C3_b	6.67	0.00	124.48	41.24	38.41	37.06	7.89	38.8	40.0	40.0	0.00	0.0
TKPbI3C2	7.11	10.29	130.30	44.08	41.13	37.38	7.08	40.2	38.9	38.0	1.03	98.0
TKPbI3C3GAMB	6.81	10.12	119.63	37.16	36.43	37.36	8.68	40.4	40.4	40.4	1.10	95.5
TKPbI3C3GAMA	6.99	10.35	132.59	43.17	43.80	38.28	7.29	38.4	38.4	38.6	0.96	100.0
TSBPBI3C3NB	4.20	9.95	85.39					22.1		25.0	0.61	100.0
TSBPBI1C3_5	4.03	10.07	81.73					21.8	21.8	22.3	0.61	95.0
TSBPBI3C3*	3.94	10.07	79.53					23.7	23.7	24.5	0.64	99.8
TSBPBI1C3_3	4.09	10.40	85.35	35.36	29.67	18.55		23.2	22.3	24.7	0.63	96.7
TSBPBI3C3BP	4.00	10.14	82.27	24.82	30.71	26.46		22.0	22.3	22.7	0.61	97.3
TSBZnI1C3	3.71	10.00	76.01	29.00	24.29	22.69		23.3	23.5	23.9	0.61	100.0
TSBPbI1C1	3.85	10.00	77.29	26.54	29.81	20.64		22.3	22.6	N.A.	0.62	96.5

F.2 - Sample Characteristics After Permeability Testing

SAMPLE_ID	H (cm)	AREA (cm2)	TOT_VOL (cm3)	W (g)	WDS (g)	G	e0	S (%)	Vv (cm3)	w (%)
TKPbI2C3	6.99	9.93	69.55	121.90	93.00	2.60	0.94	85.2	33.63	30.8
TKPbI2C1	7.16	10.29	73.70	123.99	94.40	2.60	1.03	79.0	37.40	31.3
TKPbI1C3	7.07	10.15	71.76	124.20	92.44	2.60	1.02	86.0	36.24	34.4
TKPbI3C1	6.95	10.24	71.14	124.95	94.66	2.60	0.95	87.2	34.73	32.0
THIXO	6.87	10.00	68.76	121.06	90.68	2.60	0.97	89.7	33.86	33.5
TKPbI3C3*	6.73	10.21	68.76	118.90	87.75	2.60	1.04	88.0	35.05	35.5
TKPbI3C3_b	6.86	10.21	70.07	120.80	89.35	2.60	1.04	88.0	35.72	35.2
TKPbI3C2	7.05	10.21	72.03	124.06	91.44	2.60	1.05	88.0	36.89	35.6
TKPbI3C3GAMB	6.83	10.15	69.29	112.36	84.35	2.60	1.14	76.0	36.85	33.2
TKPbI3C3GAMA	6.90	10.29	70.98	126.34	95.00	2.60	0.94	91.0	34.40	33.0
TSBPBI3C3NB	4.25	10.07	42.80	82.97	69.49	2.66	0.64	80.6	16.70	19.4
TSBPBI1C3_5	4.08	10.07	41.09	79.05	67.39	2.66	0.62	74.2	15.70	17.3
TSBPBI3C3*	3.96	10.07	39.88	76.76	64.83	2.66	0.64	76.5	15.60	18.4
TSBPBI1C3_3	4.13	10.35	42.72	82.37	69.75	2.66	0.63	76.4	16.50	18.1
TSBPBI3C3BP	4.05	10.15	41.09	80.02	67.60	2.66	0.62	79.0	15.70	18.4
TSBZnI1C3	3.81	10.07	38.38	73.51	61.93	2.66	0.65	76.8	15.10	18.7
TSBPbI1C1	3.89	10.15	39.43	75.43	63.60	2.66	0.65	76.2	15.50	18.6

F.3 - "Isotherms" of Adsorption

F.3.1 - Freundlich Adsorption Isotherms

$$q = \frac{(C_0 - C) * V}{M} \qquad \text{(F.1)}$$

where: V = volume = 40 ml;
M = mass = 4 grams => V/M = 10 ml/g;
C_0 = initial concentration of *Pb* in the solution (ppm);
C = equilibrium concentration of *Pb* in the solution (ppm).

Obs.: (C_0-C) is the amount adsorbed; this was obtained directly from the supernatant after the "extraction" procedure.

F.3.1.1 - Kaolinite

C_0 (mg/l)	C_0-C (mg/l)	C (mg/l)	q $(g/g)*10^{-5}$
131.5	70.5	61.0	71.0
161.5	95.7	65.8	95.7
346.5	185.1	161.4	185.0
708.6	279.5	429.1	280.0
1185.2	284.0	901.2	284.0
1354.0	393.4	960.6	393.0
1802.5	345.7	1456.8	346.0
1807.7	342.0	1465.7	342.0
2321.0	376.4	1944.6	376.0
2369.0	326.5	2042.5	327.0

The regression analysis gives the following parameters for the power curve fitting (Equation (F.2)) :

$$q = aC^b \qquad \text{(F.2)}$$

a = 0.000173; b = 0.4162; and

R^2 = 0.89.

F.3.1.2 - Sand/Bentonite

C_0 (mg/l)	C_0-C (mg/l)	C (mg/l)	q (g/g)*10^{-5}
442.4	386.6	55.8	387.0
1076.1	641.3	434.8	641.0
1451.9	778.9	673.0	779.0
1776.6	888.4	888.2	884.0
1971.2	812.5	1158.7	813.0
2336.5	774.0	1562.5	774.0
2531.1	947.2	1583.9	947.0
2903.9	823.7	2080.2	824.0
3664.6	874.7	2789.9	875.0

The regression analysis gives the following parameters for the power curve fitting (Equation (F.2)) :

a = $1.74 * 10^{-3}$; b = 0.216; and

R^2 = 0.955.

F.3.2 - Adsorption Characteristic Curves for Compacted Kaolinite

The Freundlich model (Equation (F.2)) was also used to draw the 4 adsorption curves drawn for samples tested in the triaxial cell: one for each slice. For those tested in the consolidation cell, see Weber (1991)). In the present case :

V = 100 ml; M = 4 grams => V/M = 25 ml/g. (Equation (F.1))

Sample	Slice	C_0 (mg/l)	C_0-C (mg/l)	C (mg/l)	q (g/g)*10^{-5}
TKPbI1C3	B(s)	1678.6	89.3	1589.3	223.3
	B		75.0	1603.6	187.5
	M		69.2	1609.4	173.0
	T		50.6	1628.0	126.5
TKPbI2C3	B(s)	1783.8	100.5	1683.3	251.3
	B		86.1	1697.7	215.3
	M		62.3	1721.5	155.8
	T		37.8	1746.0	94.5
TKPbI2C1	B(s)	235.1	31.4	203.7	78.5
	B		24.5	210.6	61.3
	M		11.6	223.5	29.0
	T		0.0	235.1	0.0
TKPbI3C3γ_b	B(s)	1735.7	98.6	1637.1	246.5
	B		83.8	1651.9	209.5
	M		61.2	1674.5	153.0
	T		48.1	1687.6	120.3
TKPbI3C3γ_a	B(s)	1735.7	111.4	1624.3	278.5
	B		88.1	1647.6	220.3
	M		58.6	1677.1	146.5
	T		45.5	1690.2	113.8

Continues

Continued

Sample	Slice	C_0 (mg/l)	C_0-C (mg/l)	C (mg/l)	q (g/g)*10^{-5}
TKPbI3C3_b	B(s)	1690.0	115.2	1574.8	288.0
	B		103.4	1586.6	258.5
	M		72.5	1617.5	181.3
	T		70.8	1619.2	177.0
TKPbI3C3	B(s)	1783.8	93.0	1690.8	232.5
	B		83.6	1700.2	209.0
	M		41.4	1742.4	103.5
	T		19.5	1764.3	48.8
TKPbI3C2	B(s)	893.1	85.4	807.7	213.5
	B		57.7	835.4	144.3
	M		38.4	854.7	96.0
	T		33.3	859.8	83.3
TKPbI3C1	B(s)	215.5	29.6	185.9	74.0
	B		24.0	191.5	60.0
	M		13.7	201.8	34.3
	T		3.1	212.4	7.8

Equation by slice:

Slice	Parameters for Equation $q = a.C^b$		
	a	b	R^2
B(s)	4.2×10^{-5}	0.557	0.950
B	2.51×10^{-5}	0.60	0.975
M	5.86×10^{-6}	0.747	0.930
T	2.71×10^{-9}	1.74	0.810

F.4 - Permeability Test Data

TSBZnI1C3: permeability test data

DT (min)	BUR_IN	BUR_OUT	VOL. IN (ml)	VOL. OUT (ml)	K IN (cm/s)	K OUT (cm/s)	P. VOL.OU ACCUM. (m	hydr. grad.
	21.80	0.10						25
331	16.05	5.60	-11.2	10.9	-2.26E-06	2.20E-06	0.75	
293	10.85	10.70	-10.4	10.2	-2.37E-06	2.32E-06	1.46	
311	15.00	8.45	-15.6	15.3	-3.34E-06	3.28E-06	2.50	
410	4.95	10.30	-19.7	19.4	-3.20E-06	3.15E-06	3.85	
189	17.05	5.85	-10.9	10.7	-3.84E-06	3.77E-06	4.59	
417	7.05	15.70	-20.0	19.7	-3.20E-06	3.15E-06	5.94	
424	5.00	19.00	-36.8	36.6	-5.79E-06	5.75E-06	8.47	
380	13.40	10.25	-20.8	20.2	-3.65E-06	3.54E-06	9.86	
305	6.10	17.10	-13.6	13.6	-2.97E-06	2.97E-06	10.80	
61	22.10	2.30	-3.6	3.6	-3.93E-06	3.93E-06	11.04	
246	14.50	9.70	-9.6	9.4	-2.60E-06	2.55E-06	12.00	
251	7.80	6.60	-13.4	13.4	-3.56E-06	3.56E-06	13.00	
172	3.40	11.00	-8.8	8.8	-3.41E-06	3.41E-06	13.60	

TSBPbI1C3_5: permeability test data

DT (min)	BUR_IN	BUR_OUT	VOL. IN (ml)	VOL. OUT (ml)	K IN (cm/s)	K OUT (cm/s)	P. VOL.OU ACCUM.	HYDR. GRAD
	10.60	5.55						
203	9.30	6.80	-2.6	2.5	-8.48E-07	8.15E-07	0.159	i = 25
196	23.25	7.35	-1.2	1.1	-4.05E-07	3.72E-07	0.229	
947	21.55	9.00	-3.4	3.3	-2.38E-07	2.31E-07	0.439	
1457	18.85	11.65	-5.4	5.3	-2.45E-07	2.41E-07	0.777	
1477	16.75	13.70	-4.2	4.1	-1.88E-07	1.84E-07	1.038	
1401	15.00	15.35	-3.5	3.3	-1.65E-07	1.56E-07	1.248	
2023	12.60	3.10	-4.8	4.8	-1.57E-07	1.57E-07	1.554	
1273	11.20	4.40	-2.8	2.6	-1.46E-07	1.35E-07	1.720	
1040	10.20	5.55	-2	2.3	-1.27E-07	1.46E-07	1.866	
3094	7.35	8.45	-5.7	5.8	-1.22E-07	1.24E-07	2.236	
1424	15.30	12.00	-7	7.1	-1.60E-07	1.65E-07	2.688	i = 50
1630	11.25	16.10	-8.1	8.2	-1.64E-07	1.66E-07	3.210	
1019	9.00	3.85	-4.5	4.5	-7.30E-08	7.30E-08	3.497	i = 100
1482	6.15	6.75	-5.7	5.8	-6.40E-08	6.50E-08	3.866	
1393	3.40	9.60	-5.5	5.7	-6.50E-08	6.80E-08	4.229	

TSBPbl1C3_3: permeability test data

DT (min)	BUR_IN	BUR_OUT	VOL. IN (ml)	VOL. OUT (ml)	K IN (cm/s)	K OUT (cm/s)	P. VOL.OU ACCUM.	hydr. grad.
	19.50	8.15						
117	18.20	9.50	-2.6	2.7	-1.43E-06	1.49E-06	0.16	i = 25
326	15.30	12.50	-5.8	6	-1.15E-06	1.19E-06	0.53	
631	11.25	16.65	-8.1	8.3	-8.27E-07	8.47E-07	1.03	
170	21.40	1.45	-2.4	2.4	-9.09E-07	9.09E-07	1.18	
370	19.10	3.85	-4.6	4.8	-8.01E-07	8.36E-07	1.47	
752	15.15	8.10	-7.9	8.5	-6.77E-07	7.28E-07	1.98	
403	12.90	2.35	-4.5	4.7	-7.19E-07	7.51E-07	2.27	
1104	7.40	8.25	-11	11.8	-6.42E-07	6.88E-07	2.98	
297	5.85	1.70	-3.1	3.3	-6.72E-07	7.16E-07	3.18	
1223	0.00	7.90	-11.7	12.4	-6.16E-07	6.53E-07	3.93	
1607	9.80	10.40	-19.5	20	-7.82E-07	8.02E-07	5.15	
1202	16.00	7.70	-14.8	15	-7.93E-07	8.04E-07	6.05	
1449	8.05	8.25	-15.9	16.3	-7.07E-07	7.25E-07	7.04	
1189	15.60	8.55	-16.4	16.6	-8.88E-07	8.99E-07	8.05	
1386	8.25	7.60	-14.7	15.1	-6.83E-07	7.02E-07	8.96	
251	16.20	2.65	-5	5.2	-6.42E-07	6.67E-07	9.28	i = 50
275	13.50	5.40	-5.4	5.5	-6.32E-07	6.44E-07	9.61	
414	9.65	9.35	-7.7	7.9	-5.99E-07	6.15E-07	10.09	
339	6.40	3.65	-6.5	6.5	-6.18E-07	6.18E-07	10.48	
242	4.05	6.10	-4.7	4.9	-6.25E-07	6.52E-07	10.78	
1000	14.10	15.95	-19.2	19.7	-6.18E-07	6.34E-07	11.98	
385	9.45	5.15	-9.2	9.6	-3.85E-07	4.02E-07	12.56	i = 100
958	11.05	18.10	-25.2	25.9	-4.24E-07	4.35E-07	14.13	
501	4.90	6.65	-12.3	12.9	-3.95E-07	4.15E-07	14.91	
929	11.35	19.50	-25.2	25.7	-4.37E-07	4.45E-07	16.47	

TSBPbl1C1: permeability test data

DT (min)	BUR_IN	BUR_OUT	VOL. IN (ml)	VOL. OUT (ml)	K IN (cm/s)	K OUT (cm/s)	P. VOL.OU ACCUM.	hydr. grad.
	20.60	0.10						
141	18.00	2.75	-1	1	-4.66E-07	4.66E-07	0.25	i=25
193	17.60	3.15	-0.8	0.8	-2.73E-07	2.73E-07	0.30	
1177	16.35	4.35	-2.5	2.4	-1.40E-07	1.34E-07	0.45	
2879	15.75	5.00	-1.2	1.3	-2.74E-08	2.97E-08	0.54	
1523	15.50	5.15	-0.5	0.3	-2.16E-08	1.30E-08	0.55	
2859	15.15	5.50	-0.7	0.7	-1.61E-08	1.61E-08	0.60	
2993	14.85	5.75	-0.6	0.5	-1.32E-08	1.10E-08	0.63	
2081	14.60	6.00	-0.5	0.5	-1.58E-08	1.58E-08	0.66	
5700	14.05	6.50	1.1	1	-1.30E-08	1.15E-08	0.73	
7761	13.45	7.10	-1.2	1.2	-1.02E-08	1.02E-08	0.81	
6652	12.95	7.60	-1	1	-1.00E-08	1.00E-08	0.87	
4382	12.60	7.95	-0.7	0.7	-1.05E-08	1.05E-08	0.92	
5770	12.10	8.40	-1	0.9	-1.14E-08	1.03E-08	0.97	

6013	9.65	1.10	-1.9	1.8	-2.08E-08	1.97E-08	1.09	
5324	8.95	1.85	-1.4	1.5	-1.73E-08	1.85E-08	1.19	
4425	8.45	2.35	-1	1	-1.49E-08	1.49E-08	1.25	
4136	7.95	2.85	-1	1	-1.59E-08	1.59E-08	1.32	
5799	7.30	3.50	-1.3	1.3	-1.47E-08	1.47E-08	1.40	
4439	6.80	4.00	-1	1	-1.48E-08	1.48E-08	1.46	
9992	5.75	5.00	-2.1	2	-1.38E-08	1.32E-08	1.59	
10089	4.70	6.05	-2.1	2.1	-1.37E-08	1.37E-08	1.73	
7680	3.90	6.80	-1.6	1.5	-1.28E-08	1.28E-08	1.83	
8161	1.95	8.80	-3.9	4	-3.14E-08	3.22E-08	2.08	i=100
293	23.45	0.45	-0.3	0.5	-1.68E-08	2.80E-08	2.12	
1134	22.90	1.00	-1.1	1.1	-1.59E-08	1.59E-08	2.19	
3162	21.45	2.45	-2.9	2.9	-1.51E-08	1.51E-08	2.37	
5441	19.15	4.85	-4.6	4.8	-1.39E-08	1.45E-08	2.68	
6114	16.65	7.30	-5	4.9	-1.34E-08	1.32E-08	3.00	
4000	15.05	8.90	-3.2	3.2	-1.31E-08	1.31E-08	3.21	
5859	12.80	2.50	-4.5	4.7	-1.27E-08	1.32E-08	3.51	
5708	10.55	4.65	-4.5	4.3	-1.30E-08	1.24E-08	3.79	
4225	8.80	6.40	-3.5	3.5	-1.36E-08	1.36E-08	4.01	
5760	6.60	8.70	-4.4	4.6	-1.26E-08	1.31E-08	4.31	
8667	3.25	12.15	-6.7	6.9	-1.27E-08	1.31E-08	4.75	
7609	19.70	3.70	-6.9	7	-1.49E-08	1.51E-08	5.21	
5367	17.30	6.10	-4.8	4.8	-1.47E-08	1.47E-08	5.52	
8830	13.45	10.05	-7.7	7.9	-1.43E-08	1.47E-08	6.03	
4543	11.40	12.05	-4.1	4	-1.48E-08	1.45E-08	6.28	
6736	8.50	15.00	-5.8	5.9	-1.42E-08	1.44E-08	6.66	
2910	23.10	1.00	-1.3	1.2	-2.70E-08	2.70E-08	6.74	i=25
4315	20.80	3.35	-4.6	4.7	-7.00E-08	7.15E-08	7.05	
5660	19.40	4.70	-2.8	2.7	-3.24E-08	3.13E-08	7.22	
4451	18.40	5.75	-2	2.1	-2.95E-08	3.10E-08	7.35	
4312	17.40	6.65	-2	1.8	-3.05E-08	2.74E-08	7.47	
5620	16.40	7.70	-2	2.1	-2.34E-08	2.46E-08	7.61	
4259	15.60	8.45	-1.6	1.5	-2.47E-08	2.32E-08	7.70	
7152	14.30	9.70	-2.6	2.5	-2.39E-08	2.30E-08	7.86	
7423	13.05	11.00	-2.5	2.6	-2.21E-08	2.30E-08	8.03	
7346	11.85	12.10	-2.4	2.2	-2.15E-08	1.97E-08	8.17	

TSBPbI3C38P: permeability test data

DT (min)	BUR_IN	BUR_OUT	VOL. IN (ml)	VOL. OUT (ml)	K IN (cm/s)	K OUT (cm/s)	P. VOL.OU ACCUM.	hydr. grad.
	14.80	0.25						
102	13.60	1.25	-2.40	2.00	-3.86E-07	3.22E-07	0.13	i = 100
223	13.12	1.60	-0.96	0.70	-7.07E-08	5.15E-08	0.17	
1107	12.20	2.40	-1.84	1.60	-2.73E-08	2.37E-08	0.27	
426	11.95	2.55	-0.50	0.30	-1.93E-08	1.16E-08	0.29	
1284	11.30	3.10	-1.30	1.10	-1.66E-08	1.41E-08	0.36	
2491	10.45	3.80	-1.70	1.40	-1.12E-08	9.23E-09	0.45	
487	10.30	3.95	-0.30	0.30	-1.01E-08	1.01E-08	0.47	

1269	9.90	4.30	-0.80	0.70	-1.04E-08	9.06E-09	0.52	
1192	9.45	0.45	-0.70	0.70	-9.64E-09	9.64E-09	0.56	
1764	8.85	0.90	-1.20	0.90	-1.12E-08	8.38E-09	0.62	
5450	7.40	2.30	-2.90	2.80	-8.74E-09	8.44E-09	0.80	
2880	6.65	3.00	-1.50	1.40	-8.55E-09	7.98E-09	0.89	
2876	5.95	3.65	-1.40	1.30	-7.99E-09	7.42E-09	0.97	
4276	4.92	1.08	-2.06	1.96	-7.91E-09	7.53E-09	1.09	
2861	4.22	1.68	-1.40	1.20	-8.04E-09	6.89E-09	1.17	
7152	2.65	3.15	-3.14	2.94	-7.21E-09	6.75E-09	1.36	
2967	15.40	3.50	-1.20	1.00	-6.64E-09	5.53E-09	1.42	
7206	14.30	4.45	-2.20	1.90	-5.01E-09	4.33E-09	1.54	
1424	13.92	0.40	-0.46	0.40	-5.30E-09	4.61E-09	1.57	
7230	12.90	1.30	-2.04	1.80	-4.63E-09	4.09E-09	1.68	
4272	12.30	1.80	-1.20	1.00	-4.61E-09	3.84E-09	1.75	
4335	11.78	2.15	-1.04	0.70	-3.94E-09	2.65E-09	1.79	
5624	11.00	2.75	-1.56	1.20	-4.55E-09	3.50E-09	1.87	
4376	10.40	3.20	-1.20	0.90	-4.50E-09	3.38E-09	1.92	
5930	9.60	3.80	-1.60	1.20	-4.43E-09	3.32E-09	2.00	i = 200
4196	8.65	0.80	-1.90	1.60	-3.72E-09	3.13E-09	2.10	
5362	7.50	1.65	-2.30	1.70	-3.52E-09	2.60E-09	2.21	
3878	6.60	2.20	-1.80	1.10	-3.81E-09	2.33E-09	2.28	
4322	5.75	2.75	-1.70	1.10	-3.23E-09	2.09E-09	2.35	
4702	4.60	3.30	-2.30	1.10	-4.02E-09	1.92E-09	2.42	
5275	3.50	4.00	-2.20	1.40	-3.42E-09	2.18E-09	2.51	
1301	21.20	0.65	-0.80	0.70	-2.52E-09	2.21E-09	2.55	i = 400
4661	20.10	1.70	-2.20	2.10	-1.94E-09	1.85E-09	2.69	
3089	19.40	2.30	-1.40	1.20	-1.86E-09	1.59E-09	2.76	
10964	16.95	4.35	-4.90	4.10	-1.83E-09	1.54E-09	3.03	
4305	15.70	0.85	-2.30	1.50	-2.19E-09	1.43E-09	3.12	
5738	14.70	1.85	-2.00	2.00	-1.43E-09	1.43E-09	3.25	
8686	13.20	3.20	-3.00	2.70	-1.42E-09	1.28E-09	3.42	
7598	11.60	4.25	-3.20	2.10	-1.73E-09	1.13E-09	3.55	
12626	9.15	5.95	-4.90	3.40	-1.59E-09	1.11E-09	3.77	
6445	8.15	6.85	-2.00	1.8	-1.30E-09	1.14E-09	3.89	
3387	7.50	7.35	-1.30	0.9	-1.60E-09	1.09E-09	3.95	
10095	16.30	1.7	-3.80	2.5	-1.55E-09	1.02E-09	4.11	
10100	14.75	3	-3.10	2.6	-1.26E-09	1.06E-09	4.28	
10076	13.30	4.25	-2.90	2.5	-1.18E-09	1.02E-09	4.37	
10078	11.95	5.5	-2.70	2.5	-1.10E-09	1.02E-09	4.6	
7217	11.05	6.35	-1.80	1.7	-1.02E-09	9.67E-10	4.7	
10062	8.80	7.4	-4.50	2.1	-1.84E-09	8.60E-10	4.83	
7210	7.30	8.15	-3.00	1.5	-1.71E-09	8.50E-10	5.02	
14377	4.40	9.6	-5.80	2.9	-1.66E-09	8.30E-10	5.12	

tot_in= -105.76 ml tot_out = 80.35 ml
delta (v_in - v_out) =25.41 ml

(leak in a secondary line IN (not leading to cell)
discovered when cleaning up equipment).

F.5 - Mass Balance Calculations Data

TKPbl3C1: results of Pb mass balance

AVG [ppm] (T1-T3) = 3.05
AVG [ppm] (M1-M3) = 13.67
AVG [ppm] (B1-B3) = 23.97
[ppm] B(S) = 29.58

W of top part = 45.06g
w% top = 35.2 (at end)
WDS(top) = 33.33g and WDSwashed = 30g/1.352 = 22.19

W of mid part = 42.51g
w% mid = 41 (at end)
WDS(mid) = 30.15g and WDSw = 21.28g

W of bot = 35.35g
w% bot = 41.1 (at end)
WDS(bot) = 25.05g and WDSw = 21.26g

W of b(s) = 6.53g
use w% for bot
WDS(b(s)) = 4.63g = WDSw

Mass Balance for Pb:

1. Ammount of Pb introduced :

   5 pore volumes = 34.73 * 5 = 173.65 ml
   [blank] = 215.5 mg/l (0.2155 g/l)
   thus, 0.2155 * 173.65/ 1000 = 0.0374 g of Pb were introduced
   (or 0.36 meq)

2. Amount Collected as Leachate:

Nothing was identified in the leachate

3. Amount adsorbed on the clay surface:

   mass in grams = [g/l] * WDS(t,m,b, or b(s)) * 100 / (1000 * 4)
   (4 g of dried soil, 100 ml of Amm. Ac. 1000 stands for 1 liter.)

   am. in the top = 0.00254 g
   am. in the mid = 0.0103 g
   am. in the bot = 0.015 g

am. in the b(s) = 0.00342g
total adsorbed = 0.031 g

4. amount in the pores:

$$\text{mass in g (t-b)} = \frac{[\text{g/l}] * \text{WDS (of the slice)} * 400 \text{ (or } 160)}{\text{WDSw (of the slice)} * 1000}$$

(400 ml were used to wash each slice; 1000 stands for 1 liter)
(in the case of B(S) only 160 ml were used to wash the soil)

am. in the top = 0.00118
am. in the mid = 0.0058
am in the bot = 0.0074
am in the b(s) = 0.0017
total in the pores = 0.0161

5. Summing up:

0.0161 (pores) + 0.031 (adsorbed) = 0.0471 g
(0.155 meq) + (0.300 meq) = (0.455 meq)
this value is 27% HIGHER than the amount introduced in the system,
(0.0374 g).

6. OBS.:
1) the pores contained 34% of the Pb found in the system;
2) 66% was adsorbed;
and the rest leached through.
3) the amount adsorbed does not exceed the value obtained
for the adsorption isotherm (3 meq/100g at 1700 ppm)

TKPbI3C2: results of Pb mass balance

AVG [ppm] (T1-T3) = 33.33
AVG [ppm] (M1-M3) = 38.39
AVG [ppm] (B1-B3) = 57.68
[ppm] B(S) = 85.39

W of top part = 44.08g
w% top = 40.2 (at end)
WDS(top) = 31.44g and WDSwashed = 30g/1.402 = 21.40g

W of mid part = 41.13g
w% mid = 38.9 (at end)
WDS(mid) = 29.61 and WDSw = 21.60g

W of bot = 37.38g
w% bot = 38.0 (at end)
WDS(bot) = 27.09g and WDSw = 21.74g

W of b(s) = 7.08g
use w% for bot
WDS(b(s)) = 5.13g = WDSw

Mass Balance for Pb:

1. Ammount of Pb introduced :

5 pore volumes = 36.89 * 5 = 184.45 ml
[blank] = 893 mg/l (0.893 g/l)
thus, 0.893 * 184.45 / 1000 = 0.165g of Pb were introduced
(or 1.59 meq)

2. Amount Collected as Leachate:

for PV=1 (alias 0.98):
Am. Pb = negligeable
for PV=2 (alias 1.85):
Am. Pb = negligeable
for PV=3 (alias 3.07):
Am Pb = negligeable
for PV=4 :
Am. Pb = 8.76 * 36.89 / 1000 = 0.323 mg = 0.000323 g
for PV=5:
Am. Pb = 152.25 * 36.89 / 1000 = 5.62 mg = 0.0056 g

total of Pb collected in the leachate = 0.006 g

3. Amount adsorbed on the clay surface:

mass in grams = [g/l] * WDS(t,m,b, or b(s)) * 100 / (1000 * 4)
(4 g of dried soil, 100 ml of Amm. Ac. 1000 stands for 1 liter.)

am. in the top = 0.0262 g
am. in the mid = 0.0284g
am. in the bot = 0.0391 g

am. in the b(s) = 0.01095g
total adsorbed = 0.10465 g

4. amount in the pores:

$$\text{mass in g (t-b)} = \frac{[\text{g/l}] * \text{WDS (of the slice)} * 400 \text{ (or } 160)}{\text{WDSw (of the slice)} * 1000}$$

(400 ml were used to wash each slice; 1000 stands for 1 liter)
(in the case of B(S) only 160 ml were used to wash the soil)

am. in the top = 0.0089 g ((0.01506*31.44*400)/(21.4*1000))
am. in the mid = 0.00413
am in the bot = 0.0091
am in the b(s) = 0.0021
total in the pores = 0.024 g

5. Summing up:

0.024 (pores) + 0.1047 (adsorbed) + 0.006 (leach.) = 0.135 g
(0.23 meq) + (1.01 meq) + (0.058 meq) = (1.3 meq)

this value is 18% lower than the amont introduced in the system.
The diff. can be attributed to experimental errors.

6. OBS.:
   1) the pores contained 17.8% of the Pb found in the system;
   2) 77.7% was adsorbed;
   and the rest leached through.
   3) the amount adsorbed does not exceed the value obtained
   for the adsorption isotherm (2.9 meq/100g at 893 ppm)

TKPbI3C3b: results of Pb-mass balance

AVG [ppm] (T1-T3) = 70.79
AVG [ppm] (M1-M3) = 72.47
AVG [ppm] (B1-B3) = 103.37
[ppm] B(S) = 115.17

W of top part = 41.24 g
w% top = 38.8 (at end)

WDS(top) = 29.71g and WDSwashed = 30g/1.388 = 21.61g

W of mid part = 38.41 g
w% mid = 40.0 (at end)
WDS(mid) = 27.43 and WDSw = 21.43g

W of bot = 37.06 g
w% bot = 40.0 (assumed = Mid)
WDS(bot) = 26.47g and WDSw = 21.43g

W of b(s) = 7.89 g
use w% for bot
WDS(b(s)) = 5.64g = WDSw

Mass Balance for Pb:

1. Ammount of Pb introduced :

   10 pore volumes = 35.72 * 10 = 357.20 ml
   [blank] = 1690 mg/l (1.690 g/l)
   thus, 1.690 * 357.20 / 1000 = 0.601 g of Pb were introduced
   (or 5.83 meq)

2. Amount Collected as Leachate:

   for PV=1 :
   Am. Pb = 0.88 * 35.72 / 1000 = 0.0314 mg = 0.0000314g
   for PV=2 :
   Am. Pb = 1.19 * 35.72 / 1000 = 0.043 mg = 0.000043 g
   for PV=3 :
   Am. Pb = 176.2 * 35.72 / 1000 = 6.294 mg = 0.006294 g
   for PV=4 :
   Am. Pb = 795.9 * 35.72 / 1000 = 28.43 mg = 0.02843 g
   for PV=5
   Am. Pb = 925.2 * 35.72 / 1000 = 33.05 mg = 0.03305 g
   for PV=6 :
   Am. Pb = 1043.2 * 35.72 / 1000 = 37.26 mg = 0.03726 g
   for PV=7 :
   Am. Pb = 1327.2 * 35.72 / 1000 = 47.41 mg = 0.04741 g
   for PV=8 :
   Am. Pb = 1375.8 * 35.72 / 1000 = 49.14 mg = 0.04914 g
   for PV=9 :
   Am. Pb = 1475.4 * 35.72 / 1000 = 52.70 mg = 0.05270 g
   for PV=10 :
   Am. Pb = 1322.4 * 35.72 / 1000 = 47.24 mg = 0.04724 g

   total of Pb collected in the leachate = 0.3016 g

3. Amount adsorbed on the clay surface:

mass in grams = [g/l] * WDS(t,m,b, or b(s)) * 100 / (1000 * 4)
(4 g of dried soil, 100 ml of Amm. Ac. 1000 stands for 1 liter.)

am. in the top = 0.0526 g
am. in the mid = 0.0497 g
am. in the bot = 0.0684 g
am. in the b(s) = 0.01623 g
total adsorbed = 0.1869 g

4. amount in the pores:

$$\text{mass in g (t-b)} = [g/l] * \text{WDS (of the slice)} * 400 \text{ (or 160)} \;/\; (\text{WDSw (of the slice)} * 1000)$$

(400 ml were used to wash each slice; 1000 stands for 1 liter)
(in the case of B(S) only 160 ml were used to wash the soil)

am. in the top = 0.027 g ((0.04944*29.72*400)/(21.61*1000))
am. in the mid = 0.0233 g
am in the bot = 0.022
am in the b(s) = 0.0061
total in the pores = 0.0784 g

5. Summing up:

0.0784 (pores) + 0.1869 (adsorbed) + 0.3016 (leach.) = 0.567 g
(0.757 meq) + (1.804 meq) + (2.911 meq) = (4.79 meq)
this value is quite similar to the amount introduced in the system, ie, 0.6037 g (only 6% lower, which can be attributed to experimental errors).

6. OBS.:
1) the pores contained 13.8% of the Pb found in the system;
2) 33% was adsorbed;
3) 53.2% leached through.
3) the amount adsorbed does not exceed the value obtained for the adsorption isotherm (3.50 meq/100g at 1690 ppm)

TKPbI1C3: results of Pb mass balance

AVG [ppm] (T1-T3) = 50.6

AVG [ppm] (M1-M3) = 69.24
AVG [ppm] (B1-B3) = 75.0
[ppm] B(S) = 89.29

W of top part = 41g
w% top = 41.3 (at end)
WDS(top) = 29.02g and WDSwashed = 30g/1.413 = 21.23g

W of mid part = 41.22g
w% mid = 45.5 (at end)
WDS(mid) = 28.33 and WDSw = 20.62g

W of bot = 38.54g
w% bot = 46.4 (at end)
WDS(bot) = 26.33g and WDSw = 20.49g

W of b(s) = 7.61g
use w% for bot
WDS(b(s)) = 5.2g = WDSw

Mass Balance for Pb:

1. Ammount of Pb introduced :

5 pore volumes = 36.24 * 5 = 181.2 ml
[blank] = 1679 mg/l (1.679 g/l)
thus, 1.679 * 181.2 / 1000 = 0.304g of Pb were introduced
(or 2.94 meq)

2. Amount Collected as Leachate:

for PV=0.5 (alias 0.78):
Am. of Pb = negligeable
for PV=1 (alias 0.98):
Am. Pb = negligeable
for PV=2 (alias 1.96):
Am. Pb = 5.65 ppm * 35.6 ml / 1000 ml = 0.2mg (2.0E-4 g)
for PV=3 (alias 2.96):
Am Pb = 59.52 * 36.4 / 1000 = 2.17 mg = 0.00217 g
for PV=4 :
Am. Pb = 815.5 * 37.46 / 1000 = 30.54 mg = 0.0305 g
for PV=5:
Am. Pb = 1190.5 * 36.24 / 1000 = 43.14 mg = 0.043 g

total of Pb collected in the leachate = 0.076 g

3. Amount adsorbed on the clay surface:

mass in grams = [g/l] * WDS(t,m,b, or b(s)) * 100 / (1000 * 4)
(4 g of dried soil, 100 ml of Amm. Ac. 1000 stands for 1 liter.)

am. in the top = 0.0367 g
am. in the mid = 0.049
am. in the bot = 0.0494
am. in the b(s) = 0.0116
total adsorbed = 0.1467 g

4. amount in the pores:

$$\text{mass in g (t-b)} = \frac{[\text{g/l}] * \text{WDS (of the slice)} * 400 \text{ (or 160)}}{\text{WDSw (of the slice)} * 1000}$$

(400 ml were used to wash each slice; 1000 stands for 1 liter)
(in the case of B(S) only 160 ml were used to wash the soil)

am. in the top = 0.0205 g ((0.0375*29.02*400)/(21.23*1000))
am. in the mid = 0.0242
am in the bot = 0.0276
am in the b(s) = 0.0049
total in the pores = 0.0772 g

5. Summing up:

0.0772 (pores) + 0.1467 (adsorbed) + 0.076 (leach.) = 0.300 g
(0.745 meq) + (1.42 meq) + (0.734 meq) = (2.90 meq)
this value is quite similar (2% difference) to the amount introduced in the system, i.e., 0.304 g.

6. OBS.:
1) the pores contained 25.7% of the Pb found in the system;
2) 48.9% was adsorbed;
and the rest, 25.3%, leached through.
3) the amount adsorbed does not exceed the value obtained for the adsorption isotherm (3.5 meq/100g at 1700 ppm)

TKPbI2C1: results of Pb mass balance

1. Ammount of Pb introduced:

5 pore vol. = 187 ml

[blank] = 235 mg/l (.235 g/l)
WDS = 95.36 g (total sample)
WDS (B(s) only) = 4.51 g

thus : .235 --> 1000 x = 0.043(or 0.424 meq) of Pb
x --> 187 mwere introduced in the sample

2. Ammount collected as leachate (total)

Nothing was collected after 5 pv's

3. Amount adsorbed by the clay (AVG between top and bottom):

General AVG = 16.86 ppm (see above)
mass in grams = [g/l] * WDS * 100 / (1000 * 4)

thus, 0.04 g were adsorbed by the clay.

4. amount in the pores (washed out)

AVG (t-b) = 3.29 ppm (see above)
mass in grams(t-b) = [g/l] * (WDS-4.51) * 400 / (21.35 * 1000)
= 0.0056 g were in the pores of the three slices

400 ml refers to the amount of D-water used for washing, and
21.35 is the amount of dry soil washed (= 30g/(1+w%))

mass in grams(b(s))= [g/l] * 4.51 * 120ml / (4.51 * 1000) (++)
= 0.00103g were in the pores of the bottom slice
(++) I used all the material I cut from the sample

summing up, 0.0066 g of Pb were found in the pore solution.

5. Summing up...

0.0066 + 0.04 = 0.0466 g were found in the system.

this value is quite similar to the amount introduced in the system, i.e, 0.0439 g. The difference (7%) can be attributed to experimental errors.

6. OBS.: 1) The pore fluid contained only 13.7% of the total Pb Pb found in the sample
2) Most of the exchangeable Pb is retained in the bottom part of the sample.

TSBZnI1C3: results of Zn mass balance

1. Preliminary data :

AVG [ppm] (T1-T3) = 56.3
AVG [ppm] (M2) = 62.5
AVG [ppm] (B1-B3) = 66.3

W of Top = 29.0 g
w% top = 23.3%
WDS (T) = 23.52g ; WDS washed = 4. * 3 = 12.00 g

W of Mid = 24.59 g
w% mid = 23.5 %
WDS (M) = 19.67 g ; WDS washed = 2 * 4 = 8.0 g

W of Bot = 22.69 g
w% bot = 23.9 %
WDS (B) = 18.3 ; WDS washed = 4 * 3 = 12 g

2. Ammount of Pb introduced:

13.6 pv's at 15.09 ml each = 205.2 ml
[blank] = 2135 ppm (2.135 g/l) AVERAGE
thus, 2.135 * 205.2/1000 = 0.438 g of Zn were introduced

3. Ammount Collected as Leachate :

for pv # 1 : Amm. Zn = 1.1 ppm * 15.09 ml/1000 ml = 0.016 mg
for pv # 1.8 : Amm. Zn = 46.1*0.8*0.01509 = 0.557 mg
for pv # 3 : Amm. Zn = 9.145 mg
for pv # 4.1 : Amm. Zn = 10.32 mg
for pv # 5.4: Amm. Zn = 19.3 mg
for pv # 7.0 : Amm. Zn = 33.9 mg
for pv # 10.5 : Amm. Zn = 84.61 mg
for pv # 12.2: Amm. Zn = 43.0 mg
for pv # 13.6 : Amm. Zn = 31.4 mg

total collected in leachate = 232.24 mg = 0.232 g of Zn

4. Amount adsorbed on the clay surface:

mass in grams (for each slice) = AVG [g/l]*WDS*100/(1000*4)
(4g of dried soil, 100 ml of Amm. Ac.; 1000 stands for 1 liter)

Amm. Pb on Top = 0.0563*23.52/40 = 0.033 g
Amm Pb on Mid = 0.031 g
Amm Pb on Bottom = 0.029 g

total adsorbed = 0.093 g

5. Ammount in the pores:

$$\text{mass in g for each slice} = \frac{[\text{g/l}] * \text{WDS} * 240 \text{ ml (160 for Mid)}}{\text{WDS washed} * 1000}$$

(240 ml were used to wash each slice ; 1000 stands for 1 liter)

amm. on Top = 0.0123 * 23.52 * 240 / (12 *1000) = 0.0058 g
amm. on Mid = 0.0115 * 19.67 * 160 / (8 * 1000) = 0.0038 g
amm. on Bottom = 0.015 * 18.3 * 240 / (12*1000) = 0.0055 g

total in the pores = 0.0151 g

6. Summing up totals :

0.0151 g (pores) + 0.093 g (leach.) + 0.232 g (ads.) = 0.34 g

This value is inferior to the 0.438 g of Zn introduced by 22%

TSBPb11C38P: results of Pb mass balance

1. Preliminary data :

AVG [ppm] (T1-T3) = 0.0 , thus AVG [g/l] = 0.0
AVG [ppm] (M1 and M2) = 9.8 ppm, thus AVG [g/l] = 0.0098
AVG [ppm] (B1-B3) = 297.1, thus AVG [g/l] = 0.297

W of Top = 24.82 g
w% top = 22.0%
WDS (T) = 20.34g ; WDS washed = 4 * 3 = 12.0 g

W of Mid = 30.71 g
w% mid = 22.3 %
WDS (M) = 25.11 g ; WDS washed = 2 * 4 = 8 g

W of Bot = 26.74 g
w% bot = 22.7 %
WDS (B) = 21.79 ; WDS washed = 4 * 3 = 12 g

2. Ammount of Pb introduced:

5 pv's at 15.7 ml each = 78.5 ml
[blank] = 2391 ppm (2.391 g/l)
thus, 2.391 * 78.5/1000 = 0.1877 g of Pb were introduced
(1.814 meq)

3. Ammount Collected as Leachate :

for pv # 1.5 : amm. Pb = 0.66 ppm*15.7 ml/1000 ml = 0.01 mg
for pv # 2 : Amm. Pb = 0.005 mg = 0.5*E-5 g
for pv # 2.5 : Amm. Pb = 0.0365 mg = 3.65*E-5 g
for pv # 3 : Amm. Pb = 0.04 mg = 4.*E-5 g
for pv # 4 : Amm. Pb = 0.008 mg = 0.8*E-5 g
for pv # 5 : Amm. Pb = 0.013 mg = 1.3*E-5 g

total of Pb collected as leachate = 0.0001125 g

4. Amount adsorbed on the clay surface:

mass in grams (for each slice) = AVG [g/l] * WDS * 100/(1000*4)
(4g of dried soil, 100 ml of Amm. Ac.; 1000 stands for 1 liter)

Amm. Pb on Top = 0.0 g
Amm Pb on Mid = 0.0098 * 25.11 / 40 = 0.0062 g
Amm Pb on Bottom = 0.297 * 21.79 / 40 = 0.162 g

total adsorbed = 0.1682 g

5. Ammount in the pores:

$$\text{mass in g for each slice} = \frac{[g/l] * WDS * 240 \text{ ml (160 for Mid)}}{WDS \text{ washed} * 1000}$$

(240 ml were used to wash each slice ; 1000 stands for 1 liter)

amm. on Top = negligeable
amm. on Mid = 0.002 * 25.11 * 160 / (8 * 1000) = 0.001 g
amm. on Bottom = 0.0081 * 21.79 * 240 / (12*1000) = 0.0035 g

total in the pores = 0.0045 g

6. Summing up totals :

0.0045 g (pores)+0.0001125 g (leach.)+0.1682 g (ads.)=0.1728 g
(0.043 meq) (0.0011 meq) (1.624 meq) (1.668 meq)

This value is inferior to the 0.1877 g (1.814 meq)
introduced by 8%.

7. Final Comments :

a) the pores contained 2.6% of the Pb found in the system;
b) 97.3% was adsorbed. Of the total adsorbed, 96.3% was adsorbed by the bottom.

TSBPbl1C3_3: Pb mass balance

1. Preliminary data :

AVG [ppm] (T1-T3) = 286.9 , thus AVG [g/l] = 0.2869
AVG [ppm] (M2) = 190.0 (M1 discarded), thus AVG [g/l] = 0.19
AVG [ppm] (B1-B3) = 295.4, thus AVG [g/l] = 0.295

W of Top = 35.36 g
w% top = 23.2%
WDS (T) = 28.7g ; WDS washed = 4. * 3 = 12.00 g

W of Mid = 29.67 g
w% mid = 22.3 %
WDS (M) = 24.26 g ; WDS washed = 2 * 4 = 8.0 g

W of Bot = 18.55 g
w% bot = 24.7 %
WDS (B) = 14.88 ; WDS washed = 4 * 3 = 12 g

2. Ammount of Pb introduced:

16.45 pv's at 16.5 ml each = 271.43 ml

[blank] = 2419 ppm (2.419 g/l) AVERAGE
thus, 2.419 * 271.43/1000 = 0.657 g of Pb were introduced
(6.35 meq)

3. Ammount Collected as Leachate :

for pv # 1 : amm. Pb=1.5ppm*16.5ml/1000ml=0.025 mg (2.5*E-5 g)
for pv # 2 : Amm. Pb = 0.13 mg = 1.3*E-4 g
for pv # 3 : Amm. Pb = 0.46 mg = 4.6*E-4 g
for pv # 4 : Amm. Pb = 0.87 mg = 8.7*E-4 g
for pv # 5 : Amm. Pb = 10.4 mg = 0.0104 g
for pv # 6 : Amm. Pb = 15.44 mg = 0.01544 g
for pv # 7 : Amm. Pb = 19.23 mg = 0.01924 g
for pv # 8 : Amm. Pb = 20.38 mg = 0.0204 g
fc pv # 9 : Amm. Pb = 22.49 mg = 0.0225 g
for pv # 10 : Amm. Pb = 21.53 mg = 0.02153 g
for pv # 12 : Amm. Pb = 39.1 mg = 0.0391 g
for pv # 14 : Amm. Pb = 49.39 mg = 0.0494 g
for pv # 16.45 : Amm. Pb = 68.72 mg = 0.0687 g

total of Pb collected as leachate = 0.2682 g

4. Amount adsorbed on the clay surface:

mass in grams (for each slice) = AVG [g/l]*WDS*100 / (1000*4)
(4g of dried soil, 100 ml of Amm. Ac.; 1000 stands for 1 liter)

Amm. Pb on Top = 28.7*0.2869/40 = 0.2059 g
Amm Pb on Mid = 0.1152 g
Amm Pb on Bottom = 0.1097 g

total adsorbed = 0.4308 g

5. Ammount in the pores:

$$\text{mass in g for each slice} = \frac{[g/l] * WDS * 240 \text{ ml (160 for Mid)}}{WDS \text{ washed} * 1000}$$

(240 ml were used to wash each slice ; 1000 stands for 1 liter)

amm. on Top = 0.0094 * 28.7 * 240 / (12 *1000) = 0.0054 g
amm. on Mid = 0.0025 * 24.26 * 160 / (8 * 1000) = 0.0012 g
amm. on Bottom = 0.0107 * 14.88 * 240 / (12*1000) = 0.00318 g

total in the pores = 0.0098 g

6. Summing up totals :

0.0098 g (pores)+0.2682 g (leach.)+0.4308 g (ads.) = 0.7088 g
(0.0946 meq) (2.59) (4.16 meq) (6.844 meq)

This value is superior to the 0.657 g (6.35 meq)
introduced by 8%.

7. Final Comments :

a) the pores contained 1.1% of the Pb found in the system;
b) 61.0% was adsorbed;
c) the remaining 37.9% leached through.
d) the amount adsorbed by each slice
(the highest is 7.13 meq/100g)
does not exceed the value obtained for the maximum
absorption on the adsorption isotherm of the S/B (soil
suspension) which is 7.95 meq/100g. This is expected.

Appendix G - High Affinity Adsorption of Pb by a S/B Mixture

G.1 - Background

This brief review is partly based on Alammawi's Ph. D. thesis (1988), who developed a model to predict the adsorption mechanisms of heavy metals next to the montmorillonite clay particle surfaces.

Basically, Alammawi (1988) re-examined the limitations of existing theories describing ion exchange equilibrium and mechanisms (e.g.: the Gouy-Chapman diffuse double layer model), and those describing the interactions between water molecules, ionic species and clay surfaces (e.g.: the DLVO theory and model). The author proposes[1] the consideration of repulsive and attractive short range forces in the diffuse double layer model and in the DLVO theory in terms of hydration energies of ion species very close to the particle surfaces.

---

[1] The works of Norrish (1954), Bolt (1956), Warkentin and Schofield (1962), Ottewill (1977), Pashley (1981), Israelachvili (1982), and Push (1982) are classical and important references given by Alammawi (1988) as support to the proposed model.

According to Yong and Mohamed (1991), a better agreement between experimental observations and computed values is possible by considering the Stern and Grahame[2] suggestions in the classical double layer model. In other words, "the charged particle surface and the immediate adjacent layer of counter ions need to be considered in the determination of the additional energy term required [for] ... the extension of the DDL model" to small particle spacing ($2d < 3$ nm). The authors tested the capability of the modified energy model (including hydration energy) in a study of particle interaction during wetting of unsaturated expansive clays. They compared the experimental results obtained by Alammawi (1988) to those of Bolt (1956) and to calculated values obtained using the Gouy-Chapman model. The results only differed at very close particle spacing, where the proposed model agrees better with the experimental observations.

In relation to the present work, this model is an useful tool in predicting and explaining the physical mechanisms of adsorption-desorption of heavy metals next to montmorillonite surfaces, including low-affinity adsorption in the diffused layer and **high affinity adsorption** in the Stern layer (inner and outer Helmholtz planes)[3].

---

[2] The concept of the Stern layer is classical and will not be explained here. The Grahame (1947) suggestion consist of the partitioning of the Stern layer into two parts: an inner Helmholtz plane (IHP) with potential ψ_{ih}, and an outer Helmholtz plane (OHP), where the potential ψ_{oh} equals the potential at the frontier between the Stern layer and the Gouy's diffuse layer.

[3] See Chapter ? for more details on low and high affinity types of adsorption.

The hypothesis, limitations, supporting theoretical considerations and development of the referred model are neither introduced nor discussed here, and can be found in various references, e.g.: Kruyt (1952), van Olphen, 1963), Yong and Warkentin (1975), Bohn et al (1979), Alammawi's Ph.D. thesis (1988), and in Yong and Mohamed (1991).

G.2 - Governing Equations[4]

The concentration of ions at the outer Helmholtz plane can be computed from the Boltzmann relationship:

$$C_2 = C_e \exp\left(\frac{z.e'.\psi_{oh}}{KT}\right) \qquad \text{(G.1)}$$

where:

$C_2 \equiv$ concentration of cations in the second layer of water, or outer Helmholtz plane (ions/m^3);

$C_e \equiv$ concentration of the cation in the bulk solution (ions/cm^3);

$z \equiv$ valence of the cation;

$e' \equiv$ electron charge $= 4.8 \times 10^{-10}$ esu;

$\psi_{oh} \equiv$ electric potential in the second layer (esu); and

$KT \equiv 0.4 \times 10_{20}$ J/ion at 20°C (0.4×10^{-13} erg/ion).

---

[4] Main references: Kruyt (1952); Alammawi (1988); and Yong and Mohamed (1991).

From the Boltzmann law, the concentration of ions in the IHP (C_1) can be found if the potential energies of the ions in the first and second layers of counter-ions are known (E_1 and E_2, respectively):

$$C_1 = C_2.\exp(\frac{E_2 - E_1}{KT}) \qquad (G.2)$$

The energy term E_2 is composed of several 'individual' energies: a) the energy loss of the water resulting from ion-dipole interactions; the energy due to: b) coulombic forces; c) dipole-dipole interactions (reduces the potential due to ion-dipole interactions); and d) dipole-negative site interactions.

In order to calculate C_1 and C_2, the potential energies E_1 and E_2, and the electric potential ψ_{oh} must be first obtained.

In the present work, E_1 and E_2 were taken from computations made by Alammawi (1988; Table 6.1). ψ_{oh} can be obtained in the following way:

a) $\sigma_t = \sigma_s + \sigma_d$ (G.3)

where: $\sigma_t \equiv$ total surface energy density (esu/cm^2) = CEC/SSA; where SSA = specific surface area of the clay particles);

$\sigma_s \equiv$ charge density of partially hydrated adsorbed cations (esu/cm^2)

σ_s = z.e'.Δx.C_i (where Δx is the thickness of a water layer = 2.8 x 10^{-8} cm);

σ_d ≡ charge density of hydrated adsorbed cations in the diffuse layer (esu/cm^2).

σ_d is given by the Gouy-Chapman equation:

$$\sigma_d = [2.\epsilon.KT\sum_{x=0}^{x=\infty} C_e.\exp(\frac{z.\epsilon.\psi_{oh}}{KT}) - 1]^{0.5} \qquad (G.4)$$

or, in a more simple form (Kruyt, 1952):

$$\sigma_d = (\frac{C_e.\epsilon.KT}{2.\pi})^{0.5} . [\exp(Y_d) - \exp(-Y_d)] \qquad (G.5)$$

where: ϵ ≡ dielectric constant of the bulk solution = 80 (water); and

Y_d ≡ scaled potential = (z.e'.ψ_{oh})/(2.KT).

If approximately 2% of accuracy is lost, for $Y_d > 1$ (Alammawi, 1988), Equation G.5 can be simplified to:

$$L_2 = \exp(Y_d) \qquad (G.6)$$

where: $L_2 = [(C_e.\epsilon.KT)/2\pi)]^{0.5}$

Combining Equations G.1, G.2, G.3, and G.6 :

$$\sigma_t = z.e'.\Delta x.C_e.\ \exp\ [(E_2-E_1)/KT].\exp(2.Y_d) + L_2.\exp(Y_d)$$

$$\sigma_t = L_1\ \exp\ (2Y_d) + L_2\ \exp\ (Y_d)$$

where: $L_1 = z.e'.\Delta x.C_e.\exp[(E_2-E_1)/KT]$

Thus:

$$\exp(Y_d) = -L_2 + \frac{\sqrt{L_2^2 + 4.L_1.\sigma_t}}{2.L_1} \qquad (G.7)$$

With Y_d obtained (all other parameters are known), C_2 can be calculated using the Equation below (similar to Equation G.1):

$$C_2 = C_e.\exp(2.Y_d) \qquad (G.8)$$

and finally C_1 can be calculated using Equation G.2.

In order to calculate the distribution of the electric potential ψ_i at any point distant x_i from the surface of the charged particle (in the diffuse double layer), the following relationships, proposed by Kruyt (1952), can be used:

where: $\chi = [(8\pi.C_e.(e')^2.z^2) / (\varepsilon.KT)]^{0.5}$

$$\chi \cdot x = LN\left[\frac{\left[\exp\frac{ze'\psi_i}{2KT} + 1\right] * \left[\exp\frac{ze'\psi_{oh}}{2KT} - 1\right]}{\left[\exp\frac{ze'\psi_i}{2KT} - 1\right] * \left[\exp\frac{ze'\psi_{oh}}{2KT} + 1\right]}\right] \qquad (G.9)$$

The electric potential ψ_i can thus be calculated at a distance x_i, and so can the concentration at this point by using the Boltzmann relationship (Equation G.1):

$$C_i = C_e \exp\left(\frac{z.e'.\psi_i}{KT}\right) \qquad (G.10)$$

G.3 - Theoretical Capacity of the Stern Layer

Total capacity of the Stern layer = $C_1 + C_2$,

where:

C_1 = concentration of *Pb* in the inner Helmholtz plane (IHP);

C_2 = concentration of *Pb* in the outer Helmholtz plane (OHP);

Given: the ion type (*Pb*), size (0.09 nm), and valence (z = +2); CEC (109 meq/100g) and SSA (855 m^2/g); $\exp[(E_1-E_2)/KT]$ = 0.20841 (Alammawi, 1988; Table 6.1); and C_e (concentration of *Pb* in the equilibrium solution), C_1 and C_2 can be

calculated in the following order (Alammawi (1988) made similar calculations for *Na* ion in his Appendix III.8):

1) σ_1 = CEC/SSA = $(1.09*10^{-4}$ equ./g)/$(855*10^4$ cm^2/g) = $1.27*10^{-10}$ equ./cm^2

2) $L1 = z.e'.\Delta_x.C_e.\exp[(E_2-E_1)/KT]$

3) $L2 = [(C_e.\varepsilon.KT)/2\pi]^{0.5}$

4) $\exp(Y_d) = [-L2 + (L2^2 + 4.L1.\sigma_1)^{0.5}]/(2.L1)$

5) $C_2 = C_e * \exp(2.Y_d)$

6) $C_1 = C_2 * \exp[(E_2-E_1)/KT]$

For any given C_e the values of C_1 and C_2 can be obtained, e.g.:

For C_e = 55.8 ppm (C_0 = 442.4 ppm)

207.2 g -----> $6.02 * 10^{23}$ atoms (M.W. of *Pb* = 207.2)

0.0558 g ----> $C_e = 1.62 * 10^{20}$ ions/litre

$C_e = 1.62 * 10^{17}$ ions/cm^3

$L1 = 2*4.8*10^{-10}*2.8*10^{-8}*1.62*10^{17}*0.20841 = 0.9075$

$L2 = [(1.62*10^{17}*80*0.4*10^{-13})/2\pi)]^{0.5} = 287.24$ (erg/cm^3)$^{0.5}$

$\exp(Y_d) = 97.603 => Y_d = 4.58 => 2.Y_d = 9.1618$

$=> C_2 = 1.54 * 10^{21}$ ions/cm^3

$$=> C_i = 3.22 * 10^{20} \text{ ions/cm}^3.$$

G.4 - Theoretical Concentrations at Various Distances (x) from the Surface

The concentration at a distance x, C_i, can be calculated in the following order:

1) $\chi = [(8\pi.C_c.(e')^2.z^2)/(\epsilon.KT)]^{0.5}$;

2) $\psi_{oh} = LN\ (C_2/C_c) * (KT/z.e')$;

3) ψ_i is obtained by trial and error using Equation G.9

where x = distance from the surface (number of water layers);

4) $C_i = C_c\ .\ \exp[(z.e'.\psi_i)/KT]$

G.5 - Comparison Between Theory and Experiments: calculations using adsorption isotherm data for the S/B mixture.

The concentrations (in ppm) used here can be found in the Appendix F.

G.5.1 - Case 1: C_c = 55.8 ppm; C_0 = 442.5 ppm; C_{ads} = 386.6 ppm

$C_c = 1.62 * 10^{17}$ ions/cm^3; $C_{ads} = 1.12 * 10^{18}$ ions/cm^3

Following the order given above:

1) $\chi = [(8\pi.1.62*10^{17}*(4.8*10^{-10})^2*2^2)/(80*0.4*10^{-13})]^{0.5} = 1.082 * 10^6$

2) $\psi_{oh} = LN(1.54 * 10^{21}/1.62*10^{17}) * (0.4*10^{-13}/(2*4.8*10^{-10})) = 3.82*10^{-4}$

The theoretical concentrations at various distances can now be calculated :

3.1) for x = 5 water layers from the surface (= 5*0.28 nm =$1.4*10^{-7}$ cm)

$$\chi.x = LN\left[\frac{\left[\exp\frac{2*4.8*10^{-10}\psi_i}{2*0.4*10^{-13}} + 1\right]*\left[\exp\frac{2*4.8*10^{-10}*3.82*10^{-4}}{2*0.4*10^{-13}} - 1\right]}{\left[\exp\frac{2*4.8*10^{-10}\psi_i}{2*0.4*10^{-13}} - 1\right]*\left[\exp\frac{2*4.8*10^{-10}*3.82*10^{-4}}{2*0.4*10^{-13}} + 1\right]}\right] = 0.1515$$

by trial and error: $\psi_i = 2.04 * 10^{-4}$

$=> C_5 = C_e * \exp[(z.e'.\psi_i)/KT] = \exp[(2*4.8*10^{-10}*2.04*10^{-4}/0.4*10^{-13}]$

$=> C_5 = 21.6 * 10^{18}$ ions/cm^3

3.2) for 3 water layers: $C_3 = 51.4 * 10^{18}$ ions/cm^3;

3.3) for 10 water layers: $C_{10} = 6.37 * 10^{18}$ ions/cm^3;

3.4) for 20 water layers: $C_{20} = 1.70 * 10^{18}$ ions/cm^3;

3.5) for 200 water layers: $C_{200} = 0.163 * 10^{18} \approx C_e$.[5]

[5] The number of water layers needed to have $C_i \approx C_e$ is a function of C_e (see calculations below).

4) Calculation of the number of ions (theoretical and experimental):

4.1) In the Stern layer:

For the IHP, the number of ions per unit area is:

$$A_{1s} = C_1 * \Delta_x$$

$$A_{1s} = 322 * 10^{18} \text{ ions/cm}^3 * 2.8 * 10^{-8} \text{ cm} = 0.9 * 10^{13} \text{ ions/cm}^2$$

For the OHP, the number of ions per unit area is:

$$A_{2s} = C_2 * \Delta_x$$

$$A_{2s} = 1540 * 10^{18} \text{ ions/cm}^3 * 2.8 * 10^{-8} \text{ cm} = 4.3 * 10^{13} \text{ ions/cm}^2$$

Thus, for the Stern layer: $A_s = 5.2 * 10^{13}$ ions/cm^2

The total number of ions in the Stern layer ($\#_s$) is:

$$\#_s = A_s * SSA * \text{mass in grams of bentonite}^6$$

$$\#_s = 5.2*10^{13} \text{ ions/cm}^2 * 855*10^4 \text{ cm}^2/\text{g} * 0.4 \text{ g} \approx \underline{1.78*10^{20} \text{ ions}}$$

---

6 Only the bentonite adsorbs metals; the participation of the sand grains is negligible. In 4 grams of the mixture (quantity used during batch equilibrium tests for the determination of the adsorption isotherm), 0.4 g of bentonite were used.

4.2) Gouy diffuse layer:

If a curve is drawn to represent the fall of *Pb* concentration with the distance from the surface, a sharp logarithmic curve would be obtained for x > 2 water layers. The integration over the distance (area below the curve) between x = 3 and x = 200 gives the number of ions per unit area in the Gouy diffuse layer. An equation is needed before the integration can be made. In the case above, the equation: $y = e^{(14.7158/x)}$ was found for a correlation coefficient, $R^2 = 0.997$. Thus:

$$A_g = \int_3^{200} y(x).dx = 390.54 * 10^{18} * 2.8 * 10^{-8} = 1.09 * 10^{13} \ ions/cm^2$$

The total number of ions in the Gouy diffuse layer ($\#_g$) is calculated as follows:

$\#_s = A_g * SSA *$ mass in grams of bentonite

$\#_g = 1.09 * 10^{13} * 855 * 10^4 * 0.4 = 3.73 * 10^{19}$ ions

4.3) Theoretical total number of ions ($\#_t$):

$\#_t = \#_s + \#_g = 17.8 * 10^{19} + 3.73 * 10^{19} = 21.3 * 10^{19}$ ions

4.4) Experimental number of ions ($\#_e$):

$\#_c = C_{ads}$ * volume of soil suspension used

$\#_c = 1.12 * 10^{18}$ ions/cm^3 * 40 cm^3 = $4.48 * 10^{19}$ ions

4.5) Analysis:

As can be seen, $\#_t > \#_c$, and $\#_c > \#_g$.

Thus the **real** number of ions in the Stern layer is given by:

$$\#_s^r = \#_c - \#_g = 0.75 * 10^{19} \text{ ions}$$

This corresponds to $\approx$ 4% of the total capacity of the Stern layer ($1.78 * 10^{20}$ ions)[7]. These ions were **specifically** adsorbed in the Stern layer (high affinity adsorption), and are more difficult to be displaced by competing ions[8].

Since 40 ml, or 40 cm^3, were used to prepare the soil suspensions:

[Stern] = $0.75 * 10^{19} / 40 = 1.875 * 10^{17}$ ions/cm^3

[Stern] = 1.875×10^{20} ions/litre

207.2 g/l -> 6.02×10^{23} atoms/l

[g/l] -> 1.875×10^{20} ions/l => [g/l] = 0.0646

---

7 The rest of the Stern layer is still occupied by *Na*, *Ca*, *Mg*, and *K* ions.

8 e.g.: NH_4^+ ions of the 'extracting' solution (ammonium acetate) used during the experimental program to recuperate the *Pb* ions adsorbed by **compacted** S/B.

$[ppm_{Stern}]$ = 64.6 ppm (14.6% of C_0; or 17% of C_{ads} = 386.6 ppm)

$(g_{ads})_{stern}$:

207.2 g -> $6.02 * 10^{23}$ ions

x -> $0.75 * 10^{19}$ ions => $x = 2.58 * 10^{-3}$ g

$(g_{ads}/g_{S/B})_{stern} = 2.58 * 10^{-3} / 4 = 6.45 * 10^{-4}$ g/g

or using the Equation (F.1):

$q\ (g/g) = [C_{ads} * V]/M = [(64.6*10^{-3}\ g/1000\ ml) * 40\ ml]/4\ g$

$q\ (g/g) = 6.46 * 10^{-4}$ g/g.

G.5.2 - Case 2: C_e = 434.8 ppm; C_0 = 1076.1 ppm; C_{ads} = 641.3 ppm

$C_e = 1.26 * 10^{18}$ ions/cm^3; $C_{ads} = 1.86 * 10^{18}$ ions/cm^3

1) $\chi = [(8\pi.1.26*10^{18}*(4.8*10^{-10})^2*2^2)/(80*0.4*10^{-13})]^{0.5} = 3.02 * 10^6$

2) $\psi_{sh} = LN\ [1.54 * 10^{21}/1.62*10^{17}) * (0.4*10^{-13}/(2*4.8*10^{-10})] = 2.96 * 10^{-4}$

Theoretical concentrations at various distances:

3.1) for x = 3 water layers from the surface (= 3*0.28 nm = $8.4*10^{-8}$ cm)

$$\chi \cdot x = LN\left[\frac{\exp[1200\psi_i] + 1}{\exp[1200\psi_i] - 1} * \frac{\exp[1200*2.963*10^{-4}] - 1}{\exp[1200*2.963*10^{-4}] - 1}\right] = 0.254$$

by trial and error:

$$\psi_i = 1.66 * 10^{-4}$$

$$=> C_3 = 67.9 * 10^{18} \text{ ions/cm}^3$$

3.2) for 5 water layers: $C_5 = 26.6 * 10^{18}$ ions/cm^3;

3.3) for 10 water layers: $C_{10} = 7.64 * 10^{18}$ ions/cm^3;

3.4) for 20 water layers: $C_{20} = 2.60 * 10^{18}$ ions/cm^3;

3.5) for **100** water layers: $C_{100} = 1.26 * 10^{18} \approx C_c$.

4.1) Stern layer (same values as in the previous case):

$$A_s = 5.2 * 10^{13} \text{ ions/cm}^2$$

$$\#_s \approx 1.78*10^{20} \text{ ions}$$

4.2) Gouy diffuse layer:

In the present case, the equation: $y = e^{15.0297/x}$ was found for a correlation coefficient, $R^2 = 0.9986$. And:

$$\int_3^{100} y(x).dx = 292.42 * 10^{18} * 2.8 * 10^{-8} = 0.82 * 10^{13} \ ions/cm^2$$

$$\#_g = 0.82 * 10^{13} * 855 * 10^4 * 0.4 = 2.80 * 10^{19} \text{ ions}$$

4.3) Total number of ions ($\#_t$):

$$\#_t = \#_s + \#_g = 17.8 * 10^{19} + 2.80 * 10^{19} = 20.6 * 10^{19} \text{ ions}$$

4.4) Experimental number of ions ($\#_e$):

$\#_e = C_{ads}$ * volume of soil suspension

$\#_e = 1.86 * 10^{18}$ ions/cm^3 * 40 cm^3 $= 7.44 * 10^{19}$ ions

4.5) Analysis:

$$\#_s^r = \#_e - \#_g = 4.64 * 10^{19} \text{ ions}$$

corresponds to $\approx$ 26% of the total capacity of the Stern layer.

$$[\text{Stern}] = 4.64 * 10^{19} / 40 = 1.16 * 10^{18} \text{ ions/cm}^3$$

$$[\text{ppm}_{\text{Stern}}] = 400 \text{ ppm (37.2\% of } C_0\text{; or 62\% of } C_{ads} = 641.3 \text{ ppm)}$$

$$(g_{ads}/g_{S/II})_{stern} = 4.0 * 10^{-3} \text{ g/g}$$

G.5.3 - Case 3: C_e = 673.0 ppm; C_0 = 1451.9 ppm; C_{ads} = 778.9 ppm

$C_e = 1.955 * 10^{18}$ ions/cm^3; $C_{ads} = 2.26 * 10^{18}$ ions/cm^3

1) χ = $3.76 * 10^6$

2) ψ_{oh} = $2.78 * 10^{-4}$

Theoretical concentrations at various distances:

3.1) for 3 water layers: $C_3 = 70.0 * 10^{18}$ ions/cm^3;

3.2) for 5 water layers: $C_5 = 27.4 * 10^{18}$ ions/cm^3;

3.3) for 10 water layers: $C_{10} = 8.15 * 10^{18}$ ions/cm^3;

3.4) for 20 water layers: $C_{20} = 3.16 * 10^{18}$ ions/cm^3;

3.5) for **90** water layers: $C_{90} = 1.955 * 10^{18} \approx C_e$.

4.1) Stern layer (same values as in the previous case):

$A_s = 5.2 * 10^{13}$ ions/cm^2

$\#_s = 1.78*10^{20}$ ions

4.2) Gouy diffuse layer:

In the present case, the equation: $y = e^{15.1428/x}$ was found for a correlation coefficient, $R^2 = 0.9987$. And:

$$\int_3^{90} y(x).dx = 285.46 * 10^{18} * 2.8 * 10^{-8} = 0.8 * 10^{13} \ ions/cm^2$$

$\#_g = 0.8 * 10^{13} * 855 * 10^4 * 0.4 = 2.74 * 10^{19}$ ions

4.3) Total number of ions ($\#_t$):

$\#_t = \#_s + \#_g = 17.8 * 10^{19} + 2.74 * 10^{19} = 20.54 * 10^{19}$ ions

4.4) Experimental number of ions ($\#_e$):

$\#_e = 2.26 * 10^{18}$ ions/cm^3 * 40 cm^3 $= 9.0 * 10^{19}$ ions

4.5) Analysis:

$$\#_s^r = \#_e - \#_g = 6.26 * 10^{19} \text{ ions}$$

This corresponds to ≈ 35% of the total capacity of the Stern layer.

$$[\text{Stern}] = 6.26 * 10^{19} / 40 = 1.57 * 10^{18} \text{ ions/cm}^3$$

[ppm in Stern] = 540 ppm (70% of C_{ads})

$$(g_{ads}/g_{S/B})_{stern} = 5.39 * 10^{-3} \text{ g/g}$$

G.5.4 - Case 4: C_e = 888.2 ppm; C_0 = 1776.6 ppm; C_{ads} = 888.4 ppm

$C_e = 2.58 * 10^{18}$ ions/cm^3; $C_{ads} = 2.58 * 10^{18}$ ions/cm^3

1) χ = $4.32 * 10^6$

2) ψ_{oh} = $2.665 * 10^{-4}$

Theoretical concentrations at various distances:

3.1) for 3 water layers: $C_3 = 70.8 * 10^{18}$ ions/cm^3;

3.2) for 5 water layers: $C_5 = 28.0 * 10^{18}$ ions/cm^3;

3.3) for 10 water layers: $C_{10} = 8.60 * 10^{18}$ ions/cm^3;

3.4) for 20 water layers: $C_{20} = 3.65 * 10^{18}$ ions/cm^3;

3.5) for **80** water layers: $C_{80} = 2.58 * 10^{18} \approx C_c$.

4.1) Stern layer (same values as in the previous case):

$A_s = 5.2 * 10^{13}$ ions/cm^2

$\#_s \approx 1.78*10^{20}$ ions

4.2) Gouy diffuse layer:

In the present case, the equation: $y = e^{15.3192/x}$ was found for a correlation coefficient, $R^2 = 0.9978$. And:

$$\int_3^{80} y(x).dx = 281.17 * 10^{18} * 2.8 * 10^{-8} = 0.79 * 10^{13} \quad ions/cm^2$$

$\#_g = 0.79 * 10^{13} * 855 * 10^4 * 0.4 = 2.69 * 10^{19}$ ions

4.3) Total number of ions ($\#_t$):

$\#_t = \#_s + \#_g = 17.8 * 10^{19} + 2.69 * 10^{19} = 20.50 * 10^{19}$ ions

4.4) Experimental number of ions ($\#_e$):

$\#_e = 2.58 * 10^{18}$ ions/cm^3 * 40 cm^3 = $10.3 * 10^{19}$ ions

4.5) Analysis:

$$\#_s^f = \#_e - \#_g = 7.61 * 10^{19} \text{ ions}$$

This corresponds to = 43% of the total capacity of the Stern layer.

[Stern] = $7.61 * 10^{19} / 40 = 1.90 * 10^{18}$ ions/cm^3

[ppm in Stern] = 655 ppm (74% of C_{ads})

$(g_{ads}/g_{S/B})_{stern} = 6.55 * 10^{-3}$ g/g

G.5.5 - Case 4: C_e = 1583.9 ppm; C_0 = 2531.1 ppm; C_{ads} = 947.2 ppm

$C_e = 4.6 * 10^{18}$ ions/cm^3; $C_{ads} = 2.75 * 10^{18}$ ions/cm^3

1) χ = $5.77 * 10^6$

2) ψ_{oh} = $2.42 * 10^{-4}$

Theoretical concentrations at various distances[9]:

3.1) for 3 water layers: $C_3 = 74.5 * 10^{18}$ ions/cm^3;

3.2) for 4 water layers: $C_4 = 44.6 * 10^{18}$ ions/cm^3;

3.3) for 5 water layers: $C_5 = 29.9 * 10^{18}$ ions/cm^3;

3.4) for 7 water layers: $C_5 = 17.1 * 10^{18}$ ions/cm^3;

3.5) for 10 water layers: $C_{10} = 10.0 * 10^{18}$ ions/cm^3;

3.6) for 15 water layers: $C_{10} = 6.5 * 10^{18}$ ions/cm^3;

3.7) for 20 water layers: $C_{20} = 5.4 * 10^{18}$ ions/cm^3;

3.8) for **60** water layers: $C_{60} = 4.60 * 10^{18} \approx C_c$.

4.1) Stern layer (same values as in the previous case):

$A_s = 5.2 * 10^{13}$ ions/cm^2

$\#_s \approx 1.78*10^{20}$ ions

4.2) Gouy diffuse layer:

In the present case, the equation: $y = e^{15.9464/x}$ was found for a correlation coefficient, $R^2 = 0.9964$. And:

---

[9] More values were needed in order to obtain a good regression.

$$\int_3^{60} y(x).dx = 286.1 * 10^{18} * 2.8 * 10^{-8} = 0.8 * 10^{13} \quad ions/cm^2$$

$$\#_g = 0.80 * 10^{13} * 855 * 10^4 * 0.4 = 2.74 * 10^{19} \text{ ions}$$

4.3) Total number of ions ($\#_t$):

$$\#_t = \#_s + \#_g = 17.8 * 10^{19} + 2.74 * 10^{19} = 20.50 * 10^{19} \text{ ions}$$

4.4) Experimental number of ions ($\#_e$):

$$\#_e = 2.75 * 10^{18} \text{ ions/cm}^3 * 40 \text{ cm}^3 = 11.0 * 10^{19} \text{ ions}$$

4.5) Analysis:

$$\#_s^r = \#_e - \#_g = 8.26 * 10^{19} \text{ ions}$$

This corresponds to ≈ 46% of the total capacity of the Stern layer.

$$[\text{Stern}] = 8.26 * 10^{19} / 40 = 2.06 * 10^{18} \text{ ions/cm}^3$$

[ppm in Stern] = 711 ppm (75% of C_{ads})

$$(g_{ads}/g_{S/B})_{stern} = 7.1 * 10^{-3} \text{ g/g}$$

G.6 - Summary of Results and Conclusions

The amounts of *Pb* adsorbed in the Stern layer were plotted with the adsorption isotherm of the S/B, as presented in Figure G.1.

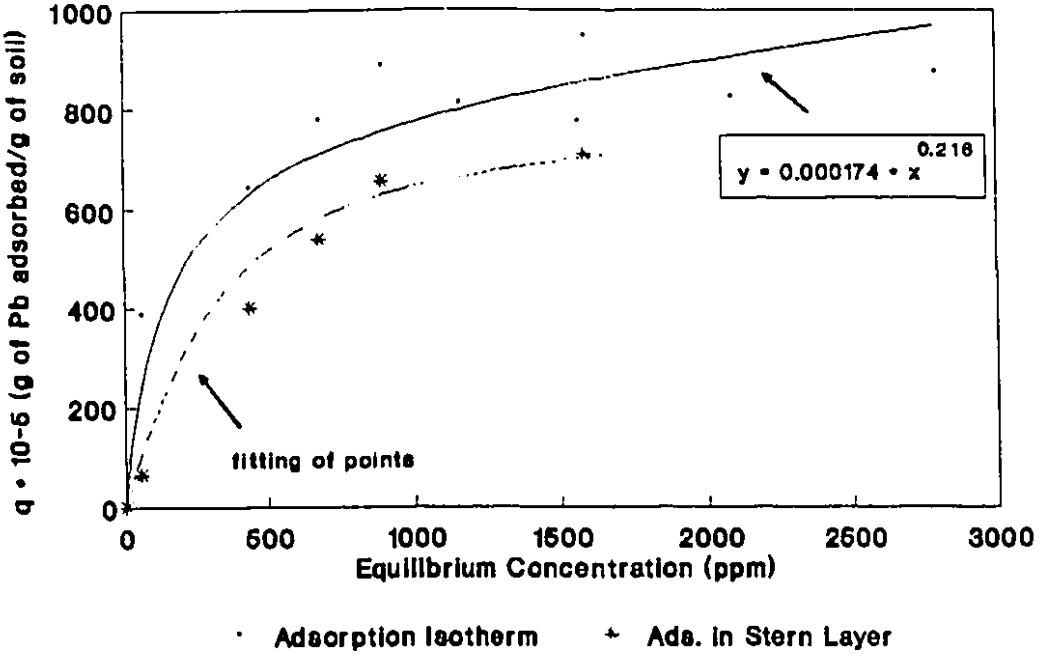

Figure G.1 - Adsorption Isotherm of S/B and Adsorption in the Stern Layer (high affinity adsorption).

It can be observed that, at the peak of adsorption, approximately 75% of the *Pb* adsorbed is packed in the Stern layer.

The presence of such high amounts of *Pb* in the Stern layer can partly explain the differences in the mass balance calculations presented in Section 4.2.5.1. Some of the lead is tightly bonded to the clay particles and will not be exchanged very easily by the ammonium ions of the extracting solution, because of the high energy needed for the exchange to occur (this subject has been also addressed in the text of Chapter 4). Indeed, as obtained from the calculations above, even at very high concentrations of *Pb* only as much as 50% of the base exchangeable cations were displaced by the *Pb* ($\#_e/\#_t \approx 54\%$ for C_e = 1583.9 ppm), evidencing how strong the bonds between the charged surfaces and the adjacent layer of ions are.